UNIVERSITÉ DE MONTRÉAL

TOWARDS ACCURATE FORECASTING OF EPILEPTIC SEIZURES: ARTIFICIAL INTELLIGENCE AND EFFECTIVE CONNECTIVITY FINDINGS

ELIE BOU ASSI
INSTITUT DE GÉNIE BIOMÉDICAL
ÉCOLE POLYTECHNIQUE DE MONTRÉAL

THÈSE PRÉSENTÉE EN VUE DE L'OBTENTION
DU DIPLÔME DE PHILOSOPHIAE DOCTOR
(GÉNIE BIOMÉDICAL)
AOÛT 2018

UNIVERSITÉ DE MONTRÉAL

ÉCOLE POLYTECHNIQUE DE MONTRÉAL

Cette thèse intitulée:

TOWARDS ACCURATE FORECASTING OF EPILEPTIC SEIZURES: ARTIFICIAL INTELLIGENCE AND EFFECTIVE CONNECTIVITY FINDINGS

présentée par : BOU ASSI Elie
en vue de l'obtention du diplôme de : Philosophiae Doctor
a été dûment acceptée par le jury d'examen constitué de :

M. DAVID Jean Pierre, Ph. D., président
M. SAWAN Mohamad, Ph. D., membre et directeur de recherche
M. NGUYEN Dang Khoa, Ph. D., membre et codirecteur de recherche
Mme RIHANA Sandy, Ph. D., membre et codirectrice de recherche
M. LESAGE Frédéric, Ph. D., membre
M. LINA Jean-Marc, Ph. D., membre externe

DEDICATION

To my beloved parents, Gladys and Georges,
Who always picked me up on time and encouraged me to go on every adventure,
Especially this one…

ACKNOWLEDGEMENTS

First and foremost, I would like to express my sincere gratitude to my advisors Prof. Mohamad Sawan, Dr. Dang K. Nguyen, and Dr. Sandy Rihana for the continuous support throughout my Ph. D. and related research. Many thanks for your patience, motivation, and immense knowledge. Your guidance helped me in all the time of research until the writing of this thesis. I could not have imagined having better advisors for my Ph. D. journey. Since the begin, you were not only research supervisors but also life mentors who have influenced a lot of decisions shaping my future career.

Beside my advisors, I would like to thank Prof. Frédéric Lesage and Dr. Philippe Pouliot who instructed me through several meetings as I was their own student. Prof. Lesage's comments and advices, especially during my comprehensive exam, were of great contribution to the work reported in this thesis.

My sincere thanks also go to the jury members namely Prof. Jean-Pierre David, Prof. Frederic Lesage, Prof. Jean-Marc Lina and Prof. Steven Dufour for their time beside their busy schedules.

I am grateful to my family who have provided me through moral and emotional support in my life. I am also grateful to my friends who have supported me along the way.

I gratefully acknowledge the funding received towards my PhD from the Natural Sciences and Engineering Research Council of Canada and Epilepsy Canada. I am also grateful to the Agence Universitaire de la Francophonie (AUF) and the Electrical Engineering Department of Polytechnique Montreal for the Excellence Doctoral Mobility and the Excellence Scholarship for Graduate Students respectively.

I would also like to thank my fellow lab mates and staff at the CHUM Epilepsy research group namely Dr. Denahin Toffa, Dr. Laurence Martineau, Daphné Perla Citherlet, Jimmy Ghaziri, Ali Kassab, Younes Zerouali, Veronique Cloutier, and Manon Robert, for our stimulating discussions, and for all the fun we had in the last four years.

And finally, last but by no means least, also to everyone in the Polystim Neurotech Laboratory, especially Laura Gagliano, Antoine Tantin, Abbas Hamoud, Leila Montazeri, Armin Najarpour, and Marie-Yannick Laplante. It was great sharing the laboratory with all of you during last four years.

RÉSUMÉ

L'épilepsie est une des maladies neurologiques les plus fréquentes, touchant près d'un pourcent de la population mondiale. De nos jours, bien qu'environ deux tiers des patients épileptiques répondent adéquatement aux traitements pharmacologiques, il reste qu'un tiers des patients doivent vivre avec des crises invalidantes et imprévisibles. Quoique la chirurgie d'épilepsie puisse être une autre option thérapeutique envisageable, le recours à la chirurgie de résection demeure très faible en partie pour des raisons diverses (taux de réussite modeste, peur des complications, perceptions négatives). D'autres avenues de traitement sont donc souhaitables. Une piste actuellement explorée par des groupes de chercheurs est de tenter de prédire les crises à partir d'enregistrements de l'activité cérébrale des patients. La capacité de prédire la survenue de crises permettrait notamment aux patients, aidants naturels ou personnels médical de prendre des mesures de précaution pour éviter les désagréments reliés aux crises voire même instaurer un traitement pour les faire avorter. Au cours des dernières années, d'importants efforts ont été déployés pour développer des algorithmes de prédiction de crises et d'en améliorer les performances.

Toutefois, le manque d'enregistrements électroencéphalographiques intracrâniens (iEEG) de longue durée de qualité, la quantité limitée de crises, ainsi que la courte durée des périodes intericales constituaient des obstacles majeurs à une évaluation adéquate de la performance des algorithmes de prédiction de crises. Récemment, la disponibilité en ligne d'enregistrements iEEG continus avec échantillonnage bilatéral (des deux hémisphères) acquis chez des chiens atteints d'épilepsie focale à l'aide du dispositif de surveillance ambulatoire implantable NeuroVista a partiellement facilité cette tâche. Cependant, une des limitations associées à l'utilisation de ces données durant la conception d'un algorithme de prédiction de crises était l'absence d'information concernant la zone exacte de début des crises (information non fournie par les gestionnaires de cette base de données en ligne). Le premier objectif de cette thèse était la mise en œuvre d'un algorithme précis de prédiction de crises basé sur des enregistrements iEEG canins de longue durée. Les principales contributions à cet égard incluent une localisation quantitative de la zone d'apparition des crises (basée sur la fonction de transfert orientée –DTF), l'utilisation d'une nouvelle fonction de coût via l'algorithme génétique proposé, ainsi qu'une évaluation quasi-prospective des performances de prédiction. Les résultats ont montré une amélioration des

performances de prédiction par rapport aux études antérieures, atteignant une sensibilité moyenne de 84.82 % et un temps en avertissement de 10 %.

La DTF, utilisée précédemment comme mesure de connectivité pour déterminer le réseau épileptique (objectif 1), a été préalablement validée pour quantifier les relations causales entre les canaux lorsque les exigences de quasi-stationnarité sont satisfaites. Ceci est possible dans le cas des enregistrements canins en raison du nombre relativement faible de canaux. Pour faire face aux exigences de non-stationnarité, la fonction de transfert adaptatif pondérée par le spectre (Spectrum weighted adaptive directed transfer function - swADTF) a été introduit en tant qu'une version variant dans le temps de la DTF. Le second objectif de cette thèse était de valider la possibilité d'identifier les endroits émetteurs (ou sources) et récepteurs d'activité épileptiques en appliquant la swADTF sur des enregistrements iEEG de haute densité provenant de patients admis pour évaluation pré-chirurgicale au CHUM. Les générateurs d'activité épileptique étaient dans le volume réséqué pour les patients ayant des bons résultats post-chirurgicaux alors que des foyers différents ont été identifiés chez les patients ayant eu de mauvais résultats post-chirurgicaux. Ces résultats démontrent la possibilité d'une identification précise des sources et récepteurs d'activités épileptiques au moyen de la swADTF ouvrant la porte à la possibilité d'une meilleure sélection d'électrodes de manière quantitative dans un contexte de développement d'algorithme de prédiction de crises chez l'humain.

Dans le but d'explorer de nouvelles avenues pour la prédiction de crises épileptiques, un nouveau précurseur a aussi été étudié combinant l'analyse des spectres d'ordre supérieur et les réseaux de neurones artificiels (objectif 3). Les résultats ont montré des différences statistiquement significatives ($p<0.05$) entre l'état préictal et l'état interictal en utilisant chacune des caractéristiques extraites du bi-spectre. Utilisées comme entrées à un perceptron multicouche, l'entropie bispectrale normalisée, l'entropie carrée normalisée, et la moyenne ont atteint des précisions respectives de 78.11 %, 72.64% et 73.26%.

Les résultats de cette thèse confirment la faisabilité de prédiction de crises à partir d'enregistrements d'électroencéphalographie intracrâniens. Cependant, des efforts supplémentaires en termes de sélection d'électrodes, d'extraction de caractéristiques, d'utilisation des techniques d'apprentissage profond et d'implémentation Hardware, sont nécessaires avant l'intégration de ces approches dans les dispositifs implantables commerciaux.

ABSTRACT

Epilepsy is a chronic condition characterized by recurrent “unpredictable” seizures. While the first line of treatment consists of long-term drug therapy about one-third of patients are said to be pharmacoresistant. In addition, recourse to epilepsy surgery remains low in part due to persisting negative attitudes towards resective surgery, fear of complications and only moderate success rates. An important direction of research is to investigate the possibility of predicting seizures which, if achieved, can lead to novel interventional avenues.

The paucity of intracranial electroencephalography (iEEG) recordings, the limited number of ictal events, and the short duration of interictal periods have been important obstacles for an adequate assessment of seizure forecasting. More recently, long-term continuous bilateral iEEG recordings acquired from dogs with naturally occurring focal epilepsy, using the implantable NeuroVista ambulatory monitoring device have been made available on line for the benefit of researchers. Still, an important limitation of these recordings for seizure-prediction studies was that the seizure onset zone was not disclosed/available. The first objective of this thesis was to develop an accurate seizure forecasting algorithm based on these canine ambulatory iEEG recordings. Main contributions include a quantitative, directed transfer function (DTF)-based, localization of the seizure onset zone (electrode selection), a new fitness function for the proposed genetic algorithm (feature selection), and a quasi-prospective assessment of seizure forecasting on long-term continuous iEEG recordings. Results showed performance improvement compared to previous studies, achieving an average sensitivity of 84.82% and a time in warning of 10 %.

The DTF has been previously validated for quantifying causal relations when quasi-stationarity requirements are met. Although such requirements can be fulfilled in the case of canine recordings due to the relatively low number of channels (objective 1), the identification of stationary segments would be more challenging in the case of high density iEEG recordings. To cope with non-stationarity issues, the spectrum weighted adaptive directed transfer function (swADTF) was recently introduced as a time-varying version of the DTF. The second objective of this thesis was to validate the feasibility of identifying sources and sinks of seizure activity based on the swADTF using high-density iEEG recordings of patients admitted for pre-surgical

monitoring at the CHUM. Generators of seizure activity were within the resected volume for patients with good post-surgical outcomes, whereas different or additional seizure foci were identified in patients with poor post-surgical outcomes. Results confirmed the possibility of accurate identification of seizure origin and propagation by means of swADTF paving the way for its use in seizure prediction algorithms by allowing a more tailored electrode selection.

Finally, in an attempt to explore new avenues for seizure forecasting, we proposed a new precursor of seizure activity by combining higher order spectral analysis and artificial neural networks (objective 3). Results showed statistically significant differences ($p<0.05$) between preictal and interictal states using all the bispectrum-extracted features. Normalized bispectral entropy, normalized squared entropy and mean of magnitude, when employed as inputs to a multi-layer perceptron classifier, achieved held-out test accuracies of 78.11%, 72.64%, and 73.26%, respectively.

Results of this thesis confirm the feasibility of seizure forecasting based on iEEG recordings; the transition into the ictal state is not random and consists of a “build-up”, leading to seizures. However, additional efforts in terms of electrode selection, feature extraction, hardware and deep learning implementation, are required before the translation of current approaches into commercial devices.

TABLE OF CONTENTS

LIST OF TABLES

LIST OF FIGURES

LIST OF SYMBOLS AND ABBREVIATIONS

3D	Three dimensional
Ach	Acetylcholine
ADTF	Adaptive directed transfer function
ANFIS	Adaptive neuro fuzzy inference system
ANN	Artificial neural network
ANOVA	Analysis of variance
AR	Autoregressive
AUC	Area under the curve
BIC	Bayesian Information Criterion
BIS	Bispectrum
CFC	Cross frequency coupling
CL	Chromosome length
Cl-	Chloride
Cm^2	Square centimeter
CNN	Cellular neural network
CNNs	Convolutional neural networks
CPU	Central processing unit
DTF	Directed transfer function
DWT	Discrete wavelets transform
ECoG	Electrocorticography
EEG	Electroencephalography
FDA	Food and drugs administration
FIR	Finite impulse response
FPR	False prediction rate
GA	Genetic algorithm
GABA	Gamma-amino-butyric acid
GC	Granger causality
HC	Hjorth complexity

HFOs	High frequency oscillations
HM	Hjorth mobility
HOS	Higher order spectra
IBM	International business machines
iDTF	Integrated directed transfer function
iEEG	Intracranial electroencephalography
IIR	Infinite impulse response
Inter	Interictal
IT	Intervention time
K+	Potassium
K-W	Kruskal Wallis
Lmax	Largest Lyapunov exponent
Mave	Mean of magnitude
mDAD	Maximum difference of amplitude of mean amplitude histograms
MEG	Magnetoencephalography
min	Minimum
MLP	Multi-layer perceptron
MPC	Mean phase coherence
MRI	Magnetic resonance imaging
mRMR	Minimum redundancy maximum relevance
MVAAR	Multi variate adaptive autoregressive
nDTF	Normalized directed transfer function
nIV	Normalized inflow
nOV	Normalized outflow
P1	Normalized bispectral entropy
P2	Normalized squared bispectral entropy
PAC	Phase amplitude coupling
PET	Positron emission tomography
PR-AUC	Precision recall area under the curve
Pre	Preictal
PSD	Power spectral density

RAM	Random access memory
RBF	Radial basis function
Relu	Rectifier linear unit
RNS	Responsive neurostimulation
ROC	Receiver operating characteristic
S1	Harmonic mean of sensitivity and specificity
SEF	Spectral edge frequency
SEP	Spectral edge power
SF	Selected features
SNR	Signal to noise ratio
SOP	Seizure occurrence period
SOZ	Seizure onset zone
SP	Specificity
SPECT	Single-photon emission computed tomography
SS	Sensitivity
SVM	Support vector machine
swADTF	Spectrum weighted adaptive directed transfer function
TIW	Time in warning

LIST OF APPENDICES

CHAPTER 1 INTRODUCTION

1.1 Epilepsy

1.1.1 General definition, prevalence, incidence, and etiology

Epilepsy is one of the most common neurological disorders affecting ~300,000 people in Canada and 70 million worldwide [1]. It was first defined by Jackson in 1873 as "an occasional sudden and excessive discharge of grey matter". This definition lasted for a long period of time, during which, investigations have given more insights into the characterization and mechanisms of this medical disorder on several levels. The fundamental elements of epilepsy are unprovoked, recurrent seizures [2] resulting from abnormal excessive hypersynchronous neuronal discharges. Seizure manifestations vary greatly depending on the site, intensity and propagation of the seizure discharge. In between seizures, brief (milliseconds) asymptomatic discharges called interictal epileptiform discharges (also known as spikes) may occur [3]. Although epilepsy can appear at any age, its incidence is higher in children and elderly (after the age of 65) [4]. The main causes of epilepsy include genetic mutations, gliosis from acquired brain insults (hypoxia, ischemia/stroke, trauma, and infection), malformations of cortical development, vascular malformations, brain tumours and degenerative disorders.

1.1.2 Epileptic seizures

A seizure is defined as a transient disturbance of brain functions due to an abnormal electrical synchronization of groups of neurons. Epileptic seizures can be divided into two main categories: focal and generalized [5]. Seizures are said to be focal when they start from a restricted area of the brain (thus in one hemisphere) while generalized seizures involved the whole of both hemispheres [6]. Focal seizures can be further classified into frontal, temporal, insular, parietal, and occipital, depending on the lobe involved at seizure onset. In generalized seizures, there is impaired consciousness from the onset as the excessive electrical discharge is widespread from the beginning. With focal seizures, earliest symptoms depend on the lobe of seizure onset (ex. visual symptoms with occipital lobe seizures, sensory symptoms in parietal lobe seizures, motor symptoms in frontal lobe seizures etc.). Consciousness is frequently not impaired at the onset of a focal seizure but such impairment may occur as the discharge spreads to larger areas of the brain

and even manifest as bilateral tonic-clonic seizures if the discharge spreads to the whole brain [6].

Studies over the last few years have suggested that network connectivity is at the centre of epilepsy. A more complex 'epileptic network' concept has replaced the classical simplistic notion of a single epileptic focus [7]. In the 'epileptic network', the synchronized activity of 'nodes' with increased excitability (or decreased inhibition) is involved in the generation of pathological interictal epileptiform discharges as well as seizures [8, 9]. Vulnerability to seizure activity in any one part of the network is influenced by the activity elsewhere in the network, and the network as a whole is responsible for epileptic discharges and seizures. The network structures are connected functionally and structurally and the seizure activity can be entrained from any of its various parts [10]. One (or more) node(s) would have a level of excitability so high, that it (they) could autonomously generate seizure onset fast oscillations, driving or entraining through excitatory connections other distant nodes (acting as relays of those fast oscillations). Seizures can subsequently propagate in a variably extensive way that might involve any region or neural structure with anatomic connections to the primary seizure network. Seizure manifestations depend on these phenomena, which in some cases can mimic a normal cognitive process or, on the contrary, disrupt it. This 'epileptic network' concept may help reconcile some observations, such as the complex electrophysiological patterns seen during many focal seizures in intracranial electroencephalography (EEG) studies, often with the involvement of several distinct structures in as much that a clear qualitative (visual) identification of the area of seizure onset is difficult and the non-negligible failure rates (from 10 to 50%, notably in refractory focal epilepsy cases with normal magnetic resonance imaging (MRI)) of classical epilepsy surgeries, which consist of the resection of a single 'epileptogenic zone'[7].

1.1.3 Electroencephalography

1.1.3.1 General definition and brief history

Because epilepsy is fundamentally the result of abnormal neuronal discharges, EEG is the single most important investigative technique for the study of epilepsy. EEG consists in an electrophysiological recording of the brain's electrical activity. The electroencephalogram (recorded signal) displays spatial and temporal voltage variations due to ionic currents flowing

within brain neurons. It is characterized by a high temporal resolution (order of ms), allowing the evaluation of dynamic cerebral functions [11].

The first reported electrical activity-based neurophysiological monitoring was performed by Canton (British neuropsychologist) in 1875 in monkeys and rabbits [12]. It took another half century until the first recording of human brain electrical activity was performed by Hans Berger (German psychiatrist) in 1924 [12]. By the 1950's EEG became widely used in clinical practice [13]. EEG is most widely used in clinical practice for the diagnosis of patients with epilepsy, suspected seizures (e.g. psychogenic seizures), unusual spells, and sleep disorders [14]. It has also been adopted to monitor the depth of anaesthesia during surgery [15]. In addition, EEG is extensively investigated in several research areas namely neuroscience, brain computer interfaces, and neuropsychology [11].

1.1.3.2 Brief background of EEG

EEG displays neuronal electrical activity resulting from the summation of inhibitory and excitatory postsynaptic potentials of large group of neurons. It is considered to be mainly produced by pyramidal cortical neurons, which are arranged in parallel, perpendicularly to the surface of the brain, and have their cell bodies mainly in layers III and V of the cerebral cortex [16]. Spatial organization of the pyramidal cortical neurons creates a cortical dipole layer, that is assumed to be the electrical source of scalp-recorded EEG signals. Scalp EEG measures brain's electrical activity by placing electrodes directly on the scalp (Figure 1.1). Thus, the electrical signal displayed on a selected channel is produced by clusters of similarly angled cortical neurons near the recording site. Each contact records a minimum of 6 cm^2 of synchronous cortical activity (10^4 – 10^6 neurons). The summed electrical activity can be modelled as a dipole (a field with negative and positive poles) [17]. Direction of the energy flow of the generated dipole is parallel to the angle of the involved pyramidal cells. Negative poles are optimally sensed when they are perpendicular to the recording electrode. In such case, the dipole's positive end is subcortical and can be only detected with depth electrodes. Thus, scalp EEG highly depends on the orientation and distance between the dipole and the corresponding recording electrode [18]. The highly resistive nature of the skull, the inhomogeneity and anisotropy of the intervening tissue as well as the head's complex geometry result in a relatively high attenuation and distortion at the EEG signal level, with amplitudes, which are around 10 times smaller than those of extracellular field potentials [11].

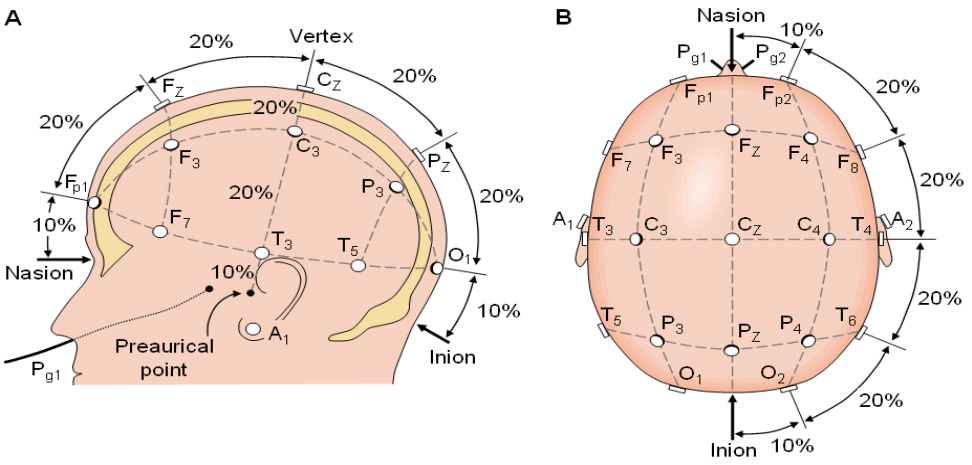

Figure 1.1 Scalp EEG electrode placement according to the 10-10 international electrode placement system [19]

1.1.3.3 Intracranial EEG

Intracranial electroencephalography (iEEG) allows to overcome the distortion of signals from the skull's resistance. It is an invasive electrophysiological investigation requiring the placement of macro-electrodes directly on the surface or inside of the brain, allowing for a higher signal to noise ratio (as compared to scalp recordings). A grid or strip of electrodes can be placed on or slipped under the brain (Figure 1.2A) to record the brain's electrical activity. Grid and strip electrodes can be complemented by depth contacts to record deep brain structures (Figure 1.2B). Thus, electrical fields generated by groups of neurons are measured intracranially. Unlike scalp EEG, electrode positions are chosen in a patient-specific manner during iEEG investigations.

1.1.3.4 EEG frequency bands

The EEG has a relatively large frequency bandwidth that can be sub-divided into well-defined rhythms or oscillatory waveforms. Main EEG rhythms are generally classified based on amplitude, frequency range, and area of the recorded brain signals [11]. The delta rhythm (0.5 – 4 Hz) is characterized by high amplitude signals usually observed in sleep over frontal and occipital areas in adults and children respectively. The theta rhythm (4 – 8 Hz) shows an irregular morphology and is characteristic of sleep and drowsiness in adults. The alpha rhythm (8 - 13 Hz) is observed over the posterior regions of the head during wakefulness. The beta rhythm (13 – 30 Hz) appears mainly in frontal and central regions during motor tasks but usually decreases during the execution of movements.

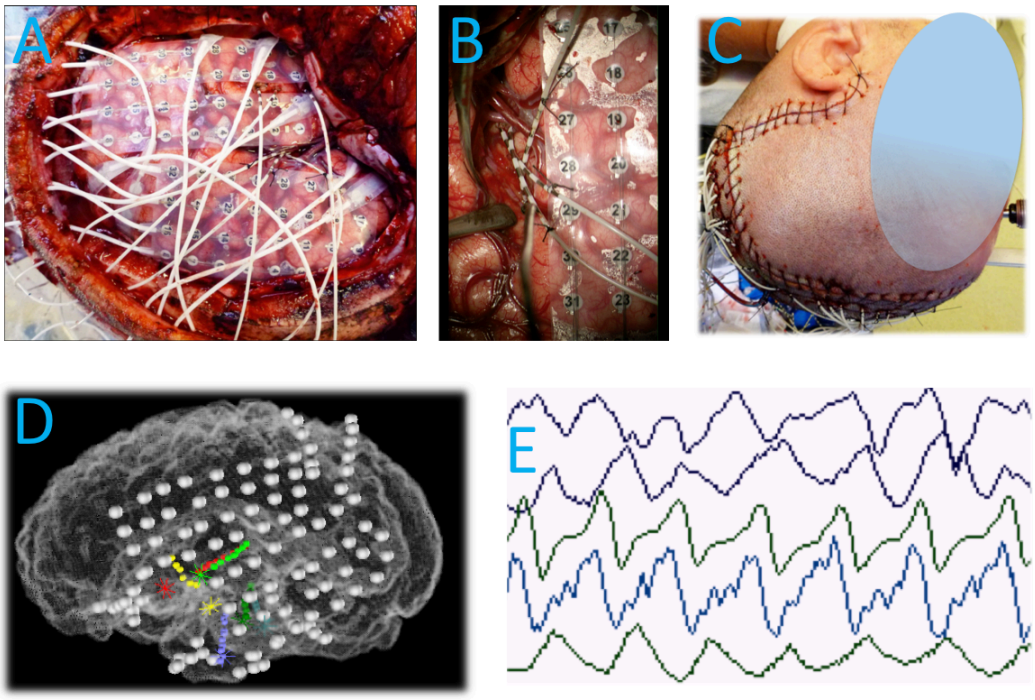

Figure 1.2 Intracranial electroencephalography. A: Intracranial study combining grid and strip electrodes as well as depth electrodes; B: Depth electrodes and grid electrodes; C: Skin flap sutured back with recorded wires tunnelling out; D: 3-D Representation of a subdural grid electrodes, strip electrodes and depth electrodes; E: Raw iEEG recordings from 5 electrode contacts.

The gamma rhythm (30 – 80 Hz) is associated with information processing, consciousness and perception.

1.1.4 The EEG in focal epilepsy

Patients with focal epilepsy exhibit focal epileptiform abnormalities. These are usually divided into a) 'interictal' discharges ('spikes') which are brief (20-200ms) asymptomatic paroxysmal EEG transients clearly distinguished from background; and b) 'ictal' discharges which are sudden focal rhythmic activity with characteristic pattern of evolution (with respect to amplitude, frequency and spatial distribution) lasting at least several seconds to minutes. These ictal discharges are generally associated with clinical seizure manifestations (electroclinical seizures) but can sometimes be clinically silent (electrical seizures) [20]. With a routine 30- min EEG, interictal spikes can be found in approximately 50% of epileptic patients (and in up to 84% by the third serial EEG).

Because routine EEGs are brief in duration, seizures are rarely captured. In circumstances when seizures need to be recorded, long-term video-EEG monitoring is performed. Long-term video-EEG monitoring is particularly useful for the evaluation of drug-refractory epileptic patients who are candidate for epilepsy surgery [21]. It may provide useful information to localize the epileptic focus that needs to be removed to ensure seizure-freedom. Electrically, seizures typically appear as a sudden rhythmic activity evolving in frequency, amplitude and distribution over time with an abrupt ending. Seizures are analysed to infer on the side (lateralization) and site (localization) of the epileptic focus. For example, rhythmic epileptic discharges over the right temporal surface electrodes at seizure onset suggest a right temporal lobe focus. During their 1-2 week stay in the epilepsy monitoring unit, several (usually 3 to 5) seizures are recorded to make sure that the patient has only one epileptic focus, rather than multiple foci. While this can be easily achieved in patients with very frequent attacks, withdrawal of anticonvulsant medication under clinical supervision may be required when seizures do not occur with sufficient regularity for proper recording [22].

When scalp EEG and complementary non-invasive studies (such as brain MRI and positron emission tomography (PET)) fail to adequately localize the focus, invasive intracranial EEG studies are generally required to delineate the focus with more precision. These studies consist of the implantation of intracranial electrodes through craniotomy or burr holes under general anaesthesia in brain regions of suspected epileptogenicity, based on presurgical non-invasive tests and hypotheses about the localization of the epileptogenic zone. A post-implantation MRI is then used to verify the precise 3D location of each electrode contact. Whereas a large cortical surface (of about 6-10 cm2) is required to generate a recordable signal by extracranial electrodes, intracranial electrodes can pick up potential changes occurring over only a few millimetres of cortex with excellent temporal resolution (~ 1ms). While intracerebral EEG overcomes the sensitivity limitations of scalp electrodes because they are closer to bioelectric sources of epileptiform activity, only a limited number may be safely implanted to minimize risk of haemorrhage, oedema or infection. With intracranial EEG, several patterns have been reported at seizure onset but the most frequent one is the sudden appearance of a low voltage fast activity discharge with subsequent increase in amplitude and decrease in frequency. Propagation may be gradual or extremely rapid to surrounding and more distant structures for variable reasons, notably because of the connectivity of involved structures. Although intracranial electrodes allow

for better definition of the epileptogenic zone, its complete delineation may sometimes remain elusive. The reason for this is, in many cases, the seizure discharge may appear quite complex by visual inspection, with rapid involvement of more than one brain region due to the rapid propagation of discharges. Finally, it must also be mentioned that inadequate intracranial electrode coverage may produce a false electrographic picture as the first signal recorded may simply represent propagation if there is no electrode over the actual seizure onset zone.

1.1.5 Treatment of epilepsy

1.1.5.1 Medical treatment of epilepsy

Following the diagnosis of epilepsy, the first line of therapy consists of the use of antiepileptic drugs. Several antiepileptic drugs are currently available on the market. The choice of the antiepileptic drug depends on several factors such as the type of seizures, the epileptic syndrome, antiepileptic drug side effects, comorbid medical conditions (such as psychiatric, renal or hepatic conditions for example), potential interactions with other drugs taken by the patients and costs [23].

While there are more than 15 antiepileptic drugs to choose from, a third of patients continue to suffer from uncontrolled seizures. An important study by Kwan and Brodie has shown that after the first antiepileptic drug used, seizures in approximately 50% of patients are controlled, while in another 10%, seizures are eventually controlled by using a second antiepileptic drug. However, for the remaining patients, whatever next drug is chosen, only 5% of the patients show eventual control [24]. Potential explanations for this drug-refractoriness include the fact that several antiepileptic drugs share the mechanisms of action (ex. several are presynaptic voltage-gated sodium channel blockers), the fact that most of these drugs were discovered/screened using the same old animal models of epilepsy, or that the patients have an intrinsic multidrug resistance mechanism. Finally, it must be noted that although majority of the epileptic patients are well controlled on medication, this may sometimes be accompanied by side effects (dizziness, fatigue, intermittent double vision, mental slowing, somnolence …). Furthermore, although a patient's epilepsy is generally well controlled, it does not necessarily mean that he cannot have breakthrough seizures from time to time. Besides, adherence to treatment is a major issue as some studies, using a variety of direct and indirect methods, indicate that 30-60% of epileptic patients do not fully adhere to their antiepileptic drug [23].

Alternative possible treatments for patients with refractory epilepsy are discussed below.

1.1.5.2 Non-medical treatment of epilepsy

Several non-medical therapies are available. The ketogenic diet is sometimes used in very specific types of drug-resistant epilepsy, notably, for some epileptic encephalopathies in young children [25]. This treatment, however, is quite challenging and long-term consequences of a high fat, low sugar diet remains uncertain particularly on growth, cardiovascular and bone health. Vagus nerve stimulation is another non-medicinal option, which consists of the chronic stimulation of the left Vagus nerve using a generator inserted under the pectoralis muscle. However, this treatment is considered a palliative treatment. Indeed, while 30-40% of patients can experience a 50% reduction of their baseline seizure frequency, less than 3% of the patients become seizure-free [26].

Epilepsy surgery is also an interesting option which consists in the surgical resection of the epileptic focus to cure seizures. In order to localize the epileptic focus to be removed, patients first need to undergo a battery of complementary non-invasive tests [27], which include: a) a good clinical history (seizure semiology can provide clues to focus localization); b) an MRI (looking for causal epileptogenic lesions); c) video-EEG monitoring (to observe seizure semiology and to characterize epileptic activity between and during seizures); and d) positron emission tomography (to reveal localized areas of abnormal glucose use). Some centers are also equipped to perform ictal single photon emission computed tomographies (revealing localized areas of increased blood flow during seizures), simultaneous EEG and functional MRI (analysing areas of transient increased blood flow and decrease in reduced haemoglobin during averaged spikes) and magnetoencephalography (to pinpoint sources of spike-triggered magnetic field disturbances). In case, these complementary non-invasive studies fail to adequately localize the epileptogenic zone, an invasive EEG study is then performed as mentioned above (required for about 25% of the patients with refractory epilepsy enrolled in the pre-surgical evaluation protocol) [27]. Despite important advances in the field of presurgical evaluation and epilepsy surgeries, it must be noted that success rates of these approaches remain modest. In temporal lobe epilepsy surgeries, the probability of becoming seizure-free is approximately 75% in lesional cases (i.e. with an MRI identifiable lesion) and only 50% in nonlesional cases. In frontal lobe epilepsy surgeries, the probability of becoming seizure-free is only 60% in lesional and a mere 35% in nonlesional cases [28]. The most obvious explanation for surgical failures is inaccurate

localization of the epileptic focus [29]. This can in part be accounted for by limitations in the current localization techniques. Furthermore, not all patients can benefit from surgery, such as patients whose epileptogenic zone overlies eloquent functionally important brain regions (language, visual and sensorimotor cortices), patients with multifocal epilepsy and patients for whom the seizure onset could not be adequately identified.

1.2 Problem statement

Because of their unpredictable nature, uncontrolled seizures represent a major personal handicap and source of worry for patients. In addition, persistent seizures constitute a considerable burden on healthcare resources, accounting for a high number of disability days or unemployment and low annual income [1, 30]. Some difficulties and challenges faced in the treatment of drug-refractory patients can be overcome by algorithms able to anticipate seizures. Seizure detection and prediction algorithms have been proposed in an attempt to deliver therapies during times of high likelihood of seizures [31]. It has been recently demonstrated that seizures are more likely to be controlled by means of closed-loop stimulations as compared to open loop strategies [32]. Although detection algorithms are currently better in terms of sensitivity (SS) and specificity (SP) than prediction algorithms, the activation of seizure-aborting interventions (such as focal cooling, electrical stimulation or release of anticonvulsants) after the electrical seizure onset means that patients could already have disabling clinical manifestations or that the brain has reached a point of no return after which it will evolve into a seizure with impaired consciousness or with bilateral tonic-clonic convulsions [33].

1.2.1 Seizure detection

Over the last decade, we and others have mainly focused on seizure detection using scalp and iEEG recordings [34, 35]. Our group has worked on: a) a low-power integrated circuit, intended for real-time epileptic seizure detection, which was tested using intracranial long-term EEG recordings from 7 patients with an average seizure detection delay of 13.5s [36]; b) a low-power closed-loop neuro- stimulator composed of a detector chip and an electrical stimulator assembled with recording electrodes [37]; and c) a responsive focal drug delivery system based on a new asynchronous seizure detector (~16s latency) [31].

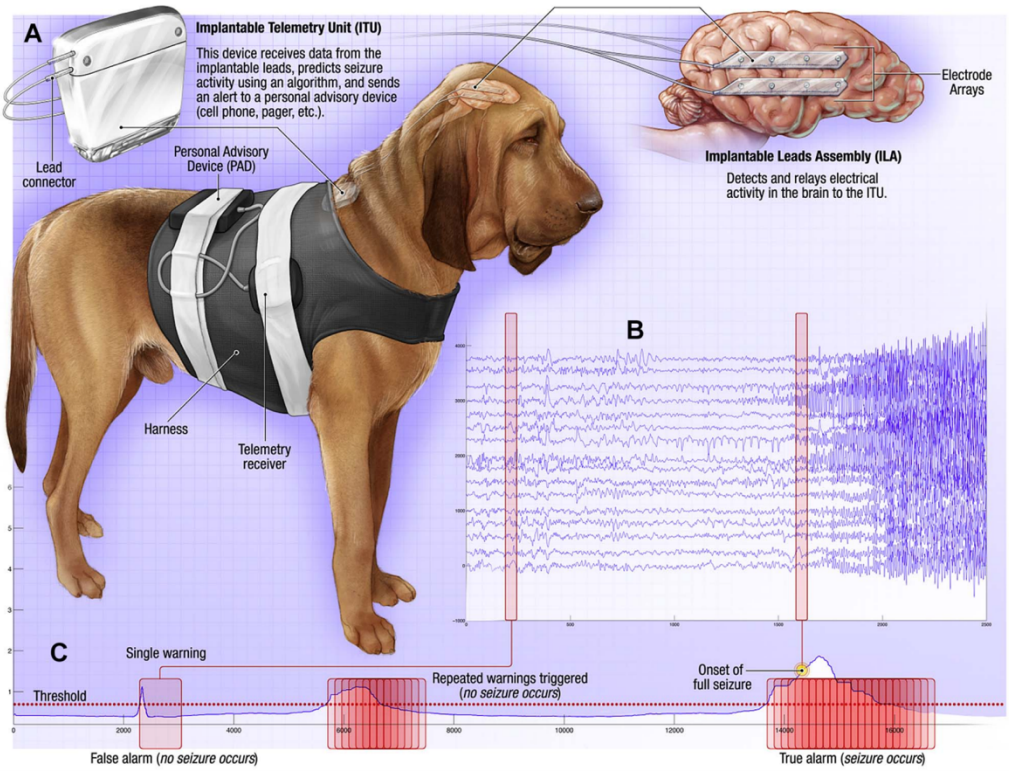

Figure 1.3 NeuroVista ambulatory monitoring device's implantation in dogs with naturally occurring focal epilepsy [38].

Recently, the responsive neurostimulation (RNS) system (NeuroPace Inc.) was approved by the food and drug administration (FDA) as an adjunctive treatment of adult patients with medically refractory focal epilepsy [39]. The device continuously monitors brain activity and provides electrical stimulation upon seizure detection. Unfortunately, reduction in seizure frequency was only modest (44% at one year) [32, 40] and the device could only retain a low number of brief detected epochs due to power and storage constraints [41]. On the other hand, the NeuroVista ambulatory monitoring device was recently proposed to continuously acquire iEEG data and transmit them to an external processing unit for subsequent storage and analysis [42]. The implantable part of the device combines a lead assembly (4 x 4-contacts' silicone strips) and telemetry unit. Intracranial EEG signals are amplified and sampled at 400 Hz within the implantable telemetry unit and then transmitted to a personal advisory device that features an embedded seizure detection algorithm, a user interface, and an email algorithm for output [42]. Interestingly, long-term continuous iEEG recordings spanning more than one year in some dogs, were recently acquired and made freely available at the ieeg.org portal.

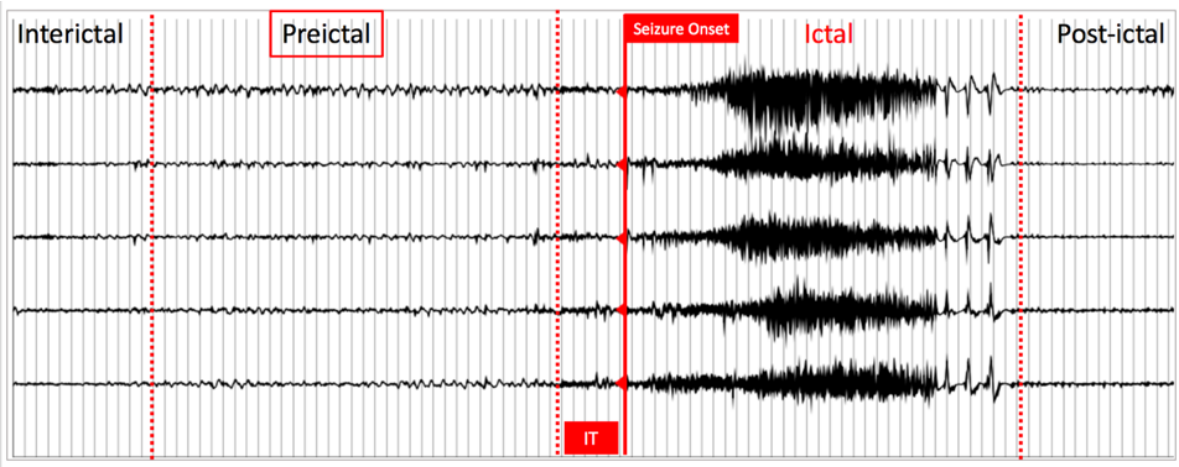

Figure 1.4 Five-channels iEEG illustrating typical epileptic brain states; IT: intervention time

Conceptually, any intervention based on seizure detection is faced with the problem that for most patients, overt clinical manifestations are already present by the time a seizure is detected (~10-15s), at which stage, aborting a seizure is more difficult (possibly past the 'point of no return'). In contrast, seizure forecasting investigates the possibility of detecting patterns before seizure onset, providing more warning time and intervention much before the point of no return.

1.2.2 Seizure prediction

Cumulative data now indicate that there is a gradual transition between the interictal (in between) and ictal (during) seizure states, known as the preictal state [43-47]. Thus, seizure prediction can be considered as the early detection of the preictal state. Figure 1.4 shows 5-channel- iEEG recordings, illustrating typical brain states. The intervention time (IT) lies between the end of the preictal period and seizure onset. Unfortunately, the ability to accurately identify the pre-seizure state remains elusive [33, 48, 49]. The guidelines proposed by Mormann et al. 2007 have paved the way to more realistic and reproducible results although less optimistic [33]. In a recent review, we critically analysed all the existing work on seizure prediction, from signal acquisition to performance evaluation [48]. Although results varied between studies, many showed acceptable performances that could be appealing for the design of advisory/intervention devices. There is, however, a great potential for improvement and optimization in the seizure forecasting framework [33, 48, 49].

Some of the critical aspects that need to be addressed to improve seizure forecasting performances are briefly discussed below:

1) In a great majority of previous seizure prediction investigations, an initial set of only six electrodes (3 focal, 3 afocal) have been used [33, 48, 49]. This is mainly because these were the only ones available in international databases, selected based on visual inspections of seizure origin and propagation by expert neurophysiologists. Snyder et al. (2008) emphasized that reliable seizure forecasting algorithms should be implemented on electrodes placed in brain areas, where preictal changes are detectable [50]. Gadhoumi et al. (2012) reported promising results by including three bipolar channels for the 4-deepest contacts implanted in the seizure onset zone [51]. In contrast, several endeavours claimed that remote channels could also carry predictive information [52, 53]. Subsequently, Gadhoumi et al. (2015) highlighted the need for including ***bilateral neocortical electrodes*** in the design of seizure predictors [49]. On the other hand, due to the explosive nature of seizure propagation through the brain, recent studies have demonstrated an imperfect visual identification of the epileptogenic regions and favour the use of quantitative functional connectivity-based methods [7, 10, 54-56].

2) Previous seizure forecasting investigations have generally looked at discontinuous recordings either from the University of Freiburg database, the European Epilepsy Database, Boston database, or local recordings. Considering the established effects of drug tapering/changes in medication, changes in vigilance states, and circadian influences on the dynamics of EEG recordings, more caution should be considered when assessing seizure forecasting performances based on such discontinuous recordings. In addition, because the discriminability of iEEG features is highly dependent on time and the non-stationary nature of EEGs can culminate in mis-estimation of algorithm performance, ***long-term continuous recordings*** that mimic real clinical scenarios, rather than discontinuous recordings, are recommended [57]. Gadhoumi et al. (2015) established that the assessment of seizure forecasting algorithms on continuous long-term EEG recordings encompassing several conditions and states is sufficient to prove its clinical validity [49].

3) Previous feature selection efforts focused on ranking methods to select the most discriminative characteristics [45, 58, 59]. Although much effort has been made towards identifying unique precursors of seizure activity, no single feature has been shown to be capable of individually characterizing the preictal state [33, 48, 49]. However, a combination of features may be able to display brain dynamics during transition to seizure [49]. Thus, it is important to

use ***incremental feature selection algorithms*** that tend to establish which combination of features is discriminative of the preictal state.

4) Spectral band power, which aims to display amplitude modulations within defined frequency bands over time, has been most commonly used in previous seizure forecasting investigations. While this feature could quantify phase changes, it failed in identifying interactions between different frequencies. In contrast, higher order spectral measures based on cross frequency coupling have been proposed to be the carrier mechanism for the relationships of global and local neuronal processes. Two recent studies in the field of seizure prediction attempted to explore cross frequency and reported promising performances [45, 60]. Investigating ***other types of frequency coupling*** may be an interesting and promising avenue for feature extraction in epileptic seizure prediction.

1.3 Objectives, hypotheses, and research work overview

The overarching goal of this thesis was the development of an accurate seizure forecasting algorithm based on continuous long-term iEEG recordings.

Our specific aims are:

AIM 1: To develop an accurate seizure forecasting algorithm, validated on *long-term continuous canine bilateral* iEEG recordings acquired using an *ambulatory monitoring device*.

We **hypothesize** that 1) an adequate selection of electrodes based on an adaptive effective connectivity approach and 2) a new incremental feature selection based on a genetic algorithm can improve seizure forecasting capabilities.

Article 1: **Elie Bou Assi**, Dang K. Nguyen, Sandy Rihana and Mohamad Sawan, A Functional-Genetic Scheme for Seizure Forecasting in Canine Epilepsy, *IEEE Transactions on Biomedical Engineering (IF: 4.288)*, 65(6), 1339-1348, June 2018, included in the journal's feature story/ website main page, https://doi.org/10.1109/TBME.2017.2752081.

This work was presented as an invited talk at the 1st Symposium on the Applications of Artificial Intelligence in Medicine (Montreal, May 2018).

AIM 2: To investigate the feasibility of accurate identification of generators and sinks of seizure activity using *high density* human iEEG recordings based on the spectrum weighted adaptive

directed transfer function (swADTF) in patients with drug-resistant epilepsy and being investigated for potential epilepsy surgery.

We **hypothesize** that the use of effective connectivity measures based on the swADTF allows an accurate identification of seizures' origin and propagation (network of seizure activity).

Article 2: **Elie Bou Assi**, Dang K. Nguyen, Sandy Rihana and Mohamad Sawan, Effective Connectivity Analysis of Operculo-Insular Seizures, *Epilepsy Research (IF: 2.49)*, submitted (July 2018).

This work was presented as part of an Investigators' workshop entitled Insular Epileptic Networks at the 71st Annual Meeting of the American Epilepsy Society (Washington DC, December 2017).

AIM 3: To assess the feasibility of seizure forecasting based on higher order spectral analysis and artificial neural networks.

We **hypothesize** that 1) capturing information about multifrequency behaviours, quantified by complex metrics, related to the concept of cross-frequency coupling and 2) the design of a classifier based on such inputs can emerge as a new avenue for seizure forecasting.

Article 3: **Elie Bou Assi**, Laura Gagliano, Dang K. Nguyen, Sandy Rihana and Mohamad Sawan, Leveraging Higher Order Spectra and Artificial Neural Networks: Towards New Precursors of Seizure Activity, *Scientific Reports (IF: 4.122)*, revised version submitted (July 2018).

This work will be presented as part of the Artificial Intelligence in Epilepsy workshop at the 2018 Canadian League Against Epilepsy Scientific Meeting (St John's, September 2018).

In parallel, additional scientific contributions were published during this thesis through auxiliary collaborative work:

Additional related Articles (2):

Elie Bou Assi, Dang K. Nguyen, Sandy Rihana, Mohamad Sawan, Towards accurate prediction of epileptic seizures: A review, Biomedical Signal Processing and Control, 34, 2017, 144-157, ISSN 1746-8094, https://doi.org/10.1016/j.bspc.2017.02.001.

Laura Gagliano, **Elie Bou Assi**, Dang K. Nguyen, Sandy Rihana, and Mohamad Sawan, Bilateral preictal signature of phase-amplitude coupling in canine epilepsy, Epilepsy Research, 139, 2018, 123-128, https://doi.org/10.1016/j.eplepsyres.2017.11.009

Conference proceedings (4):

Elie Bou Assi, Dang K. Nguyen, Sandy Rihana, and Mohamad Sawan, "A hybrid mRMR-genetic based selection method for the prediction of epileptic seizures," *2015 IEEE Biomedical Circuits and Systems Conference (BioCAS)*, Atlanta, GA, 2015, pp. 1-4.

Elie Bou Assi, Dang K. Nguyen, Sandy Rihana, and Mohamad, "A 2D clustering approach investigating inter-hemispheric seizure flow by means of a Directed Transfer Function," *2016 3rd Middle East Conference on Biomedical Engineering (MECBME)*, Beirut, 2016, pp. 68-71.

Elie Bou Assi, Dang K. Nguyen, Sandy Rihana and Mohamad Sawan, "Refractory epilepsy: localization, detection, and prediction," 2017 IEEE 12th International Conference on ASIC (ASICON), Guiyang, 2017, pp. 512-515.

Laura Gagliano, **Elie Bou Assi**, Dang K. Nguyen, and Mohamad Sawan, Bicoherence of intracranial EEG: A novel precursor of seizure activity in canine epilepsy, submitted to the 2018 2nd IEEE Life Sciences conference, Montreal, 2018.

Related Conference abstracts (3):

Elie Bou Assi, Dang K. Nguyen, Sandy Rihana, M. Sawan, "On the proper selection of electrodes for seizure forecasting in canine epilepsy" International Conference on Technology and Analysis of Seizures, 20-23 Aug. 2017

Laura Gagliano, **Elie Bou Assi**, Dang K. Nguyen, Sandy Rihana, M. Sawan, "Bilateral Preictal Signature of Phase Amplitude Coupling in Canine Epilepsy" International Conference on Technology and Analysis of Seizures, 20-23 Aug. 2017

Elie Bou Assi, Dang K. Nguyen, Sandy Rihana, M. Sawan, "Dimensionality reduction in seizure prediction studies" (Epilepsy Currents), 69th Annual Meeting of the American Epilepsy Society, 4-8 Dec. 2015

This thesis is organized as follows: Chapter 2 reviews the general framework of reliable algorithmic seizure prediction studies, discussing each component of the whole block diagram. It explores steps along the pathway from signal acquisition to adequate performance evaluation that should considered in the design of an efficient seizure advisory/intervention system. Chapter 3 briefly introduces different signal processing approaches used in this thesis. Chapters 4, 5, 6 consist of published/submitted papers that addresses the 3 main objectives of this work. Chapter 7 and 8 respectively elaborates a general discussion and conclusion of the entire thesis.

CHAPTER 2 LITERATURE REVIEW

To date, very interesting reviews of seizure prediction have been published [33, 49], but none has been specifically dedicated to classification methods in an algorithmic seizure prediction framework. We start by presenting basic conventions and considerations for reliable seizure prediction. Various seizure prediction approaches adopted by the epilepsy research community are discussed while paying special attention to algorithmic studies because of their applicability in seizure advisory/intervention implantable devices. The basics, history, and advancements in algorithmic studies are detailed in a block-by-block fashion. We have reviewed state-of-the-art achievements in each block, highlighting signal processing methods that have contributed to progress and yielded realistic evidence in the field. Several acquisition modalities are covered, focusing on intracranial (iEEG) and/or scalp EEG recordings. The algorithmic studies reviewed are based on personal and international databases as well as long-term recordings with ambulatory devices. Feature extraction covers linear and nonlinear methods with both univariate and multivariate approaches. Prominent feature selection techniques, classifiers as well as regularization functions are compared. The discussion section emphasizes current issues and required considerations with analyses of the progress made in each block.

2.1 State-of-the-art

2.1.1 Basic conventions in seizure prediction studies

Seizure detection employs algorithms that aim to detect seizure onset. Seizure prediction looks at the possibility of forecasting seizure occurrence and is therefore intended for fulfillment much earlier than detection. This review focuses solely on algorithmic seizure prediction studies. Published works were selected to cover different signal processing strategies proposed in a seizure forecasting framework. When several studies using similar processing approaches were found, only those adhering to the recommendation for reliable seizure prediction were selected [33]. Studies proposing novel methods, but not adhering to the reliable forecasting recommendations, were discussed, highlighting potential pitfalls. Numerous investigations have demonstrated gradual transition between interictal (in-between) and ictal (during) seizure states, known as the preictal state [49]. Thus, seizure prediction can be considered as early detection of the preictal state. Some recent studies have added the notion of intervention time (IT) or seizure horizon [38]. IT, assumed to lie between the end of the preictal period and seizure onset, should

ensure enough time for intervention and help to distinguish seizure prediction from simple seizure detection.

2.1.2 Different approaches to seizure prediction

Seizure prediction is an active research topic dating back to the 1970s. In a detailed review on the predictability of epileptic seizures, Mormann et al. [33] presented a chronological overview of seizure prediction studies and their findings. Early approaches searched for precursors from scalp EEG with linear methods, such as autoregressive modeling [61, 62]. Then, studies suggesting the possibility of preictal phenomena started emerging. The latter – generally based on nonlinear dynamics [63] – were, however, limited to investigations of the preictal state, without taking the normal brain state into account. They were followed by proof-of-principle and controlled studies on predictability that tackled the issue of specificity by making comparisons between preictal and interictal states. Although these early findings were optimistic, the absence of statistical validation and reproducibility was a major constraint in the development of clinical devices. They led to a phase that Mormann et al. [33] called "the rise of skepticism", during which studies based on extensive databases revealed poorer performance than earlier ones. It highlighted the need for statistical validation and long-term multi-day EEG recordings made possible at the turn of the millennium due to booming mass storage capability. Current seizure prediction approaches can be grouped into 2 main categories: analytical/statistical and algorithmic. Since the main goal of prediction studies is seizure control, it can be achieved by implementing algorithms able to track the preictal state. Accurate seizure-prediction algorithms may open possibilities for on-demand, EEG-triggered interventions once the preictal state is detected. Below, we review algorithm-based studies in a methodological manner, discussing each component of the whole block diagram.

2.1.3 Algorithmic-based studies

These studies, which implement algorithms to detect the preictal state based on EEG recordings, typically start by preprocessing EEG signals to enhance their quality, extract different features able to display preictal state dynamics, and then select the most discriminative ones as inputs to the classifier. Most seizure prediction algorithms have a regularization function as a postprocessing step to smooth classifier output. Performance of the algorithm is then evaluated (Figure 2.1).

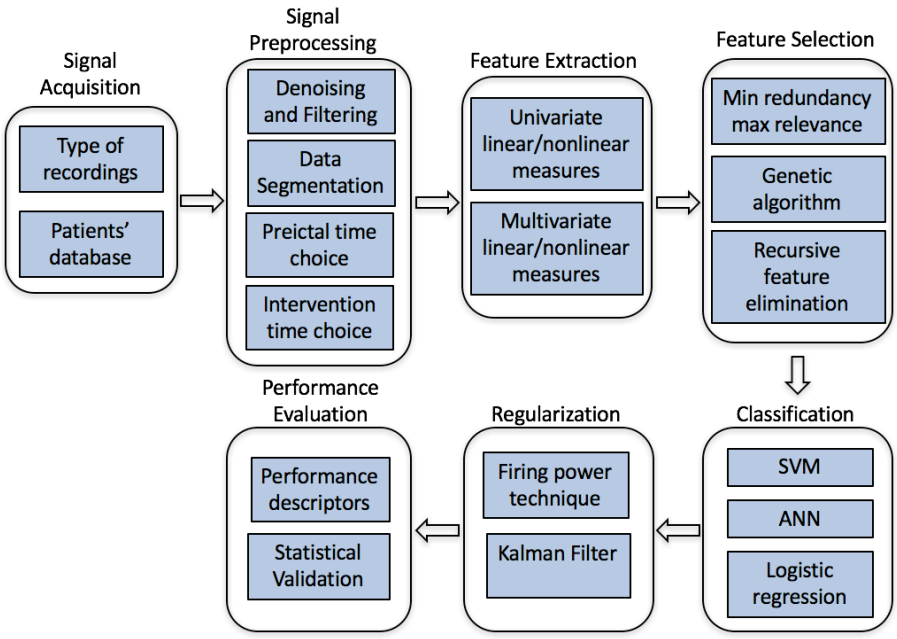

Figure 2.1 Typical block diagram of algorithmic-based studies

2.1.3.1 Signal acquisition

2.1.3.1.1 Recording type: scalp EEG vs iEEG

Both scalp and iEEG recordings have been considered in seizure prediction studies. Scalp EEG captures brain activity with equally-spaced surface electrodes glued to the skin while iEEG involves intracranial electrodes positioned in areas of suspected epileptogenicity identified from available clinical, structural and functional data collected prior to implantation [64]. Several studies have explored the utility of scalp recordings for seizure prediction [33]. For example, Teixeira et al. [65] compared the performance of a subject-specific algorithm on scalp EEG, iEEG and mixed scalp and iEEG recordings. Performance values were slightly better in terms of sensitivity and false prediction rate (FPR) with scalp EEG (sensitivity=73.55%±24.83%; FPR=0.28 h^{-1}±0.28 h^{-1}) than intracranial recordings (sensitivity=67.66%±21.83%; FPR=0.39 h^{-1}±0.37 h^{-1}). However, when comparing statistical significance of the results with the Kruskal-Wallis (K-W) test (p=0.01), these differences were found to be nonsignificant. Rasekhi et al. [66] tested the preprocessing effects of 22 linear univariate features on the performance of seizure-prediction methods and concluded that scalp EEG (sensitivity=76.67%, FPR=0.08 h^{-1}) fared better than iEEG recordings (sensitivity=68.7%, FPR=0.33 h^{-1}). Their work was, however, limited by the small number of subjects and lacked statistical validation.

Table 2.1 Recent studies comparing scalp and iEEG performances

Authors	Year	Recording type	Number of patients	Sensitivity (%)	FPR (h^{-1})	Statistical testing
Bandarabadi et al. [45]	2015	Scalp	16	73.98	0.06	None*
		iEEG	8	78.36	0.15	None*
Teixeira et al. [65]	2014	Scalp	227	73.5±24.83	0.28±0.28	K-W
		iEEG	42	67.66±21.83	0.39±0.37	K-W
Rasekhi et al. [66]	2013	Scalp	8	76.67	0.08	None
		iEEG	2	68.7	0.33	None

*No statistical testing was undertaken to compare scalp and iEEG recordings

In a recent study of spectral power quantification between 2 spectral bands of 2 channels, Bandarabadi et al. [45] reported comparative performance of scalp (sensitivity=73.98%; FPR=0.06 h^{-1}) and iEEG (sensitivity=78.36%; FPR=0.15 h^{-1}) recordings. Higher FPR values were attributed to the fact that more features were selected in the case of scalp EEG compared to iEEG signals (11.5 vs. 6.6 on average). Hence, the performance of seizure prediction algorithms on scalp EEG electrode recordings (obtained within the confines of a supervised epilepsy monitoring unit) would appear to be just as good as or superior to iEEG recordings, probably because the former can provide information on general brain state rather than localized information. It must be remembered, however, that on a practical level, iEEG recordings are more suitable for chronic intervention devices, as continuous surface EEG recordings during daily activities are impractical and fraught with artifacts. Table 2.1 summarizes the findings of recent seizure-prediction studies comparing scalp and iEEG performances.

2.1.3.1.2 Patient database

Early studies were based on local databases acquired from patients undergoing evaluation for epilepsy surgery. These investigations were limited to the analysis of short periods prior to seizures, small numbers of patients and limited amounts of ictal events, which restricted the possibility of assessing algorithm specificity over the interictal period. Schulze-Bonhage et al. (2011) [67] used the nonparametric correlation coefficients of Kendall's tau [68] and found statistically significant correlations in the sensitivity of seizure prediction systems with number of seizures and average recording duration. They raised the need for long-term recordings containing a higher number of seizures and allowing reliable estimation of algorithm sensitivity and specificity, ideally in prospective testing [67].

Table 2.2 Web-based seizure-prediction databases

Database	Number of subjects	Number of seizures	Type of recordings	Total hours of EEG recordings (h)	Sampling frequency (Hz)
Flint Hills	10	59	iEEG	1,419	239.74
Boston	23[p]	198	Scalp	940	256
Freiburg	21	88	iEEG	708	256
European Epilepsy Database	250	2,400	Scalp and/or iEEG	More than 40,000	250-2,500

p: the database includes recordings from pediatric patients

Several web-based databases have emerged in recent years, such as those from the University of Bonn, the University of Freiburg and Boston Children's Hospital. European Database on Epilepsy [69] is the largest currently-available seizure prediction database, containing 2,500 seizures and 45,000 h of EEG recordings acquired from more than 250 patients, 50 of whom underwent iEEG with up to 122 channels sampled at 250-2,500 Hz. Table 2.2 lists the sizes and specifications of web-based seizure prediction databases in terms of subject and seizure numbers, EEG recording type and duration as well as sampling frequency. Apart from such databases of EEG signals acquired in epilepsy-monitoring units, recent studies [38, 70, 71] have started adopting signals provided by the NeuroVista ambulatory monitoring system which allows continuous iEEG data over months, albeit from a small number of contacts [41]. Cook et al. [70] prospectively assessed the performance and safety of a seizure advisory system in 15 NeuroVista-implanted patients. It would be highly valuable to the seizure prediction community should such long iEEG recordings of naturally-occurring seizures become available in the future. Deploying the same device, Howbert et al. [38] evaluated the feasibility of seizure prediction in 3 dogs with naturally-occurring focal epilepsy. Fortunately, the data from their study are freely available on the iEEG portal (https://www.ieeg.org/).

2.1.3.2 Signal Preprocessing

This step is usually employed in any EEG analysis and attempts to remove artifacts, increase signal-to-noise ratio, and prepare signals for adequate feature extraction

2.1.3.2.1 Denoising and filtering

Since seizure-prediction algorithms are still in their exploratory, proof-of-principle stage, major approaches cover band-pass filtering of recorded signals into frequency ranges of interest

as well as removing bad segments identified by visual inspection [72]. Temporal filtering with digital filters, such as Infinite impulse response (IIR) and Finite impulse response (FIR) filters, has been mainly undertaken for seizure prediction [59, 73]. Since FIR filters induce a linear phase response, zero phase filtering is performed by applying them to the signal, inverting it in time, reapplying the FIR filters and then inverting the signal back [59, 74]. This results in zero phase distortion [75]. On the other hand, IIR filters have demonstrated good and uniform acceptance in EEG frequency of interest with quasi-no ripples in stop- and pass-bands [73]. Park et al. [72] explored the impact of spatial (bipolar) and/or time-differential methods on seizure prediction performance. They concluded that both approaches improved the sensitivity and specificity of seizure prediction with better results after spatial preprocessing. Bandarabadi et al. [46] found that space differential preprocessing decreases the discriminability between preictal and interictal classes in iEEG recordings.

2.1.3.2.2 Data segmentation

To extract features from preprocessed EEG recordings, they should be segmented into smaller windows assumed to have similar characteristics meaningful to EEG analysis. The duration of these windows in the context of EEG analysis in epilepsy has varied from 5 to 60 s. Park et al. [72] adopted moving window analysis engaging a 20-s window with half overlap. Others decided on a 5-s window with no overlap [45, 59, 65, 66]. Such a relatively short window is considered to be a compromise between the ability to capture specific patterns and stationarity assumptions. Howbert et al. [38] tested a segment of 1 min with no overlap in a study investigating the feasibility of seizure prediction in dogs with naturally-occurring epilepsy. Moghim and Come [43] adopted a 5-s window for EEG signal segmentation, then averaged features over long-term (180-s) and short-term (9-s) segments. These authors concluded that long-term outperformed short-term features.

2.1.3.2.3 Preictal time choice

Although early investigations into the feasibility of seizure forecasting date back more than 25 years, no standard or optimal preictal time slot has yet been defined. The American Epilepsy Society's seizure prediction challenge (https://www.kaggle.com/c/seizure-prediction) adopted a preictal time of 1 h prior to seizures, with a fixed intervention time of 5 min. Some studies have chosen fixed preictal times, such as 2 min [76], 20 min [77], 30 min [72], and 90 min [38], while

others have considered several different preictal times. In an extensive study, Teixeira et al. [65] tested 4 different preictal times (10, 20, 30, and 40 min) and observed no significant differences in terms of sensitivity, but longer preictal time was found to significantly reduce FPR. These authors concluded that preictal time of 30.47 min was the most appropriate average value, leading to a patient-specific best predictor. Because a firing power technique was included for regularization in their study, which structurally decreased FPR levels when longer preictal times were used, care should be taken before generalizing the results to studies using other regularization methods. Bandarabadi et al. [45] tested the same 4 preictal times and reported an optimal average of 33.7 min. In a study comparing 30 different features, Mormann et al. [47] adopted 4 different preictal times based on prior literature: 5, 30, 120 and 240 min. Recently, Bandarabadi et al. [46] searched for the optimal preictal time using a statistical measure based on amplitude distribution histogram (ADH). They varied preictal periods from 5 to 180 min prior to electrographic seizure onset and chose the one maximizing the discriminability between interictal and preictal periods. Interestingly, optimal preictal time was found to significantly vary between seizures even for the same subject. They reported an average of 44.3 min with optimal values ranging from 5 to 173 min. Conversely, Moghim and Come [43] proposed a preictal time-varying algorithm called Advanced Seizure Prediction via Pre-Ictal Relabeling. Preictal time was varied from 0 to 20 min prior to seizure with seizure occurrence period (SOP) fixed at 5 min. These authors started by fixing a 5-min window that ended at seizure onset. This window corresponds to the t=0 predictive model. Then, with a 1-min step, the window was moved far from seizure onset until t=20 min. The algorithm can be reformulated as starting from 0 until 20 min intervention time with steps of 1 min and constant SOP of 5 min. The authors [43] evaluated performance of the proposed algorithm by S1 score (harmonic mean of sensitivity and specificity) and claimed performance superiority of the predictive model corresponding to t=1 min. Although optimal preictal time was not declared, it can be assumed to be 6 min. When comparing performance variations across patients among all predictive models, those corresponding to t=0 (seizure prediction between 0 and 5 min in advance) or t=14 min (seizure prediction between 14 and 19 min in advance) were the most reliable. Considering that each study uses a different algorithmic strategy, performance comparison is not reliable at this stage. However, it is clear that no preictal time can be considered optimal or standard.

2.1.3.2.4 Intervention time choice

The study by Moghim and Come [43] gave optimistic results. The performance superiority of predictive models (t=1 min) and (t=14 min) ensures that, although not adopted in early studies, relatively longer intervention times may be investigated for seizure prediction. In contrast, using an Ngram-derived seizure prediction method Eftekhar et al. [78] analyzed three ITs (10, 20, and 30 min) with a SOP of 10 min and found that shorter ITs (10 min) resulted in increased sensitivity. Schelter et al. [79] reported sensitivity as function of IT. Investigated ITs ranged between 2 and 40 min while FPR and SOP were fixed to 0.15 FP/h and 10 min respectively. Although this study included only the first 4 patients of the Freiburg seizure prediction database, interesting results were reported. Findings revealed a patient specific pattern of the SPH resulting in above chance performances when choosing adequate ITs (patients 1 and 4). A significant prediction performance was observed in ITs within 4-12 min and 18-24 min for patients 1 and 4, respectively. No specific conclusions could be deduced from patients 2 and 3 whose sensitivities did not beat those achieved by an unspecific predictor but, in general, lower ITs increased sensitivity results. It is highly recommended that these interesting findings be validated on a larger dataset. In an attempt to use a uniform set of parameters across all patients, the same group [80] adopted a fixed IT of 2 min achieving average sensitivities of 82% and 89% using the dynamic similarity index and the mean phase coherence, respectively. Similarly, recent seizure prediction studies adopting a fixed intervention time of 5 min have reported promising performances [38, 71]. Such classification strategies would allow more intervention time with chronic implantable devices.

2.1.3.3 Feature extraction

An extensive list of features has been proposed [33], and EPILAB is a MATLAB toolbox for computing the main features used in seizure prediction [73]. Some features are based on univariate measures while others include information extracted from a combination of multiple channels and are called multivariate. Features have been also classified as linear and nonlinear [33]. Mormann et al. [33] presented an extensive review of features, along with their mathematical formulation, used in seizure forecasting studies until 2007. In what follows, we will limit ourselves to most prominent characterizing measures while reviewing recent proposed methodologies in each subsection. No specific type of features has been validated as the best, but Mormann et al. [47] reported that combining multivariate and univariate features results in better

predictive systems. In an extensive study supported by statistical validation and performance assessment, Mormann et al. [47] compared 30 bivariate and univariate features found in the literature. Bivariate measures exhibited higher statistical significance with constant baseline and were able to reveal preictal changes at least 240 min before seizures. On the other hand, preictal characteristics were found 5-30 min before seizures with univariate measures. An interesting outcome in this study was that linear features performed almost equally and sometimes even better than nonlinear ones. This finding was validated by Harrison et al. [81] who showed that when tested on long-term EEG recordings, the most promising nonlinear features were not predictive at all. McSharry et al. [82] established that nonlinear measures (correlation density) did not increase forecasting performance. They explained that the nonlinear nature of a signal does not necessarily require complicated nonlinear measures [33, 82]. Park et al. [72] assessed the linear features of spectral power, and explained the limitations of nonlinear measures in terms of computational intensiveness along with the difficulty in using them in real-time algorithms embedded in chronic-intervention, implantable devices. As addressed by McSharry et al. [82], the use of nonlinear measures can only be justified if they outperform linear features.

2.1.3.3.1 Univariate linear measures

Statistical measures, such as variance, skewness and kurtosis, have been adopted in several seizure prediction studies. Aarabi et al. [83] reported increased kurtosis and decreased variance during the preictal state. In addition, spectral band power features have been shown to be effective in EEG signal classification and have been considered extensively in seizure prediction. Five standard frequency bands have been defined in classical EEG analysis: delta (0.5-4 Hz), theta (4-8 Hz), alpha (8-13 Hz), beta (13-30 Hz) and gamma (30-128 Hz). Mormann et al. [47] reported power transfer from low to high frequencies during the preictal state. Since EEG signals contain much more power in the low-frequency range, a normalization procedure is usually preferred [45, 72]. It consists of computing relative spectral power by dividing the power in each of these frequency bands by the total power of the signal. Compared to other frequency bands, gamma band features have demonstrated their suitability for seizure prediction [59, 72]. Netoff et al. [84] suggested splitting the wide gamma band into 4 sub-bands (30-47, 53-75, 75-97, 103-128 Hz). This particular splitting excludes powerline interference from the data, enhancing the discriminatory power of features. Hjorth mobility (HM) and Hjorth complexity (HC) have been shown to increase during the preictal state [47]. In a comparative study of 30 features, Mormann

et al. [47] evaluated the performance of measures for which changes occur constantly on a similar level and on the same channel(s) across all seizures. HM and HC were found to be the best univariate performers. Furthermore, since power in an EEG signal dominates below 40 Hz, spectral edge power has been proposed as the lowest frequency up to which half of total power is contained in a signal. It is considered to be a characterizing measure of signal power distribution [85]. Decorrelation time, defined as first zero crossing of the autocorrelation function, has been reported to decrease prior to seizures [47, 73]. Moghim and Come [43] computed accumulated energy by summing the successive values of energy from a series of time-moving windows and ascertained that long-term energy (180 s) outperformed short-term energy (9 s) features. Although signal energy has been successfully employed in some seizure prediction studies, Mormann et al. [47] noted that it was unable to discriminate between preictal and interictal states above chance levels. In several seizure prediction studies, EEG signals were modeled as an autoregressive (AR), moving average model, and several parameters that described its evolution, such as prediction error, served as features. It was stated that EEG signals are more likely to be predicted by an AR model during the preictal period and thus prediction error decreases [73]. Direito et al. [58] discerned that AR model predictive error was the best predictor in patients exhibiting the highest performance values. However, no statistical validation was undertaken. Gadhoumi et al. 2013 [86] demonstrated the ability of wavelets' energy to achieve above-chance prediction performances in 7 of 17 patients with medial temporal lobe epilepsy. Table 2.3 reports univariate features employed in seizure prediction.

2.1.3.3.2 Univariate nonlinear measures

Based on the fact that the brain passes through several dynamic states, a set of nonlinear features derived from the dynamic systems' theory has been proposed, such as correlation dimension [87], largest Lyapunov exponent [63], and dynamic similarity index [77]. Mormann et al. [47] observed an increase in correlation dimension prior to seizure onset, while Lehnertz and Elger [87] reported a decrease 5-25 min prior to seizure onset. Largest Lyapunov (L_{max}) exponent quantifies the convergence of nearby state-space trajectories. Although the first investigations revealed a decrease in L_{max} several minutes before seizures [63], the contradictory results obtained indicate an increase 30 min prior to seizure onset [47].

Table 2.3 Prominent univariate features used in algorithmic seizure prediction studies

Authors	Year	Dataset	Measure	Type	Preictal time (min)	Patients	Type of recordings	SS (%)	SP (%)/ FPR (h^{-1})	Statistical validation
Howbert et al. [38]	2014	Melbourne (ambulatory)	Spectral power	Linear	90	3[γ]	iEEG	78.6[a] %	0.08[a] h^{-1}	Comparison with poisson-process predictor
Teixiera et al. [65]	2014	EPILEPSIAE	Decorrelation time	Linear	10, 20, 30, 40	278	Scalp	73.55 ± 24.83 %	0.28 ± 0.28 h^{-1}	Kruskal-Wallis test of significance
			Energy							
			HM and HC							
			Relative power							
			Statistics							
			SEP and SEF				iEEG	67.66 ± 21.83 %	0.39 ± 0.37 h^{-1}	
			AR model error							
			Wavelets energy							
Gadhoumi et al. [86]	2013	Personal	Wavelets energy and entropy	Linear	6.3-22[δ]	18	17	85%	0.35 h^{-1}	Comparison with random predictor
Park et al. [72]	2011	FSPEEG	Relative spectral power	Linear	30	18	iEEG	97.5 %	0.27 h^{-1}	No
Netoff et al. [84]	2009	FSPEEG	Relative spectral power	Linear	5	9	iEEG	77.78 %	0 h^{-1}	No
Mormann et al. [47]	2005	Personal	Energy	Linear	5, 30, 120, 240	5	iEEG	67.66 ± 21.83 %	0.39 ± 0.37 h^{-1}	Seizure time surrogates
			HM and HC							
			Relative power							
			Statistics							
			SEP and SEF							
			AR model error	Non-linear						
			Wavelets energy							
			Local flow							
			Algorithmic complexity							
			Loss of recurrence							
Moghim and Come [43]	2014	FSPEEG	Signal energy	Linear	variable	21	iEEG	91.14 %	99.55 %	Comparison with random and baseline predictors
			DWT							
			Correlation dimension	Non-linear						
			Lyapunov exponent							
C. Alvarado- Rojas et al. [88]	2014	EPILEPSIAE	Phase amplitude CFC	Non-linear	60	53	iEEG	66* %	0.33* h^{-1}	Comparison with random predictor
Sackellares et al. [89]	2006	Personal	Largest Lyapunov exponent	Non-linear	30	10	iEEG	80-100[§] %	0.56-0.71 h^{-1}	Comparison to periodic and random naïve predictors
					60				0.27-1.4 h^{-1}	
					90				0.19-0.29 h^{-1}	
					120				0.15-0.24 h^{-1}	
					150				0.12-0.18 h^{-1}	
					180				0.10-0.16 h^{-1}	
Winterhalder et al. [90]	2003	Personal	Similarity index	Non-linear	30	21	iEEG	42 %	0.15 h^{-1}	No
Aschenbrenner-Scheibe et al. [91]	2003	FSPEEG	Correlation dimension	Non-linear	10, 20, 50	21	iEEG	8.3-38.3 %[6]	0.1	No
Lehnertz et al. [87]	2001	Personal	Correlation dimension	Non-linear	n.m.	59	iEEG	47 %	0 h^{-1}	No
Le Van Quyen et al. [77]	1999	Personal	Dynamic similarity index	Non-linear	20	13	iEEG	n.m.	n.m.	No

SS: sensitivity; SP: specificity; FPR: False Prediction Rate; FSPEEG: Freiburg seizure prediction EEG database; [γ]: the study involves 3 dogs implanted with the NeuroVista ambulatory monitoring device; [a]: average across 3 dogs; n.m.: not mentioned; [δ]:actual duration of preictal period varied depending on the availability of continuous preictal data; [6]: depends on length of prediction window; [§]: sensitivity was fixed at 80 and 100% while FPR was reported; * average across 7 patients with statistical significant results

A comparative study of 30 linear and nonlinear features by Mormann et al. [47] found that univariate nonlinear measures (correlation dimension, Lyapunov exponent) were unable to significantly perform better than chance. Le Van Quyen et al. [77] proposed the dynamic similarity index as a measure of similarity between reference and moving test windows. However, by the turn of the millennium, the reliability of initial optimistic results was questioned by Winterhalder et al. [90] and Aschenbrenner-Scheibe et al. [91]. Other nonlinear univariate measures, such as correlation entropy [92], marginal predictability [93], state space dissimilarity, local flow and algorithmic complexity, have been proposed, but lack of reproducibility limited their use in future studies [33]. Recently, motivated by the fact that human iEEG studies have identified spatially-distributed modulation of cortical high frequency oscillations in the gamma band by theta oscillations and slow waves, recent studies have adopted slow modulation of high-frequency gamma activity as a measure of brain excitability [88]. Interaction between the phases of low frequency bands and the amplitudes of gamma sub-bands was quantified by measuring mean coupling phases. Interestingly, prospective testing disclosed above chance preictal changes in 13.2% of patients. The proposed method demonstrated performance superiority (sensitivity and specificity) compared to predictions based on relative power in traditional frequency bands.

2.1.3.3.3 Bivariate linear measures

With increasing insights into the mechanisms and functional connectivity of epileptic networks, bivariate approaches studying synchronization between brain regions have been reported to be efficient in tracking the preictal state. Table 2.4 summarizes prominent bivariate features used in seizure prediction studies. The main goal of using these features is to investigate how interaction between several brain regions modulates epileptic seizure activity. As a measure of lag synchronization, the maximum of normalized cross-correlation served to quantify the similarity of 2 time series x_i and y_i [94] and has been employed in seizure prediction [47]. A comparative study of bivariate features found maximum cross-correlation to be one of the most discriminative bivariate measures [47]. Recently, Bandarabadi et al. [45] extended the use of spectral power to a bivariate approach. With normalized power in each of the standard EEG bands, the proposed feature quantifies cross-power information between 2 different frequency bands and channels.

Table 2.4 Prominent bivariate features used in algorithmic seizure prediction studies

Authors	Year	Dataset	Measure	Type	Preictal time (min)	Patients	Type of recordings	SS (%)	FPR (h^{-1})	Statistical validation
Bandarabadi et al. [45]	2015	EPILPESIAE	Bivariate spectral band power	Linear	10,20,30,40	24	iEEG or scalp	75.8	0.1	Comparison with random predictor
Mormann et al. [95]	2003	Personal	Cross-correlation		240	10	iEEG	86	0	Surrogate data testing
Mormann et al. [47]	2005	Personal	Max cross-correlation		5, 30, 120, 240	5	iEEG	n.m.	n.m.	Seizure time surrogates
			Mean phase coherence*	Non-linear						
			Conditional probability*							
			Shannon entropy*							
			Measures for non-linear independence							
Mirowski et al. [96]	2009	FSPEEG	Wavelet synchrony		120	15	iEEG	71	0	Seizure time surrogates
Winterhalder et al. [97]	2006	FSPEEG	Mean phase coherence Lag synchronization index		30	21	iEEG	60	0.15	Comparison with random predictor
Iasemidis et al. [98]	2005	Personal	Dynamic entrainment		120	2	iEEG	82	0.15	No
Le Van Quyen et al. [99]	2005	Personal	Phase locking value		Variable	5	iEEG	70	n.m	No
Mormann et al. [52]	2003	Personal	Mean phase coherence		240	18	iEEG	81	0	No

SS: sensitivity; FPR: False Prediction Rate; n.m.: not mentioned; FSPEEG: Freiburg seizure prediction EEG database; *: applied to phase variables based on both the Hilbert Transform and Wavelet Transform

These authors tested the proposed bivariate feature as well as traditional spectral power as inputs to a feature-selection method based on maximum difference of amplitude distribution histograms (mDAD) and concluded that bivariate spectral power was selected as the best in 90% of cases.

2.1.3.3.4 Bivariate nonlinear features

Bivariate nonlinear measures have also been deployed in seizure prediction and show good predictive performances [33]. Measures based on mutual information and similarity between channels have been studied to characterize synchrony level between EEG channels [100]. Iasemidis et al. [98] proposed dynamic entrainment, a multichannel version of the Lyapunov exponent, and demonstrated good predictive power with relatively low FPR. Le Van Quyen et al. [99] evaluated the suitability of phase-locking values for all pairs of EEG channels placed over the temporal lobe, with sliding window analysis on 15 frequency bands performed over the entire dataset. These authors stated that a specific state of synchronization could be observed in 70% of cases during a relatively long preictal time of several hours. No general trend of synchronization was evident, but changes were most often localized in the primary epileptogenic zone and occurred within the 4-15 Hz frequency band. Mormann et al. [52] studied mean phase coherence

(MPC) and reported a drop in synchronization during the preictal state. This same group [95] compared MPC and maximum linear cross-correlation in a follow-up investigation. They saw similar performance with both synchronization methods in terms of predictive power as well as anticipation times. Similarly, Winterhalder et al. [97] studied short-term changes of increasing and decreasing synchronization during the preictal state via MPC and the lag synchronization index. Unlike those of Mormann et al. to [52], their results revealed non-uniform changes in synchronization. They stated that evaluating increasing as well as decreasing synchronization may yield significant prediction performance. These results are concordant with those reported in [47]. They suggest that such measures perform better than a random predictor with both increased and decreased synchronization during the preictal state. Mirowski et al. 2009 [96] evaluated combinations of different bivariate features and machine-learning approaches and found wavelets synchrony with convolutional networks as the most successful prediction scheme. The proposed methodology allowed achieving 71% sensitivity and 0 false alarms in 15 patients. In addition, indexes based on conditional probability and Shannon entropy have been proposed [101] as measures of phase synchronization [47]. Mormann et al. [47] compared 8 different bivariate nonlinear features [47] and found MPC, the Shanon entropy index, and the conditional probability index to be the best nonlinear bivariate measures.

2.1.3.4 Feature selection

Since transition from the interictal to the ictal state consists of complex mechanisms, prediction algorithms usually combine several features in an attempt to cover brain dynamics. This results in high dimensional feature spaces. It is thus crucial to select the most discriminative features that will best contribute to identification of the preictal state. Some may be redundant while others can be confounding and degrade classifier performance. Several feature selection methods have been used in seizure prediction studies, such as ReliefF [43], minimum normalized difference of percentiles [102], mDAD [102], forward selection [38], minimum redundancy maximum relevance (mRMR) [59, 103], and genetic algorithm (GA) [58, 59]. We will discuss the latter 2 methods in this review because of their extensive citation. Table 2.5 summarizes prominent feature selection and classification methods used in seizure prediction studies.

Table 2.5 Prominent feature selection and classification methods used in algorithmic seizure prediction studies

Authors	Year	Feature type	Selection method	Initial set	Red. set	Classifier	Classifier type	SS (%)	SP (%)/ FPR (h^{-1})	Stat. valid
Bandarabadi et al. [102]	2012	Bivariate linear	mRMR	435	9.1	Binary SVM (RBF kernel)	Non-linear	60.87 %	0.11 h^{-1}	No
			mDAD		8.75			76.09 %	0.15 h^{-1}	
Bou Assi et al. [59]	2015	Univariate linear	mRMR	224	28			86.07 %	79.13 %	No
			GA		44.2			87.09 %	85.71%	
			mRMR & GA		5			90.28 %	88.53 %	
Direito et al. [58]	2011	Univariate linear	mRMR	200.44	132			42.56 * %	73.44 * %	No
			GA					47.89 * %	81.59 * %	
Moghim and Come [43]	2014	Univariate linear and non-linear	ReliefF	204	14	Multi-class SVM (RBF kernel)		91.14 %	99.55 %	Yes
Teixeira et al. [65]	2014	Univariate linear	-	132	-			73.73 %	0.19 h^{-1}	Yes
						MLP ANN		74.17 %	0.29 h^{-1}	
						RBF ANN		69.14 %	0.42 h^{-1}	
Bou Assi et al. [59]	2015	Univariate linear	GA	224	44.2	ANFIS		82.0 %	77.6 %	No
Rabbi et al. [104]	2013	Univariate and bivariate non-linear	-	4	-			80 [6] %	0.46 [6] h^{-1}	No
Mirowski et al. [96]	2009	Bivariate non-linear	Lasso algorithm	6300[§]	Variable	CNN		71.0 %	0 h^{-1}	Yes
Howbert et al. [38]	2014	Univariate linear	Forward selection	96	10	Logistic regression	Linear	78.66 %	0.08 h^{-1}	Yes

SS: sensitivity; SP: specificity; FPR: False Prediction Rate; *: Average calculated over 3 subjects; 6: sensitivity at specificity reported for a preictal time of 45 min; §: patterns of bivariate features containing 60 consecutive frames (5 min) of 105 simultaneous features.

The mRMR algorithm ranks features by criteria of maximum relevance and minimum redundancy, defined in terms of cost function. While mutual information is one of the most common cost functions [45, 59, 103], several metrics have been proposed, all having the same principle and relying on criteria of similarity. In [58], the mRMR cost function was based on statistical F-testing as a measure of relevance and Pearson's correlation as a measure of redundancy and used to reduce feature dimensions from 4,410 to the first 132 ranked features. Bandarabadi et al. [102] employed the mRMR method based on a mutual information criterion to decrease feature dimensions from 435 to an average of 9.1 features. Recently, our group [59] also adopted the mRMR paradigm combined with a GA for optimal selection of electrode-feature combinations, allowing the selection of the first 28 ranked features out of 224 electrode-feature combinations. Although the number of features was reduced from 224 to 28, predictor performances were comparable using a support vector machine (SVM) with a radial basis function (RBF) kernel. Mean sensitivity was 86.07% and specificity was 79.13% after mRMR compared to mean sensitivity of 84.49% and specificity of 80.11% with the entire feature set.

GAs tend to replicate the principles of biological evolution. Starting from an initial, random population, the strongest recombine to survive and adapt to their external environment. Inspired

by natural evolution, GAs generate solutions to optimization problems based on mutation, crossover, inheritance and selection. Several GA types in terms of selection method, genetic structure, and fitness function have been tested in seizure-prediction studies. In [58], genetic structure is a binary string that includes features as well as classifier hyper-parameters. An Elitist Non-dominated Sorting-based GA was included for the selection stage. Ataee et al. [105] proposed a GA-based method that optimizes selection of the best feature vector as well as its optimal window length. GA fitness function was based on Fisher Discriminant Ratio. These authors stated that window length and feature vector should be chosen simultaneously. However, it is not clear if out-of-sample testing was performed in this study. In [59], genetic structure was a binary string in which each feature was a binary number. The fitness function was classification loss according to a K-Nearest-Neighbor classifier. It is important to mention that since GA is an iterative procedure that aims to find an optimal combination of features, the size of the selected subset is not fixed and may vary. Our group [59] showed that, after GA feature selection, reducing their number from an average of 221.2 to 44.2 features, the selected subset of features (SS=87.09%; SP=85.71%) outperformed the whole set (SS=85.49%; SP=80.11%) in terms of sensitivity and specificity. Direito et al. [58], who conducted a comparative study of mRMR, GA, and Recursive feature elimination, concluded that dimensionality reduction improved predictor performance but that the best selection method was patient-specific. As in [58], the optimal selection method was subject-specific with mRMR and GA combination always achieving the best performance. It is noteworthy that ranking selection methods is limited by the requirement of fixing the size of the selected subset of features. Five different sizes of feature subsets were assessed in [102]: 3, 5, 10, 20 and 40. The authors stated that the best size was selected in such a way that performance was close to an optimal predictor (SS=100%; SP= 0 FP/h) in a patient-specific manner. The mean number of selected features was 8.75. Unfortunately, it was not reported if such optimization was performed on the training sample or on the whole set. Selection on the whole set may give overoptimistic results. Direito et al. [58] fixed the number selected at the first 132 highly-ranked features, but it was not clear why they chose this number. Moghim and Come [43] fixed the number of selected features at 14, stating that it would facilitate the benchmarking results of a previous study [106]. In [59], our group fixed the number of electrodes at 2 per feature, then tested a GA to select combination of the most discriminative features. The advantage of a GA is that it does not require fixing the size of the selected feature

subset. Feature selection was only performed on the training set. An average number of 5 features was selected when combining mRMR with GA and rose to 44.2 with the GA only. Interestingly, reducing the number of features to 5 (SS: 90.28%; SP: 88.53%) increased predictor performance with an SVM.

2.1.3.5 Classification

Based on the features selected, a prediction scheme that detects preictal changes should be implemented. Two main approaches have been proposed and they form the core of algorithmic seizure prediction studies [73]. The first is threshold-based while the second involves machine-learning techniques to detect the preictal state. In what follows, we focus on prominent classifiers in seizure prediction.

2.1.3.5.1 Support vector machines

SVMs, currently the most popular approach in supervised machine-learning, have been adopted in a large number of seizure-prediction studies in their binary form [45, 59, 72] and extrapolated to multi-class form [65]. An SVM is a margin classifier that implements a separating hyper-plane that maximizes the distance between the nearest training points. Two hyper-parameters need to be defined with such a decision boundary: cost and cost factor. Optimal pairing of these parameters can be achieved with cross validation [72] or grid search [43, 45, 65]. One of the problems facing machine-learning techniques in seizure prediction studies is the imbalance between preictal and non-preictal samples. Obviously, the number of non-preictal samples is much larger than the number of preictal samples, and classifiers usually tend to be more accurate over the class with the greater number of training samples [107]. Several approaches have been taken to address this issue, such as reducing the number of interictal samples by resampling, resulting in a balanced number of samples between the 2 classes [45, 65]. Park et al. [72] deployed cost-sensitive support vector machines to handle imbalances in sample numbers. This type of SVM is implemented by setting higher misclassification penalties on preictal data than on non-preictal data. SVMs have proved to outperform other types of classifiers in terms of sensitivity and specificity. In a study of 278 patients from the European Epilepsy Database, Teixeira et al. [65] compared the performance of 3 classifier types: an SVM, an artificial neural network (ANN) with a multilayer perceptron (MLP) structure and an ANN with a RBF structure. Interestingly, considering different processing possibilities, this comparison included 224,928

different classifier structures. These authors found that performance of the prediction algorithm significantly depended on classifier type (K-W test, $p<0.01$) with better SVM performance in terms of FPR. Our group [59] also discerned performance superiority with a SVM compared to an Adaptive Neuro-Fuzzy Inference System (ANFIS) in terms of sensitivity and specificity. However, due to the small population size, no statistical testing or validation was undertaken. SVMs are linear classifiers but can produce non-linear decision boundaries using the kernel trick. Although several kernel functions have been explored, the Gaussian Radial Basis Function kernel is the most widely used in seizure prediction [45, 59, 66, 72].

2.1.3.5.2 Artificial and cellular neural networks

ANNs have the ability to produce nonlinear decision boundaries while assembling several artificial neurons. The general structure consists of an input layer, a hidden layer, and an output layer. These classifiers are known as universal approximators because of their capacity to approximate any continuous function if a sufficient number of neurons and layers are given. However, they are sensitive to overtraining and may fail with non-adequate input features. While several studies have looked at ANNs in the field of seizure prediction, few have adhered to the requirements for practical seizure prediction. Costa et al. [106] compared the performance of 6 different ANN architectures for predicting epileptic seizures: RBF, Feed-Forward Back Propagation, Layer-Recurrent, Feed-Forward Input Time-Delay Back Propagation, Elman, and Distributed Time Delay. While they reported optimistic results, the lack of adequate performance evaluation limited the significance and reproducibility of their findings. Teixeira et al. [65] compared the performance of 2 different ANN structures: MLP and RBF. K-W testing showed that MLP outperformed the RBF classifier in terms of FPR with no statistically significant differences in terms of sensitivity. Interestingly, these authors [65] found 2,000 or 4,000 epochs to be adequate, considering the number of hidden layers and neurons included. Cellular neural networks (CNNs) are a subset of ANNs where only local connections between cells are allowed. They have been adopted in recent seizure-prediction studies owing to their capability of universal computation and massive computing power [108, 109]. They have been mainly employed in an attempt to approximate synchronization degree and nonlinear dynamics in EEG signals. ANFISs have been explored in seizure prediction and combine a Sugeno Type Fuzzy Inference unit for classification rules with an ANN to increase and adapt learning capabilities. Rabbi et al. [104] tried an ANFIS to predict epileptic seizures with both linear and nonlinear features. They stated

that the proposed method achieved the highest sensitivity of 80% and FPR of 0.46 h^{-1}. However, their study was limited to 36 h of iEEG recordings in 1 patient, raising doubts about reproducibility of the results. Our group [59] targeted linear univariate features with several selection methods and demonstrated that combining an ANFIS with a GA yielded promising results.

2.1.3.5.3 Logistic regression

Logistic regression is a linear classifier parameterized by weights and biases. Training the classifier consists of finding adequate weights optimized by minimizing a predefined loss function. Although this classifier sets linear decision boundaries, it has been successful in seizure prediction. In a recent study that investigated the feasibility of seizure forecasting in canine epilepsy, Howbert et al. [38] engaged the logistic regression classifier to detect the preictal state based on spectral power features and were able to beat a random predictor in all 3 dogs with acceptable FPR and sensitivities. Mirowski et al. [96] evaluated the performance of bivariate synchronization features with 3 different classifiers: SVM, Logistic Regression, CNNs. Although the best results were obtained by combining wavelet coherence and CNNs, the logistic regression classifier allowed perfect seizure prediction in 14 out of 21 patients from the University of Freiburg Database.

2.1.3.6 Regularization

After classification, a regularization function should be added to attenuate the number of false alarms. Methods taking into account temporal signal dynamics, such as Kalman filtering [110] or the firing power technique [73], have been employed. The main goal is to improve classifier specificity by constraining alarm generation.

Firing power is a measure that quantifies the number of predictions classified as preictal during the SOP. If this measure exceeds a normalized threshold, an alarm is generated. Several studies recently adopted the firing power technique in their prediction schemes and reported relatively good results [45, 65]. Teixeira et al. [65] and Bandarabadi et al. [45] adopted a fixed threshold of 0.5. C. Teixeira et al. [111] compared different thresholds (0.10, 0.15,…, 0.85) and showed that in general lower FPRs were achieved with low threshold values. No optimal threshold value was reported.

Chisci et al. [110] were the first to take the Kalman filtering approach as a regularization method to smooth SVM classifier output. It is a statistical paradigm that produces estimates tending close to true measurements. With estimated AR coefficients as inputs to an SVM, these authors compared the performance of the proposed method with that of a non-regularized classifier on iEEG in 9 patients from the University of Freiburg database. Significant improvement in performance was reported but no statistical testing was done. Kalman filtering was subsequently successful in other studies [72, 110]. Park et al. [72] went with second-order discrete-time Kalman filtering to smooth undesired fluctuations of SVM outputs.

Teixeiria et al. [111] compared both regularization measures and found that the "firing power" method was more conservative in raising alarms. These authors justified its superiority by the fact that it maintains longer memory of classification dynamics and creates time constraints for alarm-raising. They stated that the number of false alarms obtained with Kalman filtering was too high and impractical for most patients [111]. However, the Kalman filtering regularization function produced relatively better sensitivities.

2.1.3.7 Performance evaluation

As with any classification problem, algorithm performance should be tested with common performance descriptors.

2.1.3.7.1 Performance descriptors

A large number of seizure prediction studies have adopted common descriptors to evaluate the performance of prediction algorithms, with mostly sensitivity and specificity being analyzed. It is important to mention that these measures should be reported on unseen test data never used for training or optimization, ideally in a prospective setting. Testing system performance on data used for training has previously led to overoptimistic results, as discussed in [33]. Several other measures have been adopted to evaluate system performance in terms of specificity, such as FPR and Time Under False Warning. As its name implies, FPR is the number of false predictions per hour. A false positive event occurs when an alarm is raised during any period other than preictal. FPR has been adopted as a measure of specificity in a large number of seizure-prediction studies [45, 47, 52, 65, 72, 95, 102, 111]. However, no minimum FPR value has been adopted as standard. Aschenbrenner-Scheibe et al. [91] used seizure frequency in presurgical monitoring settings as reference to define maximum acceptable FPR. Considering a mean of 3.6 seizures per

day, the clinical applicability of open-loop algorithms with FPR higher than 0.15/h was questioned [49]. Such comparison is not always valid, since although the number of generated alarms is comparable, false prediction means that these alarms are not generated at the correct time. Triggering interventions during low seizure likelihood or omitting them during the preictal period may limit seizure control effectiveness. Interestingly, some recent studies have reported FPR to be less than 0.15/h. Bandarabadi et al. [45] ascertained average FPR of 0.1 h^{-1} with bivariate spectral power methodology. In a comparative study of 278 patients from the European Epilepsy Database, Teixieira et al. [65] established that some predictors were able to predict at least half of the seizures with FPR of less than 0.15 h^{-1}. Howbert et al. [38] found FPR of less than 0.12 h^{-1} in data on 3 dogs implanted with a long-term monitoring system.

2.2 Discussion

Although much effort has been expended towards better prediction of epileptic seizures, the translation of current approaches and algorithms into commercial clinical devices is still not possible. The guidelines proposed by Mormann et al. [33] have paved the way for more realistic and reproducible albeit less optimistic results. Analytical and algorithmic studies have provided evidence that transition to the seizure state is not random and that a certain build-up leads to seizures. Heterogeneity between studies supports the fact that ictogenesis mechanisms are probably complex and suggests that the approaches taken to deal with this state should be envisaged with more precaution. In what follows, we discuss, summarize and analyze the progress made in main blocks of the seizure prediction framework.

As already suggested in the earlier review [33], no single feature can be considered as standard on its own to characterize preictal state. However, combination of univariate and bivariate features may be a good choice. Two recent studies in the field of seizure prediction attempted to explore cross frequency coupling in their feature extraction block [45, 88] and generated promising results compared to traditional spectral power features. The implemented features were based on univariate phase-amplitude coupling as well as bivariate amplitude-amplitude coupling. Investigating other types of coupling may be a tempting idea for feature extraction in epileptic seizure prediction.

Combining several features to track the preictal state may increase feature space dimensions, triggering the need for feature selection algorithms. Although the vast majority of seizure prediction studies confirmed the need for subject-specific, individually-tailored algorithms, few

have reported the most discriminative features across all subjects. It may be reminded that out-of-sample testing should be considered in feature selection. Samples for feature selection should never be used for performance evaluation.

Several types of classifiers have been investigated in seizure-prediction studies. Comparison is difficult due to the heterogeneous aspect of preprocessing, input features and patient data. Several authors have shown that combination of linear features and nonlinear classification methods is a good approach. It has been adopted in several prediction schemes, especially those involving SVMs with nonlinear kernels, and yielded relatively good performances [45, 65, 72]. Logistic regression, a linear classification method, has yielded acceptable results [96]. It is important to mention that the use of non-complex classifiers, employing relatively simple decision boundaries, is worthwhile.

Both Kalman filtering and firing powers have been able to reduce FPR in seizure-prediction studies [45, 65, 72]. Deploying such advanced postprocessing techniques to achieve reliable performance, one could question the statistical existence of a preictal state. Herein lies the importance of performance evaluation, especially methods employing extensive statistical validation and comparison with random predictors. Proof-of-principle studies [65] conducted on a large cohort of patients (278) and employing reliable statistical validation and testing techniques, have demonstrated the existence of preictal state. At this stage, the performance improvement after applying such post processing techniques can be explained by the fact that they decrease the vulnerability of seizure-prediction systems to brain vigilance states.

The studies covered in this review have generally looked at discontinuous recordings either in the University of Freiburg database, the European Epilepsy database, or local recordings. Because the discriminability of iEEG features is highly dependent on time and the non-stationary nature of EEGs can culminate in mis-estimation of algorithm performance, long continuous recordings that mimic real clinical scenarios rather than discontinuous recordings are recommended.

CHAPTER 3 THEORY AND METHODOLOGY

This chapter summarizes signal processing approaches used in chapters 4, 5, and 6 namely in terms of EEG signal processing and classification as well as effective connectivity measures.

3.1 EEG signal processing and classification

3.1.1 Feature extraction

3.1.1.1 Univariate linear features

As explained in the literature review, univariate linear features have been adopted in recent studies [43, 65, 72] and showed a better predictive performance than non-linear ones [47]. Traditional univariate linear features, most prominent in the EEG seizure prediction literature with reproducible performances were adopted in this work and are briefly explained: statistical moments, relative spectral power, Hjorth parameters, spectral edge frequency and power, and decorrelation time.

3.1.1.1.1 Statistical moments

Considering a discrete time series x_i, the variance is the second statistical moment and reflects the energy content of a signal (1).

$$\delta^2 = \frac{1}{N-1}\sum_{i=1}^{N}(x_i - \bar{x})^2 \quad (1)$$

The skewness is the third statistical moment and is a measure of symmetry (2).

$$X = \frac{1}{N}\sum_{i=1}^{N}\left(\frac{x_i}{\delta}\right)^3 \quad (2)$$

The kurtosis is the fourth statistical moment and reflects a measure of flatness of the amplitude distribution (3).

$$k = \left[\frac{1}{N}\sum_{i=1}^{N}\left(\frac{x_i}{\delta}\right)^4\right]^{-3} \quad (3)$$

3.1.1.1.2 Relative spectral band power

Spectral band power was computed by calculating the average power in each frequency range of interest as integrated across the periodogram of the signal [112]. As discussed in the literature review, the relative spectral power feature (RSP) will be computed based on standard EEG frequency bands and the wide gamma band will be split into four further sub-bands. This results in the following frequency bands: delta (0.5- 4 Hz), theta (4-8Hz), alpha (8-13 Hz), beta (13-30

Hz) and gamma (30-47, 53-75, 75-97, 103-128 Hz). In order to get the relative spectral power, each of the frequency bands is divided by the total power of the signal.

3.1.1.1.3 Hjorth parameters

Hjorth parameters have been extensively used to quantitatively describe the temporal dynamics of EEG signals in seizure prediction and have shown to increase during the preictal state [47]. The HM (5) reflects the mean frequency of a signal while the HC (6) is an estimate of its bandwidth.

$$Activity = Var(x(t)) \tag{4}$$

$$Mobility = \sqrt{\frac{Activity\left(\frac{dx(t)}{dt}\right)}{Activity\left(x(t)\right)}} \tag{5}$$

$$Complexity = \frac{Mobility\left(\frac{dx(t)}{dt}\right)}{Mobility\left(x(t)\right)} \tag{6}$$

where x(t) is a time series.

3.1.1.1.4 Spectral edge frequency and power

The spectral edge frequency (SEF) has been defined as the minimum frequency (below 40 Hz) up to which 50% of the power is contained in a signal. It is considered as a characterizing measure of the power distribution of a signal [85]. The Spectral Edge Power (SEP) is the corresponding half power up the spectral edge frequency.

3.1.1.1.5 Decorrelation time

The decorrelation time is defined as the first zero crossing of the autocorrelation function. As shown in (7), the autocorrelation function is an estimation of the degree of similarity between a signal x_i and a delayed version of itself $x_{i-\tau}$.

$$A(\tau) = \frac{1}{(N-1)\sigma^2}\sum_{i=1}^{N-\tau} x_i x_{i-\tau} \tag{7}$$

The autocorrelation function can have values between -1 and 1. An autocorrelation value of 1 reflects an optimal positive correlation while a value of -1 reflects an optimal negative correlation. Initially (τ =0), the autocorrelation function is equal to 1. Considering a non-periodic signal such as the EEG, A (τ) decreases with increasing values of τ. The slower the autocorrelation function decreases, the stronger are the linear correlations of the signal.

Therefore, the decorrelation time can be considered as an estimate of the strength of the linear correlations. A drop in the decorrelation time had been reported prior to seizures [47, 73].

3.1.1.2 Univariate nonlinear features

The commonly used spectral band power feature in seizure prediction studies display amplitude modulations within defined frequency bands over time. While this feature is able to quantify phase changes, it fails identifying the interactions between different frequencies. Cross-frequency coupling (CFC) among different frequency bands has been recently proposed to be the carrier mechanism for the relationships of local and global neuronal processes [113]. Two recent studies in the field of seizure prediction have attempted to explore specific types of CFC in their feature extraction block [45, 88]. The implemented features were based on a phase-amplitude [88] CFC and amplitude-amplitude CFC [45]. As already discussed, recent iEEG studies found a modulation of cortical high frequency oscillations in the gamma band (40-120 Hz) by slow cortical potentials [114]. As emphasized in [88], low frequency oscillations seem to trigger high frequency oscillations. M. Le Van Quyen et al, 2014 [88] focused on coupling between the phase of slow oscillations (slow wave and theta) and the amplitude of different sub-bands of gamma rhythms in a univariate manner. Interestingly, the authors compared the proposed methodologies with predictions based on the individual power in each frequency band (delta, theta, gamma) and found superior performance when quantifying the coupling between different frequency bands. Recently, M. Bandarabadi et al, 2015 [45] proposed a new bivariate feature for the prediction of epileptic seizures and reported promising results (Sensitivity= 75.8% and FPR= 0.1 h^{-1}). Although not termed as cross frequency coupling, the proposed feature (discussed in the literature review) quantifies the cross-power information between two different frequency bands and two different channels (across all possible combinations) by calculating the ratio between the normalized PSD among different channels and frequency bands combinations. The authors used a selection method that performs a ranking of the input features (bivariate/univariate PSD); relative, bivariate spectral power features were selected as the best in 90% of the cases. The mentioned previous studies [45, 88] are both prospective and follows methodological recommendations for practical seizure prediction studies [33]. Therefore, there is recent evidence that coupling between different frequencies may better discriminate the preictal state. Using phase-amplitude coupling, C. Rojas et al, 2014 [88] identified preictal changes above chance levels in 13.2% of patients. Bandaradabi et al, 2015 [45] found promising results using the cross-

frequency information based on spectral power which only take into consideration the amplitude of the signal. In contrast, the bispectrum (BIS) measure have been proposed to take into consideration both the amplitude of the signal and the degree of phase coupling between two frequencies.

3.1.1.2.1 Higher order spectra

Higher order spectral analysis is an advanced signal processing method that allows exploring the existence of quadratic (and cubic) non-linearities. In contrast to traditional power spectrum which quantifies the power of a time series over frequency, HOS analysis employs the Fourier transform of higher order correlation functions investigating non-linear coupling information. The bispectrum splits the skewness (third order moment) of a signal over its frequencies quantifying the coupling between a signal's oscillatory components. The bispectrum, quantifying oscillatory relationships between basic frequencies f1, f2, and their harmonic component "f1+f2" is computed from the Fourier transform of the third-order correlation (8).

$$Bis(f_1, f_2) = \lim_{T \to \infty} \left(\frac{1}{T}\right) E[X(f_1 + f_2)X^*(f_1)X^*(f_2)] \quad (8)$$

where X(f) is the Fourier transform of a time series x(t), (*) is the complex conjugate, and E denotes the arithmetic average estimator over time duration T.

3.1.1.2.2 Higher order spectra features

In order to characterize and compare time series, quantitative features must be extracted from the bispectral density array. Bispectrum analysis yields a 3D mapping of the level of interaction between all frequency triplets in the signal. In order to characterize and compare time series, quantitative features must be extracted. In this work, three features were computed from the non-redundant region: the mean magnitude (Mave) of the bispectrum, the normalized bispectral entropy (P1) and the normalized squared bispectral entropy (P2). The mathematical equations of extracted features are briefly explained:

The first feature, bispectrum's mean of magnitude (Mave) (9), has been commonly used to extract quantitative information from the bispectrum [115, 116].

$$Mave = \frac{1}{L}\sum_{\Omega} |Bis(f_1, f_2)| \quad (9)$$

where L is the total number of sample points in the bispectral density array non-redundant region (Ω).

In an attempt to extract regularity from bispectrum plots, normalized bispectal entropy (P1) and normalized bispectral squared entropy (P2) have been recently proposed [115] and were used in this work (10) and (12):

$$P_1 = -\sum_n p_n log p_n \quad (10)$$

$$p_n = \frac{|Bis(f_1,f_2)|}{\sum_\Omega |Bis(f_1,f_2)|} \quad (11)$$

$$P_2 = -\sum_n q_n log q_n \quad (12)$$

$$q_n = \frac{|Bis(f_1,f_2)|^2}{\sum_\Omega |Bis(f_1,f_2)|^2} \quad (13)$$

where *n=0, 1, ... L-1*; L is the total number of sample points in the bispectral density array non-redundant region (Ω).

3.1.2 Feature selection: genetic algorithm

As already discussed in the literature review, no single feature had been found capable to individually characterize the preictal state, but a combination of features may be able to display brain dynamics during the transition to seizures. Thus, a Genetic Algorithm (GA) (described in the literature review) was be used in this study since it allows finding which combination of features is discriminative of the preictal state rather than performing a ranking of the features. In addition, the advantage of using a GA is that such an iterative algorithm doesn't require fixing the size of the selected subset of features. The computation requirements of the GA were considered as an obstacle towards the development of predictors in studies which didn't perform electrodes selection [58]. In its simplest form, a GA requires a genetic representation and a fitness function. While several presentations have been proposed, the standard one is an array of bits. In feature selection, generally each bit can be considered as a feature. Binary bit representations have been adopted where 1 means that the feature is discriminative of the classification target and 0 otherwise [58, 59]. The fitness function can be considered as the cost function that will ensure the convergence of the problem into a good potential solution. Thus, it is important to note that the GA doesn't perform a ranking of the features in terms of their discriminative power but tends to find a good feature combination for the given problem. This structure can be an advantage in seizure prediction studies where a combination of features, each displaying a certain aspect of brain dynamics, have shown a better performance than using individual features [33].

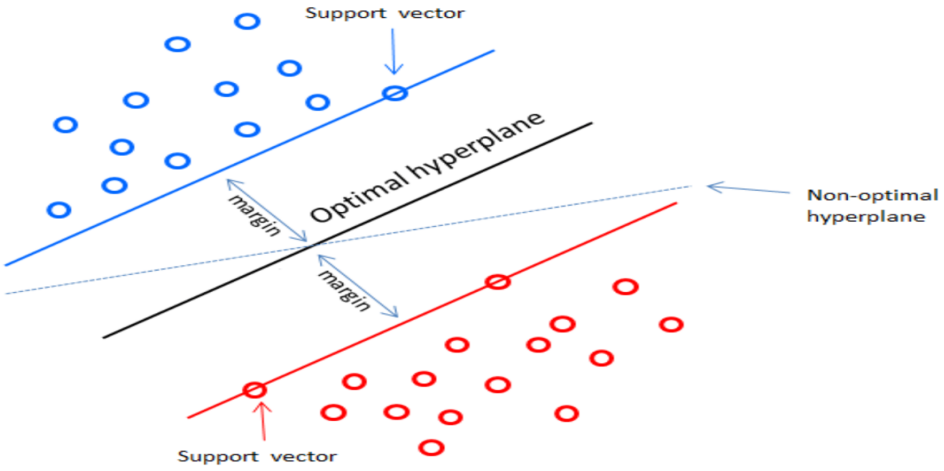

Figure 3.1 Support vector machine optimal linear hyperplane

After defining the fitness function and the genetic representation, the GA initializes an initial population of chromosomes and then improves it through generations. The general algorithm is briefly explained: After selecting an initial random population, a proportion of the individuals is selected to create a new population. The selected individuals are generally the ones with the best fitness. Then a combination of genetic operators (crossover and mutation) is used to generate the following generation. Crossover and mutation are applied on a pair of parents from the initial population to create a new solution (child). This process is repeated until reaching a certain termination condition such a maximum number of generations or a minimum value of the fitness function. Several types of genetic algorithms in terms of selection methods, genetic structure, and fitness function have been used in seizure prediction studies and have been discussed in the literature review.

3.1.3 Classification

3.1.3.1 Support vector machine

Several studies have demonstrated the superiority of SVMs over other supervised machine learning techniques in seizure prediction and were discussed in the literature review. As shown in Figure 3.1, the main idea behind support vector machines is to separate classes using a linear hyperplane (14).

$$f(x) = w^T x + b \tag{14}$$

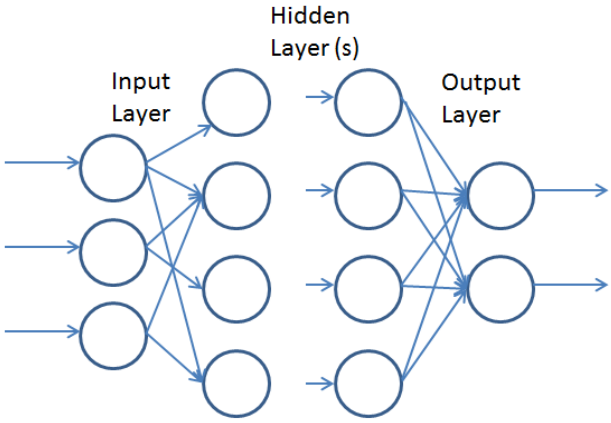

Figure 3.2 Multi-layer perceptron network architecture

However, using the kernel trick, these are capable of projecting the data into a higher dimensional non-linear space. It often happens that data non-separable in the original space become separable in a high dimensional space. Several kernels have been used in EEG classification such as the Gaussian, Radial Basis Function (RBF), polynomials and Multilayer Perceptron. The RBF kernel (15) is the most exploited in seizure prediction [45, 58, 59, 65, 72] and will be used in this study.

$$K(x,y) = exp\left(\frac{-|x-y|^2}{2\sigma^2}\right) \quad (15)$$

where x and y are the input feature vectors and σ is the scale parameter. This hyperplane tends to maximize the distance between the nearest training points (margins) what increases generalization capabilities and makes SVMs more resistant to overtraining. Using such a decision boundary, two hyper parameters need to be defined: the cost (C) and the cost factor (R). Actually, while searching for the hyperplane that maximizes the margins between the support vectors, some of the training points may be misclassified. The cost is the tradeoff between the classification margins and the non-separable or misclassified samples. On the other side, the cost factor is the trade-off between the number of false positives and false negatives.

3.1.3.2 Multi-layer perceptron

A multi-layer perceptron (MLP) classifier has the capability of reproducing nonlinear decision boundaries while assembling several neurons. MLP is one the most commonly used feedforward artificial neural networks architecture and consists of an input layer, one or multiple hidden layers, and an output layer. MLP classifiers are known as universal approximators since they can approximate any continuous function when subject to enough neurons and layers. Network

training and weights optimization is performed by backpropagation, a supervised learning technique. Each neuron requires a linear activation function, which maps its weighted inputs to its output. Figure 3.2 shows the typical architecture of an MLP network.

3.1.4 Regularization function

As discussed in the literature review, this step is considered as a post-processing that regularizes the output of the classifier to reduce the number of false alarms. C. Teixeira et al. 2012 [111] showed that the firing power technique is more conservative than the Kalman filter. Thus, the firing power method will be used in this project and is briefly explained: A sliding window equal to the preictal time is considered in which a measure of the number of samples classified as preictal is calculated (16):

$$fp[n] = \frac{\sum_{k=n-\tau}^{n} O[k]}{\tau} \quad (16)$$

Where fp [n] is the firing power at time point n, O[k] is the output of the classifier and τ is the number of samples in the preictal time. In most of the cases, a fixed firing power threshold is fixed at 50 % (fp =0.5) above which an alarm is generated. After alarm generation, a new alarm can only be raised at a time at least equal to the considered preictal time only if the threshold is crossed in an ascending way [73].

3.2 Effective connectivity measures

3.2.1 Directed Transfer Function

The directed transfer function (DTF) is a multichannel extension of the Granger causality using a multivariate autoregressive model. The Granger causality is a method used to determine whether a time series is useful in predicting another one [117]. Recently several directed connectivity measures based on the theory of Granger causality have been proposed in an attempt to discern neuronal sources of epileptic activity [118, 119] and provided promising results in the identification of generators of ictal activity. Some of them were based on pairwise measures while other extended to multivariate approaches. Kus et al, 2004 [120] compared directions of activity propagation between pairwise estimates of granger causality and coherences with the multivariate DTF. Based on simulated data and experimental EEG signals, the authors found that the DTF method was better in estimating the sources/generators of ictal activity. Actually, pairwise causality measures have an innate inconvenient when applied to multivariate signals

such as the multichannel EEG. In such case, spurious causal connections may appear between electrodes or regions of interest when no such coupling exists. The mathematical principles of the DTF, a multivariate approach, are explained and were used in this thesis for the determination of ictal generators and sinks. As already stated, the DTF is defined in terms of a multichannel autoregressive model (MVAR). As depicted in equation (17), a MVAR model is a parametric time series representation that describes each channel as a linear combination of its own past and the past activity of all other channels added to an uncorrelated white noise.

$$x_n = \sum_{m=1}^{p} A_m x_{n-m} + e_n \quad (17)$$

where x_n is a multichannel signal at time point n containing k channels (18), e_n is the uncorrelated white noise matrix (19) and A_m is the matrix containing the coefficients of the MVAR model at a time delay m.

$$x_n = [x_1(n),\ x_2(n), \dots, x_k(n)]^T \quad (18)$$

$$e_n = [e_1(n),\ e_2(n), \dots, e_k(n)]^T \quad (19)$$

The DTF attempts to examine the causal relation between the signals in the frequency domain. Thus equation (18) is Fourier transformed as follows (20):

$$E(f) = A(f)X(f) \quad (20)$$

where E (f), X (f) are the Fourier transforms of the error and time series matrices; A (f) is the Fourier Transform of the coefficient matrix and expressed as follows (21):

$$A(f) = -\sum_{m=0}^{p} A_m e^{-j2\pi fm} \quad (21)$$

Assuming that A (f) is non-singular and thus invertible, equation (20) can be reformulated as follows (22):

$$X(f) = A^{-1}(f)E(f) = H(f)E(f) \quad (22)$$

H (f) is defined as the transfer matrix of the process and is a k x k matrix. Interestingly, the elements of the transfer matrix H_{ij} (f) express the causal relations at frequency f from channel x_j to channel x_i. The DTF is then estimated in terms of the transfer function and estimates the flow from channel x_j to channel x_i (23):

$$DTF_{ij}(f) = \left|H_{ij}(f)\right|^2 \quad (23)$$

Kaminski et al, 2001 [121] demonstrated the equivalence between DTF and Granger causality. In almost all studies [54, 122], the DTF is normalized with respect to the incoming inflow in such a way that the normalized DTF (nDTF) quantifies the ratio of the inflow from signal j to signal i with respect to all inflows to signal i at frequency f (24).

$$nDTF_{ij}(f) = \frac{|H_{ij}(f)|^2}{\sum_{k=1}^{K}|H_{ik}(f)|^2} \quad (24)$$

As clear, the current formulation of the DTF quantifies the amount of outflow of activity at a specific frequency. As it is dedicated to analyze quasi-stationary segments of seizure activity which span over a spectral band of frequency, the integrated DTF (iDTF) had been proposed [123] and consists of integrating the nDTF over the desired frequency band (25).

$$iDTF_{ij} = \frac{1}{f_2-f_1}\sum_{f=f_1}^{f_2}\frac{|H_{ij}(f)|^2}{\sum_{k=1}^{K}|H_{ik}(f)|^2} \quad (25)$$

3.2.2 Spectrum weighted adaptive directed transfer function

The adaptive directed transfer function (ADTF) allows investigating time-varying connectivity patterns and does not entail stationarity requirements. It is based on a multivariate adaptive auto regressive model (MVAAR) [124] (26):

$$X(t) = \sum_{i=1}^{p} A(i,t)X(t-i) + E(t) \quad (26)$$

where X(t) is a multivariate signal, A (i, t) is a matrix gathering time varying model coefficients, E(t) is the error matrix and p is the model order. Non-linear Kalman filtering, based on a combination of observation and state space equations, is used to estimate model's time varying coefficients [124]. The frequency domain transfer matrix H_{ij} (f, t) is obtained by Fourier transforming equation (26). H_{ij} (f, t) displays causal relations from the electrode j to electrode i at time instant t and frequency f. Although the clinical validity of the ADTF has been demonstrated [124], Mierlo et al. 2013 found that at some frequency f and time t, the term $H_{ij}(f,t)$ may be high even though power of signal j is relatively low [125].

They subsequently proposed the swADTF in which H_{ij} (f, t) is divided by the auto spectrum of the sending channel (27).

$$swADTF_{ij}(\mathrm{t}) = \frac{\sum_{f=f_1}^{f_2}|H_{ij(f,t)}|^2 \sum_{k=1}^{K}|H_{jk(f,t)}|^2}{\sum_{l=1}^{K}\sum_{f'=f_1}^{f_2}|H_{il(f',t)}|^2 \sum_{s=1}^{K}|H_{ls(f',t)}|^2} \quad (27)$$

where f1 and f2 are frequency bounds of interest, and K is the total number of channels.

Mierlo et al. 2013 demonstrated how the auto-spectrum can be estimated out of the coefficients and residuals of the MVAAR [125]. Considering equation (22), the power spectral density matrix can be calculated as follows (28):

$$\begin{aligned} S(f) &= X(f)X^*(f) = H(f)E(f)E^*(f)H^*(f) \\ &= H(f)\Sigma_e H^*(f) = H(f)\sigma_e I H^*(f) = \sigma_e H(f)H^*(f) \end{aligned} \quad (28)$$

where * represents the complex conjugate and $\sum_e$ is the noise covariance matrix. Assuming that the error time series can be represented by an uncorrelated white noise, the covariance matrix $\sum_e$ can be approximated by a diagonal matrix σI. Thus, the auto-spectrum of a channel x_i can be estimated as in (29):

$$S_{ii}(f) = \sigma_e \sum_{k=1}^{K} H_{ik}(f) H_{ki}^{*}(f) = \sigma_e \sum_{k=1}^{K} |H_{ik}(f)|^2 \quad (29)$$

3.2.3 Outflow and inflow of seizure activity

Seizure activity outflow and inflow were extracted from the DTF or swADTF transfer matrix (TF). As H_{ij} quantifies seizure activity flow from channel x_j to channel x_i, summing and normalizing along columns of the transfer matrix determine outflow from x_j to all remaining electrodes (30):

$$nOV(j) = \frac{\sum_{i=1}^{K} TF_{ij}}{K} \quad (30)$$

for j=1 to K, where K is the number of iEEG channels, and TF is the transfer matrix.

Similarly, integrating and normalizing across lines of the transfer matrix quantifies normalized inflow values (nIV) from all channels to channel x_i (31):

$$nIV(i) = \frac{\sum_{j=1}^{K} TF_{ij}}{K} \quad (31)$$

for i=1 to K, where K is the number of iEEG channels, and TF is the transfer matrix.

3.2.4 Statistical significance of causal links: surrogate data testing

This is an essential step to remove the links that may create spurious interactions between the EcoG channels. It is mainly performed to validate the statistical significance of the causal interaction among the channels. Since the DTF have a highly non-linear relation with the time series from which it is derived, and thus the estimators' distribution under the null hypothesis of no connectivity is not well established, a non-parametric statistical analysis should be used. As discussed in the performance evaluation section of the literature review, a non-parametric statistical method based on surrogate data testing has been proposed [126] and used in several source localization studies [54, 124]. In summary, it consists of randomly and independently shuffling the phases of the Fourier transform to create a new surrogate time series. This procedure is repeated several times to obtain an empirical distribution of the DTF values under the null hypothesis of no causal interaction. This distribution is then used to assess the statistical significance of causal interactions.

CHAPTER 4 ARTICLE 1 A FUNCTIONAL-GENETIC SCHEME FOR SEIZURE FORECASTING IN CANINE EPILEPSY

Elie Bou Assi[1], Dang K. Nguyen[2], Sandy Rihana[3], and Mohamad Sawan[1]

[1]Polystim Neurotech Lab, Institute of Biomedical Engineering, Polytechnique Montreal, Montreal, QC, Canada

[2]University of Montreal Hospital Center (CHUM), University of Montreal, Montreal, QC, Canada

[3]Biomedical Engineering Department, Holy Spirit University of Kaslik (USEK), Jounieh, Lebanon

This article addresses the first objective of this thesis, namely the design of an accurate seizure forecasting algorithm, based on long-term continuous canine bilateral iEEG recordings. This paper was published in IEEE Transactions on Biomedical Engineering (Vol. 65, No. 6, June 2018) and was selected as a feature article for the IEEE TBME journal website. This work was awarded a travel grant (Alliance for Epilepsy Research) for presentation at the International Conference on Technology and Analysis of Seizures (ICTALS2017, Minneapolis, 2017).

4.1 Abstract

Objective: The objective of this work is the development of an accurate seizure forecasting algorithm that considers brain's functional connectivity for electrode selection. *Methods:* We start by proposing Kmeans-directed transfer function, an adaptive functional connectivity method intended for seizure onset zone localization in bilateral intracranial EEG recordings. Electrodes identified as seizure activity sources and sinks are then used to implement a seizure-forecasting algorithm on long-term continuous recordings in dogs with naturally-occurring epilepsy. A precision-recall genetic algorithm is proposed for feature selection in line with a probabilistic support vector machine classifier. *Results:* Epileptic activity generators were focal in all dogs confirming the diagnosis of focal epilepsy in these animals while sinks spanned both hemispheres in 2 of 3 dogs. Seizure forecasting results show performance improvement compared to previous studies, achieving average sensitivity of 84.82% and time in warning of 0.1. Conclusion: Achieved performances highlight the feasibility of seizure forecasting in canine epilepsy. *Significance:* The ability to improve seizure forecasting provides promise for the development of EEG-triggered closed-loop seizure intervention systems for ambulatory implantation in patients with refractory epilepsy.

Index Terms: Classification, Directed Transfer Function, epilepsy, feature extraction, functional connectivity, seizure forecasting, genetic algorithm

4.2 Introduction

Epilepsy is a chronic condition characterized by recurrent seizures (or 'ictus') resulting from abnormal and excessive neuronal discharges. The most common form of treatment is long-term medication, to which 30% of patients are refractory. Brain surgery is recommended when medical therapy fails. The outcome of surgery depends on the accurate localization of foci. Seizure manifestations (semiology) and surface electroencephalographic (EEG) epileptiform discharges are key features of broad anatomical localization, which can be further refined with appropriate neuroimaging tests and intracranial EEG (iEEG) recordings [1]. Despite decades of research, the rate of epilepsy surgery failures in patients with drug-refractory seizures remains significant (30% of temporal and 50% of frontal lobe surgeries) [1]. A potential explanation is the inaccurate determination of seizure onset zones (SOZ) by expert neurophysiologists visually interpreting EEG. Indeed, epileptic activity triggered in SOZ can rapidly propagate to remotely-connected brain areas (part of the epileptic "network") that can be falsely identified as regions to be resected since intracerebral electrodes can only cover a small fraction of the brain. While the historical and traditional way to understand higher-level brain systems (such as seizure generation mechanisms) is to decompose the brain into distinct anatomical regions with specific local properties and functions, modern approaches focus on the analysis and modeling of networks, emphasizing connectivity, interaction, and synchronization on both local and large scales [2]. In a recent review of methods identifying epileptic neuronal networks and their own clinical findings, Stephan and Lopes da Silva [2] re-evaluated the concept of dichotomic classification of focal and generalized epilepsies and emphasized that, in both situations, specific epileptogenic networks are involved in seizure activity. Many methods have been designed to study the principle of functional connectivity and the dynamics of neuronal networks, such as those related to the Granger Causality (GC) concept [3] or directed transfer function (DTF), that extends GC to multichannel causality and has been successfully applied in epilepsy [2], [4], [5].

Besides brain surgery, refractory epilepsy can benefit from algorithms able to anticipate seizures. Recent research is currently oriented towards the prediction of epileptic seizures long in advance to accommodate acute interventions.

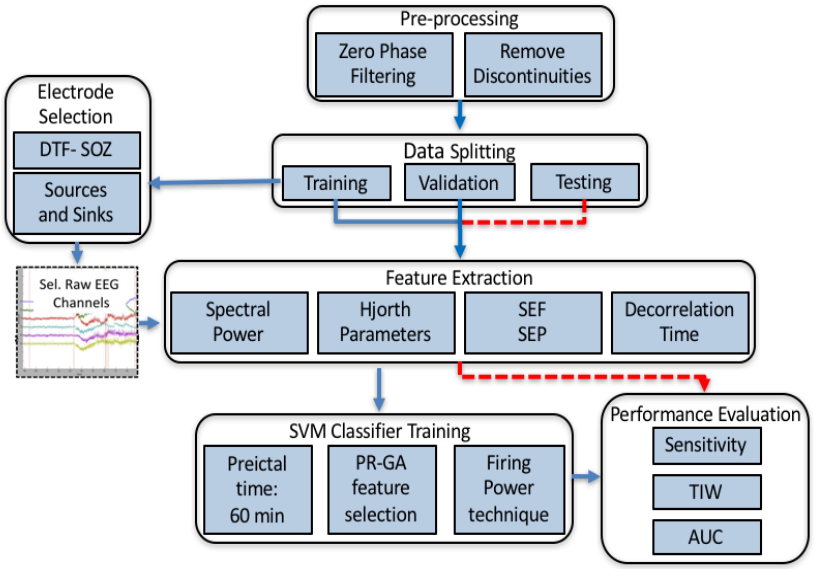

Figure 4.1 Framework of proposed seizure-prediction algorithm; The first cluster in each dog was used for training and validation (seizure used for training were not included in validation or testing); All remaining clusters were completely held out during algorithm development and were used for testing. DTF-SOZ: direct transfer function-seizure onset zone; SEF: spectral edge frequency; SEP: spectral edge power; PR-GA: precision recall-genetic algorithm; TIW: time in warning; AUC: area under the curve.

Although early seizure prediction investigations lacked adequate statistical rigor, recent studies have demonstrated that the transition to seizures is not random [6], [7], [8]. Paucity of iEEG recordings, limited amounts of ictal events and short duration of interictal periods are major obstacles to adequate assessment of seizure forecasting. In addition, these recordings are usually acquired in spatially-confined areas of suspected epileptogenicity ascertained on an individual basis after semiology and non-invasive, presurgical tests. Recently, long-term continuous bilateral iEEG recordings were acquired from dogs with naturally-occurring epilepsy using the implantable NeuroVista ambulatory monitoring device [9]. Canine epilepsy is a suitable model of human epilepsy with homologous clinical representation, electrophysiology, clinical therapeutic response, and epidemiology [10]. Howbert et al [11] proposed a seizure prediction algorithm combining spectral band power features and a logistic regression classifier in 3 dogs implanted with the NeuroVista monitoring device. The same group [12] extended these investigations to inter-electrode synchrony features in conjunction with a support vector machine (SVM). However, one of the major caveats of using these long-term canine iEEG recordings in seizure-prediction investigations was non-a priori knowledge of SOZ.

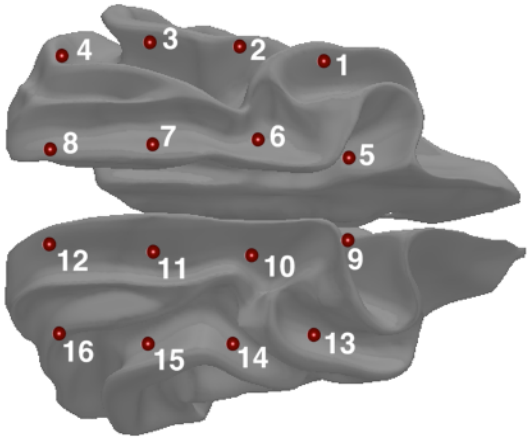

Figure 4.2 Approximate positioning of iEEG electrodes. The 3D canine brain mesh was generated by segmentation and reconstruction of magnetic resonance imaging canine brain scans on Matlab.

Our group [5] recently proposed a DTF-based adaptive method for the appraisal of seizure activity sources and sinks in multichannel bilateral iEEG recordings. In this work, we validated the suggested method and then exploited it to assess SOZ extent. A seizure-prediction algorithm was implemented on electrodes selected with Kmeans-DTF. A preprocessing step was undertaken to filter EEG recordings and remove discontinuities encountered upon device/electrode breakage.

Fourteen features were extracted from iEEG recordings and used as inputs to a genetic algorithm (GA) for feature selection. A new fitness function, based on precision-recall area under the curve (PR-AUC), was proposed and tested for problem optimization. The selected combination of features was used for classification with a probabilistic SVM. A post-processing step, based on the firing power technique, smoothed the classifier's output. Figure 4.1 depicts the methodological framework developed in this work.

4.3 Materials and methods

4.3.1 Database

Dogs were implanted with the NeuroVista ambulatory monitoring device for iEEG recordings [9]. Numbers of seizures and long-term recordings suitable for seizure prediction were adequate in 3 out of 7 dogs [11]. Data were acquired at 400 Hz through 4-bilateral 4-contact electrode strips (2 over each hemisphere) with a standardized protocol [9]. Dogs underwent continuous iEEG and video monitoring at the University of Minnesota canine epilepsy assessment unit.

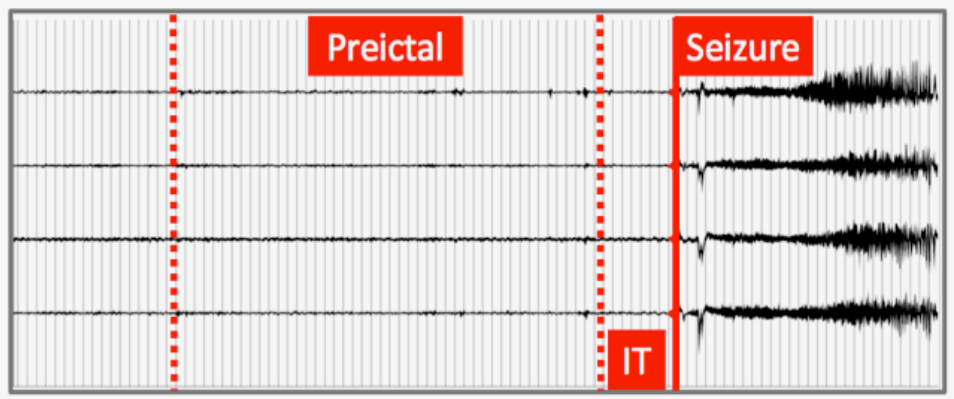

Figure 4.3 Four-channel iEEG recording showing preictal time and IT

For more technical and demographic details about canine iEEG recordings in this work, readers are referred to [11] and [12]. On average, recordings duration was 326±127 days including a total of 125 seizures. Figure 4.2 shows approximate positioning of the implanted electrodes. The 3D canine brain mesh was generated by segmentation and reconstruction of magnetic resonance imaging canine brain scans on Matlab©. The data are publicly available through the iEEG.org portal [11]. This type of recording allowed exploration of inter-hemispheric SOZ extent. Studies involving data acquisition and labeling were previously approved by the University of Minnesota Institutional Animal Care and Use Committee [11].

4.3.2 Kmeans-DTF: SOZ extent

Previous seizure-forecasting studies frequently lacked adequate electrode selection [8]. To address this drawback, we designed an adaptive, quantitative framework to evaluate SOZ extent in bilateral iEEG recordings. In [5], we tested DTF, a prominent multichannel causality measure to quantitatively define ictal activity generators and sinks in 1 of the dogs implanted with the NeuroVista device. Here, we extended these investigations to localize SOZ in 3 dogs with naturally-occurring focal epilepsy and then implemented a seizure-prediction algorithm using electrodes identified as seizure activity sources and sinks.

4.3.2.1 Directed transfer function

DTF is a multichannel causality estimate based on a multivariate autoregressive (AR) model. Kaminski et al [13] demonstrated equivalence between DTF and GC in determining whether a time series is useful in forecasting others. While several bivariate-directed connectivity measures have been proposed, multivariate approaches, namely, DTF, have proven to outperform pair-wise

methods [14]. The latter techniques are innately inconvenient when applied to multivariate signals, such as EEG recordings. In such cases, spurious causal connections may appear between electrodes or regions of interest, even when no coupling exists. The mathematical principles of DTF are briefly explained: as shown in (1), a multivariate AR model is a parametric time series representation that expresses each EEG channel as a linear combination of its past activity and that of all other EEG channels added to uncorrelated white noise:

$$x_t = \sum_{d=1}^{p} A_d x_{t-d} + e_t \quad (1)$$

where x_t is the k-channel signal at time point t and e_t is the uncorrelated white noise matrix while A_d contains 2D coefficients of the multivariate AR model at time delay d.

Equation (1) is Fourier-transformed in the DTF formulation, allowing causal interactions in the frequency domain to be examined, as shown in (2):

$$E(f) = A(f)X(f) \quad (2)$$

where A(f), E(f), and X(f) are Fourier transforms of coefficient, error and time series matrices, respectively.

Assuming that A(f) is invertible and non-singular, (2) can be reformulated as (3):

$$X(f) = A^{-1}(f)E(f) = H(f)E(f) \quad (3)$$

for k-channel signals, where H(f) is a k x k matrix and defines the transfer matrix. $H_{ij}(f)$ elements quantify causal relations at frequency f from channel x_j to channel x_i. Transfer matrix $H_{ij}(f)$ is then normalized with respect to incoming flow, allowing the ratio of inflow from channel xj to channel x_i to be quantified with respect to all inflows to x_i at a frequency f (4):

$$nDTF_{ij} = \frac{|H_{ij}(f)|^2}{\sum_{k=1}^{K}|H_{ij}(f)|^2} \quad (4)$$

As DTF is dedicated to analyzing quasi-stationary seizure epochs spanning a frequency band, integrated DTF (iDTF) is employed by integrating normalized DTF over the frequency band of interest.

4.3.2.2 Statistical significance of causal interactions

Statistically validating the significance of causal interactions is an essential step in any connectivity analysis simulation. Since DTF has a highly non-linear relationship with the time series from which it is derived, the distribution of estimators under the null hypothesis of no-interaction is not well-established. Thus, a non-parametric statistical test was included: surrogate data testing [4]. In summary, surrogate data testing consisted of randomly and independently

shuffling Fourier transform phases to create new surrogate time series. This procedure was repeated several times to obtain an empirical distribution of DTF values under the null hypothesis of no causal interaction. This distribution then served to assess the statistical significance of causal interactions.

4.3.2.3 Seizure activity outflow and inflow

Seizure activity outflow and inflow were extracted from the DTF matrix and considered as features of an unsupervised Kmeans-clustering algorithm. As H_{ij} quantifies seizure activity flow from channel x_j to channel x_i, summing and normalizing along columns of the transfer matrix determine outflow from x_j to all remaining electrodes (5):

$$nOV(j) = \frac{\sum_{i=1}^{K} iDTF_{ij}}{K} \quad (5)$$

for j=1 to K ($i \neq j$), where K is the number of iEEG channels.

Similarly, integrating and normalizing across lines of the transfer matrix quantifies normalized inflow values (nIV) from all channels to channel x_i (6):

$$nIV(i) = \frac{\sum_{j=1}^{K} iDTF_{ij}}{K} \quad (6)$$

for i=1 to K ($j \neq i$), where K is the number of iEEG channels.

Usually, electrodes with relatively high nOV and nIV are defined as sources and sinks of seizure activity respectively [4], [5].

4.3.2.4 Kmeans clustering: seizure activity sources and sinks

Previous DTF-based SOZ localization studies fixed a threshold for normalized outflow values (nOV) to determine seizure activity sources [4], [5]. In this work, we propose a clustering approach which attempts to adaptively evaluate seizure activity sources and sinks. Several assumptions support our motivation for such a scheme. First, employing adaptive, unsupervised clustering ensures the identification of a population with relatively normal outflow and inflow values (electrodes not implied in the network of seizure activity) compared to those featuring abnormal values (seizure activity sources and sinks). In contrast to previous studies, we assumed that seizure activity sources/generators feature high nOV and low nIV compared to sinks with low nOV and high nIV. Electrodes not implied in the network of seizure activity may exhibit low nOV and nIV. The separation hyperplane based on nOV and nIV is found using Kmeans

clustering, an adaptive partitioning algorithm. Clustering ensures minimizing intra-class variance while maximizing inter-class variance [15].

4.3.3 Seizure-prediction algorithm

As discussed in the introduction, one of the major caveats concerning these long-term iEEG recordings in previous seizure prediction investigations was non-a priori knowledge of SOZ extent. In this work, after employing automated functional connectivity analysis (Kmeans-DTF), a seizure prediction algorithm was implemented on electrodes identified as seizure activity sources and sinks.

4.3.3.1 Preprocessing

Long term continuous iEEG recordings of dogs with naturally occurring epilepsy are used in this study. A finite impulse response 6th order Butterworth band pass filter was used to select EEG frequencies of interest [0.5-180 Hz] [16]. Forward-backward filtering was performed to maintain signal phases intact [15]. As sketched in Figure 4.3, preictal time of 1 hour was considered with intervention time (IT) of 5 minutes. Such IT ensured enough time for intervention prior to any seizure manifestation. Continuous interictal segments were chosen from the whole recording with a restriction of 4 hours prior to or after seizure. A post-ictal state of 15 minutes was considered to avoid any contamination by ictal data. Thus, seizures separated by at least 1 hour 20 minutes were considered.

4.3.3.2 Feature extraction

Univariate linear features adopted in recent seizure prediction studies [7] manifested better predictive performance than non-linear features [8], [17]. Fourteen linear univariate features, most prominent in the EEG seizure prediction literature with reproducible performances, were extracted from iEEG signals in non-overlapping 1-minute windows [8]: relative spectral band power (9 features), Hjorth mobility and complexity, spectral edge frequency and power, and decorrelation time. Spectral power features were extracted from standard EEG bands while splitting the gamma band into 4 sub-bands: delta [0.5-4] Hz, theta [4-8] Hz, alpha [8-13] Hz, beta [13-30] Hz, gamma 1 [30-47] Hz, gamma 2 [53-75] Hz, gamma 3 [75-97] Hz, gamma 4 [103-128] Hz, and total power [0.5-180] Hz. Each of the spectral power features was divided by the total power of the signal.

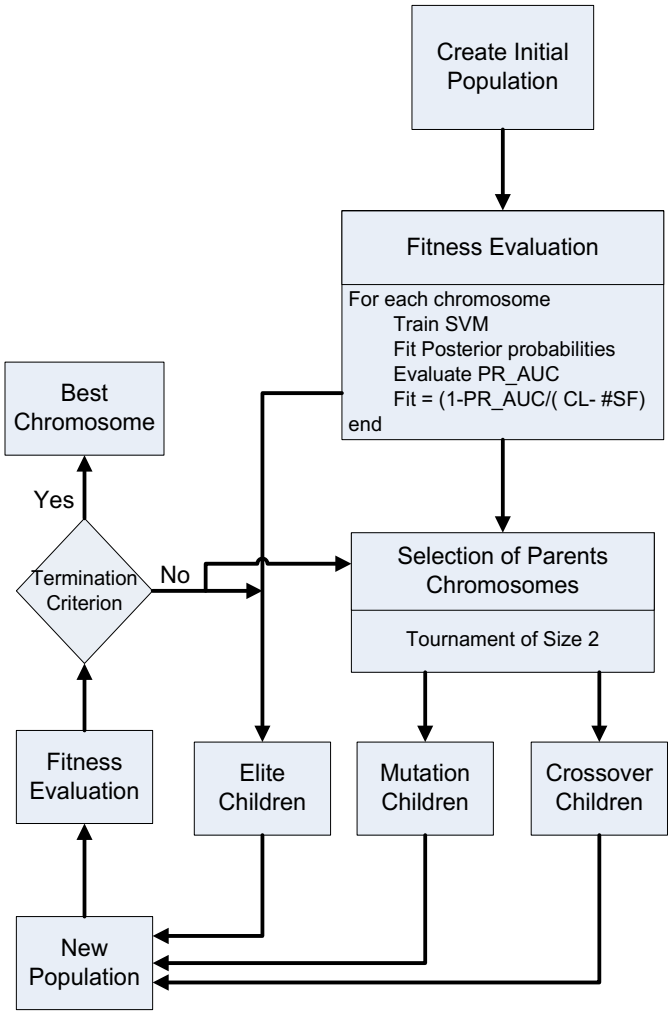

Figure 4.4 Flowchart of proposed PR-based genetic algorithm. SVM: support vector machine; PR_AUC: precision recall-area under the curve; CL: chromosome length; #SF: number of selected features

4.3.3.3 Feature selection: precision-recall genetic algorithm

Although much effort has been put into identifying unique precursors of seizure activity, no single feature has been found capable of individually characterizing the preictal state. However, a combination of features may be able to display brain dynamics during transition to seizure. Thus, a genetic algorithm in this work will allow us to establish which combination of features is discriminative of the preictal state rather than ranking them. In addition, the advantage of a GA is that such an iterative algorithm does not require fixing the size of the selected subset of features. The computation requirements of GAs are considered to be obstacles to the development of predictors in studies which did not perform electrode selection [18], [19].

Table 4.1 Data splitting into train, validation, and test

Dog ID	# of recording days	# of Seizures	Training and Validation (# of seizures)	Testing (# of seizures)
A0002	451	83	37 days (11)	414 days (72)
A0003	197	27	22 days (7)	175 days (20)
A0004	330	15	26 days (5)	304 days (10)

In its simplest form, a GA requires genetic representation and fitness function. While several presentations have been proposed, the standard is an array of bits. In feature selection, each bit represents a feature. Binary representations have been adopted where 1 indicates that the feature is discriminative of the classification target and 0 indicates otherwise [18].

The fitness function can be considered as the cost function that will ensure convergence of the problem into a potentially good solution. Thus, it is important to note that the GA does not rank features in terms of their discriminative power but tends to find good feature combination for the given problem. This structure can be an advantage in seizure prediction studies where a combination of features, each displaying a certain aspect of brain dynamics, performed better than looking at individual features [8].

After defining fitness function and genetic representation, the GA initializes an initial population of chromosomes and then improves it through generations. Figure 4.4 is a flowchart of the proposed precision-recall genetic algorithm (PR-GA).

After selecting an initially-randomized population, a proportion of individuals were selected to create a new population. The selected individuals were those with the best fitness.

Then, a combination of genetic operators (crossover and mutation) was used to generate the next population. Crossover and mutation were applied on a pair of parents from the initial population to create a new solution (child). This process was repeated until a termination criterion, maximum number of generations or minimum value of the fitness function was reached.

Receiver operating characteristic (ROC) curves, which display relationships between the number of correctly-classified positive and negative examples, are recommended when evaluating binary decision problems. However, they cannot be employed as a fitness function of an optimization problem, such as a GA when large skew occurs in class distribution (preictal vs interictal), since they may show interictal-biased, overoptimistic performance [20]. Precision-recall curves have

been reported to provide more reliable information on algorithm performance [20]. Davis and Goadrich [20] noted that an algorithm which optimizes PR-AUC augments the ROC-Area under the curve (ROC-AUC), but the inverse is not always valid. Subsequently, the PR-AUC was used in this work as a fitness function of the GA. The PR-AUC allows inclusion of the whole interictal training set in the algorithm's cost function (no need for under-sampling interictal training/validation data). The proposed GA iterates through 150 generations with an initial population equal to twice the chromosome length (number of electrode-feature combinations) [21]. Based on trials, cross-over and mutation probabilities were fixed at 0.8 and 0.1, respectively. A tournament of size 2 was used for the selection process.

4.3.3.4 Classification: probabilistic support vector machine

Several recent seizure prediction investigations have demonstrated the superiority of SVMs over other supervised machine learning techniques [7]. The main idea behind SVMs is to separate classes using a linear hyperplane. Interestingly, with the kernel trick, they are capable of projecting the data into high-dimensional, non-linear space. The RBF kernel (7) was the most employed in seizure prediction and adopted in this work:

$$K(x,y) = exp\left(\frac{-|x-y|^2}{2\sigma^2}\right) \quad (7)$$

where x and y are input feature vectors, and σ is scale parameter. Hyperplanes tend to maximize the distance between the nearest training points (margins), which increases generalization capabilities and makes SVMs more resistant to overtraining. SVM hyper-parameters were found through a hold-out validation grid search. In this work, a probabilistic SVM was implemented by fitting Plat's posterior probabilities [22]. Output was a normalized score (0-1) quantifying preictal state probability.

4.3.3.5 Output regularization: firing power

This step was considered as post-processing which regularizes the classifier's output to reduce the number of false alarms. Teixeira et al. reported that the firing power technique was more conservative than the Kalman filter in terms of alarm generation [23]. Thus, it was included in this work and explained briefly: a sliding window equal to preictal time was considered in which the number of samples classified as preictal was calculated (8):

$$fp[n] = \frac{\sum_{k=n-\tau}^{n} O[k]}{\tau} \quad (8)$$

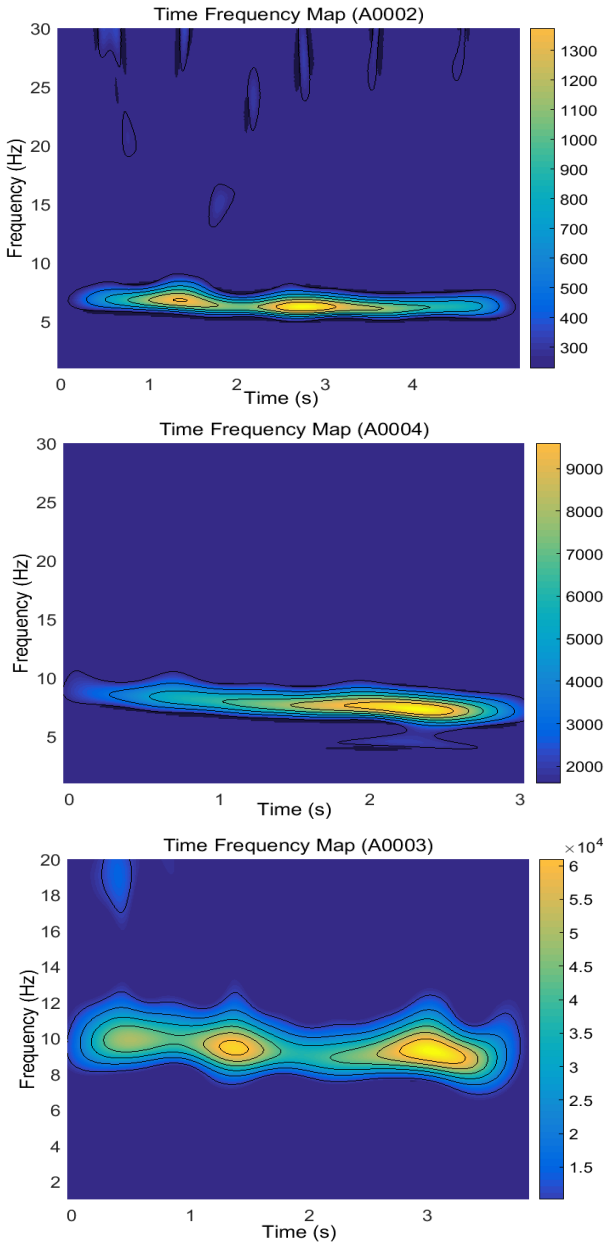

Figure 4.5 Time frequency-energy distribution of seizure onset patterns in each dog

where fp[n] is firing power at time point n, O[k] is the classifier's output, and τ is the number of samples in the preictal state.

4.3.4 Data splitting

Previous seizure-prediction studies lacked adequate performance assessment, giving overoptimistic results. In this work, we ensured reliable performance evaluation while employing frameworks that imitated real clinical scenarios.

Table 4.2 Functional connectivity results averaged across 3 seizures per dog

Dog ID	Sources	Sinks	Frequency range (Hz)
A0002	2, 3, 4	1, 5, 6	(5-8)
A0003	11	1, 2, 4, 9, 14, 16	(8-12)
A0004	13	1, 2, 3, 4, 6, 7, 9, 11, 14	(5-9)

In these continuous, long-term iEEG recordings, seizures occurred in cluster/seizure bursts. Data were grouped into training, validation, and testing. The first cluster in each dog was considered for training and validation while all remaining clusters were targeted for testing. Held-out validation made sure seizures undergoing connectivity analysis were not subjected to validation. Preictal data were divided on a seizure-per-seizure basis to avoid any contamination/time-correlation of the data. Table 4.1 states the number of recording days and number of seizures for each dog as well as data distribution across training, validation and testing.

4.3.5 Performance evaluation

Following the recommendations for reliable and practical seizure prediction systems [17], performance was assessed rigorously in this work. It was evaluated on held-out long-term and continuous test data using 3 measures: sensitivity, time in warning (TIW), and ROC-AUC. TIW is a measure of specificity, representing the fraction of interictal time classified as preictal over interictal duration.

4.4 Results

This section was grouped into 2 main parts showcasing functional connectivity simulations and performance results of the seizure-prediction algorithm. The former covers data segmentation and adequate multivariate AR model order, frequency band of interest, iDTF computation and statistical validation, while the latter discusses performance evaluation, comparison to previous work and selected feature distribution. All methods were implemented on Matlab©. Functional connectivity simulations were performed with eConnectome open source Matlab© Toolbox [24].

4.4.1 Kmeans-DTF: SOZ extent

4.4.1.1 Data segmentation and multivariate autoregressive model

Connectivity analysis was undertaken in 3 seizures per dog. A 3- to 7-second window after seizure onset was selected during regular, highly synchronous EEG activity to ensure quasi-stationarity [4]. In addition, time-varying power spectra were analyzed for each window to make sure frequency content remained stable. As is common in all studies of DTF as a basis for connectivity analysis, optimal AR model order was selected by finding the minimum on Bayesian information criterion (BIC) plots. Segments for which it was impossible to find a clear minimum on BIC plots were discarded as they could have given rise to spurious, non-relevant links. iEEG recordings were fitted with a multivariate AR model by solving Yule-Walker equations with the multichannel Levinson algorithm. Model orders ranged from 2 to 4.

4.4.1.2 Wavelet time-frequency analysis

Wavelet time frequency analysis was based on Morlet mother wavelet to ascertain the frequency range of interest for each seizure. Stereotypical seizure onset patterns were apparent in each dog with a similar frequency range for all seizures of a given dog. Figure 4.5 reports the time-frequency energy distribution of seizure onset patterns.

Upper and lower bounds of frequency bands were 5 to 8 Hz, 8 to 12 Hz, and 5 to 9 Hz for dogs A0002, A0003, and A0004, respectively. Chosen bounds corresponded to frequencies with power values higher than half the maximum power.

4.4.1.3 Transfer matrices computation

iDTFs were computed on the basis of AR coefficients to quantify flow causal patterns within frequency ranges identified through time-frequency analysis. A statistical significance level of 0.01 was considered, and phase shuffling was repeated 1,000 times for each seizure. Three seizures per dog whose onset patterns were adequate for connectivity analysis were selected and then averaged. Figure 4.6 displays averaged transfer matrices H_{ij} for each dog. As already explained, H_{ij} revealed causal interactions from channel x_j to x_i. Although no thresholding or selection was performed, electrodes 11; 2, 3, 4; and 13 could be considered as sources of seizure activity in dogs A0002, A0003 and A0004, respectively.

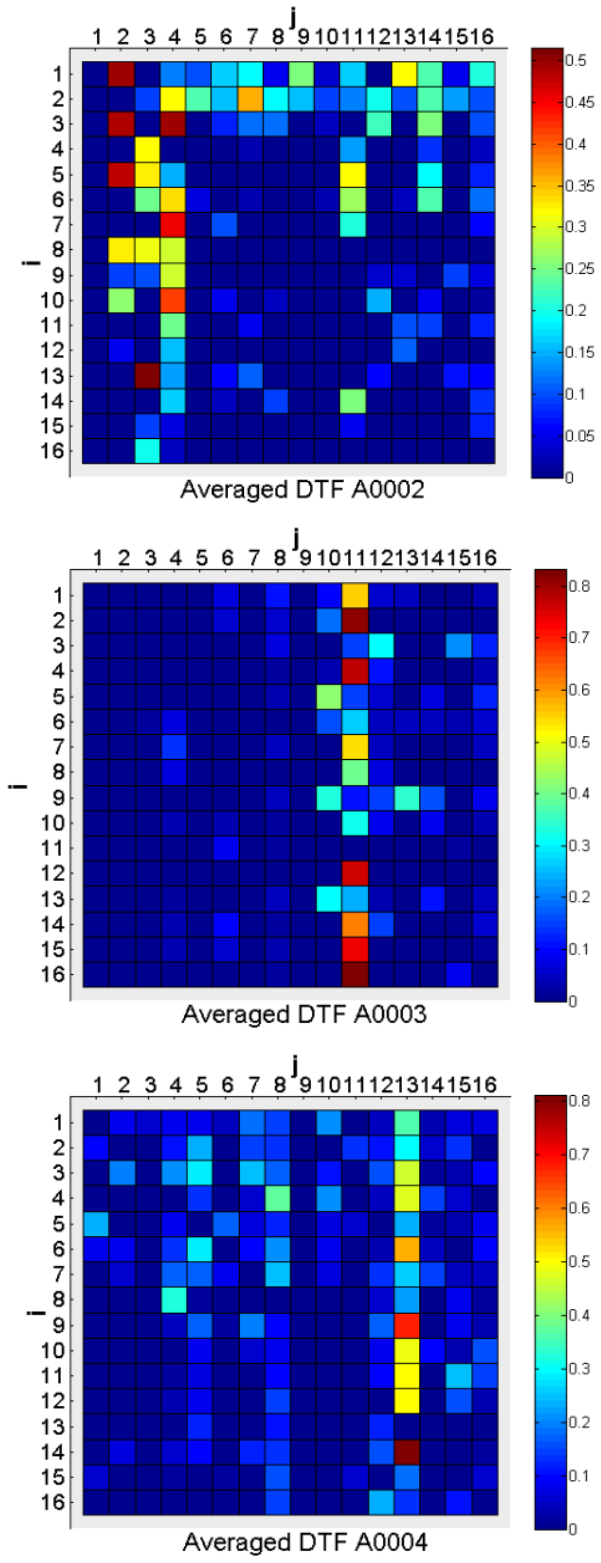

Figure 4.6 Averaged DTFs of all dogs. Electrodes 2, 3 and 4 were identified as sources of seizure activity in dog A0002, 11 in dog A0003, and 13 in dog A0004.

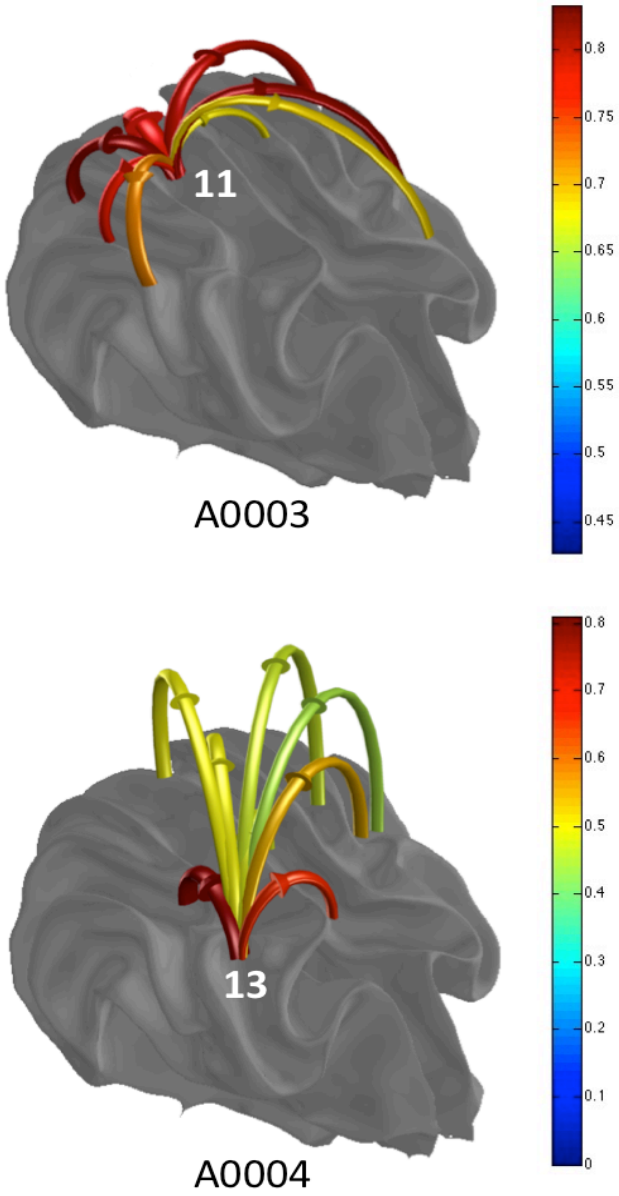

Figure 4.7 Strength of causal interactions in dogs A0003 and A0004. The results highlight inter-hemispheric seizure flow during seizure initiation, even in dogs with focal epilepsy

4.4.1.4 Adaptive selection of sources and sinks

As mentioned in Section II.B.4, seizure activity sources and sinks were identified adaptively via a 3-class Kmeans-clustering approach. Table 4.2 illustrates the connectivity analysis results for each dog, namely, seizure activity sources and sinks, seizure onset patterns, and identified frequency range. Seizures evaluated for source and sink localization were not appraised in validation or testing.

4.4.1.5 Inter-hemispheric activity flow

Interestingly, inter-hemispheric seizure activity flow was apparent in 2 out of 3 dogs with naturally-occurring epilepsy. Epileptic activity generators were focal in all dogs (left hemisphere in A0002 and right hemisphere in A0003 and A0004), confirming the diagnosis of focal epilepsy in these animals. However, seizure activity sinks spanned both hemispheres in dogs A0003 and A0004, indicating communication between both hemispheres during seizure initiation. Figure 4.7 shows causal interaction strength averaged across 3 seizures in dogs A0003 and A0004.

4.4.2 Seizure-prediction algorithm

The results of seizure-prediction performance are presented along with selected feature distribution and compared with previous efforts to implement a seizure prediction algorithm in the same canine database.

4.4.2.1 Seizure prediction: performance evaluation

The proposed forecasting algorithm was implemented on seizure activity sources and sinks as they are involved the most in the epileptogenic network. Table 4.3 presents the performance evaluation results in terms of sensitivity, TIW and AUC. The whole proposed framework was implemented, including the proposed PR-GA. The restriction of 4 hours before or after seizures was not applied on the testing set where continuous iEEG recordings were used. Ictal and post-ictal data were removed from the test continuous recording and their duration was subtracted from interictal duration while calculating TIW. Alarms falling within the IT window were considered as false alarms. Firing power threshold was subject-specific. It was determined by searching different possibilities (from 0 to 1 with 0.05 increments) and choosing the one achieving highest AUC on the validation set. As shown in Fig. 4.8, the firing power technique operates using a moving window equal to preictal time in which the number of samples classified as preictal was calculated. After threshold crossing (in an ascending way), an alarm was raised for a duration equal to the preictal time (meaning the dog can have a seizure at some point in the next hour). No other alarms were permitted during the warning period. Average sensitivity of 84.42%, TIW of 0.1, and AUC of 0.87 were achieved with 1-hour preictal time (5 min IT).

4.4.2.2 Comparison with previous work

Interestingly, the long-term canine data in this work are freely available through the iEEG.org portal which allows benchmarking with studies sharing the same databases.

Table 4.3 Seizure-forecasting results

Dog	# of seizures	# of selected electrodes	Preictal time	# of electrode feature combinations	Population size (GA)	Firing power threshold	SS (%)	TIW	AUC
A0002	83	6	60 min	21	168	0.35	87.50	0.21	0.83
			30 min	19		0.30	91.66	0.09	0.91
A0003	27	7	60 min	24	196	0.30	81.25	0.08	0.86
			30 min	24		0.35	81.25	0.19	0.81
A0004	15	10	60 min	21	280	0.35	85.71	0.01	0.92
			30 min	18		0.35	71.42	0.21	0.85

Howbert et al implemented a seizure prediction algorithm, combining spectral power features with a logistic regression classifier, and reported their results on the same 3 dogs in our study [11]. Table 4.4 compares this study with previous works [11]. Although different algorithmic strategies were adopted in both studies, which restricted direct inference, the proposed methodology delivered higher performance. Higher sensitivity and lower TIW were noted for all 3 dogs. Recently, a seizure prediction competition was held on Kaggle.com reporting promising performances [25]. Direct result comparisons with our findings is difficult as different perspectives were adopted in the competition namely, data structure, human and canine recordings and generic algorithmic strategies. The contest required classification of non-continuous 10-minute intracranial EEG clips labeled as “preictal” and “interictal” and testing data was provided in a random order. In this manuscript, the algorithm operated on long-term continuous intracranial EEG recordings. Competition administrators tailored an adaptive data structure dedicated for data science competitions (differentiate between preictal and interictal clips by assigning a single score to each 10-min clip). In this work, we used all continuous iEEG recordings available through the iEEG.org portal. The Kaggle seizure prediction contest involved both human and canine iEEG recordings. Our study involves only canine recordings. The objective of the contest was to find a single algorithm able to classify preictal and interictal labeled clips. In this work, we designed subject-specific algorithms individually tailored for each dog. Although points discussed above restrict direct inference, comparable results were achieved. The mean AUC score on the held-out data was 0.74 (Six Winning teams, Max: 0.79, Min: 0.59) in the Kaggle context. Our algorithm achieved an average AUC of 0.87 when considering a preictal time of 1 hour with a 5-min IT on held-out test data.

Table 4.4 Comparison with previous work

Dog	SS (%) in this work	TIW in this work	SS (%) in [11]	TIW in [11]
A0002	87.50	0.21	66.7	0.2
A0003	81.25	0.08	73.3	0.3
A0004	85.71	0.01	75.9	0.1
Average	**84.82**	**0.1**	**71.96**	**0.2**

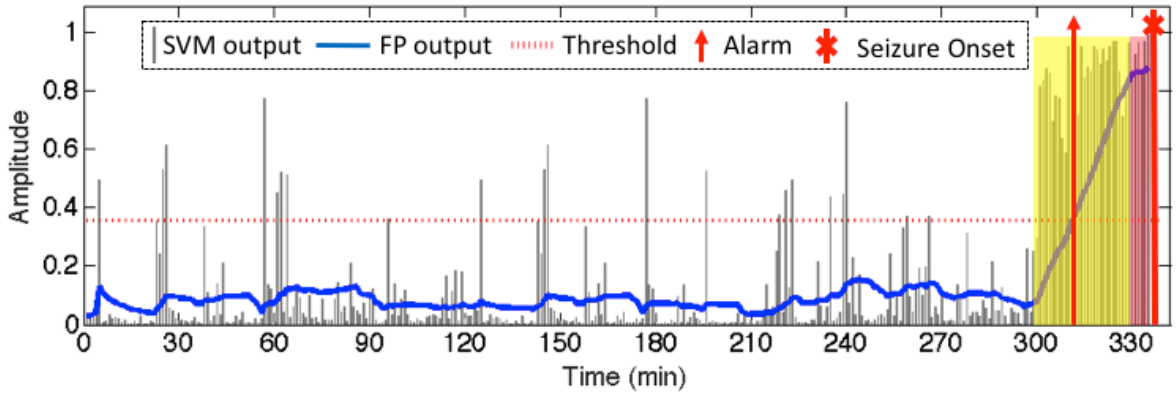

Figure 4.8 Alarms generation based on the Firing power technique. Area highlighted in yellow and red respectively depict a 30 min preictal time and 5 min IT. Blue and black lines represent the firing power output and probabilistic support vector machine output respectively. The vertical red line and arrow respectively indicates seizure onset and generated alarm. Any alarm generated during the preictal period (highlighted in yellow) is considered as true

4.4.2.3 Selected features distribution

The selected features in each of the 3 dogs were different, confirming the need for patient-specific, individually-tailored algorithms. Band power features, mainly the gamma band, were selected most frequently (37%). These features have already demonstrated their superiority in seizure-prediction studies [7], [8], [17], [26]. Figure 4.9 reports selected feature distribution in all 3 dogs.

4.4.2.4 Preictal time choice

Since recent seizure prediction investigations have reported good performances for preictal times in the range of 30 minutes [7], [8], [27], a similar preictal period with 5-minutes intervention time was also adopted in this work. As seen in Table III and in line with previous findings, preictal

time was subject-specific with better average performance for a preictal time of 1 hour with a 5-min intervention time.

4.5 Discussion

The benefits of this study confront 2 research communities. We start by proposing a quantitative and automatic functional connectivity framework to localize SOZ in bilateral iEEG recordings of dogs with naturally-occurring epilepsy. Then, a seizure-prediction algorithm is implemented on electrodes in the identified SOZ. The purpose behind proposing such a methodology is to prospectively determine if electrodes within SOZ allow good prediction of epileptic seizures and thus contain ictal activity generators. This could lead to better and more precise delineation of epileptogenic zones. Such promising performances may encourage researchers to prospectively perform quantitative source localization methods for presurgical evaluation. To our knowledge, no previous seizure prediction investigations have undertaken functional connectivity-based electrode selection prior to implementing their seizure prediction algorithm. With this methodology, we assume that selecting electrodes through functional connectivity analysis allows the identification of those recording electrical potentials over seizure activity generators and sinks and are thus more suitable for seizure forecasting.

In all 3 dogs, seizure activity sources were focal and localized in 1 hemisphere, confirming the focal nature of epilepsy in these animals. However, seizure spread shows an inter-hemispheric nature, which indicates that, although not adopted in earlier seizure prediction studies, bilateral iEEG recordings may represent added value in seizure forecasting.

In addition, Kmeans-DTF allowed a sort of electrode selection based on raw data and overcoming computation constraints of the GA.

In the seizure prediction part, we ensured rigorous methodology and adequate performance evaluation to avoid overoptimistic results. The following points were considered:

- Continuous, long-term iEEG recordings
- Data splitting into training, validation and testing
- Held-out validation and testing
- Splitting on a seizure-per-seizure basis to avoid contamination or time correlation
- Scaling parameters (Z-score) were computed on train sets only and used for validation and testing.

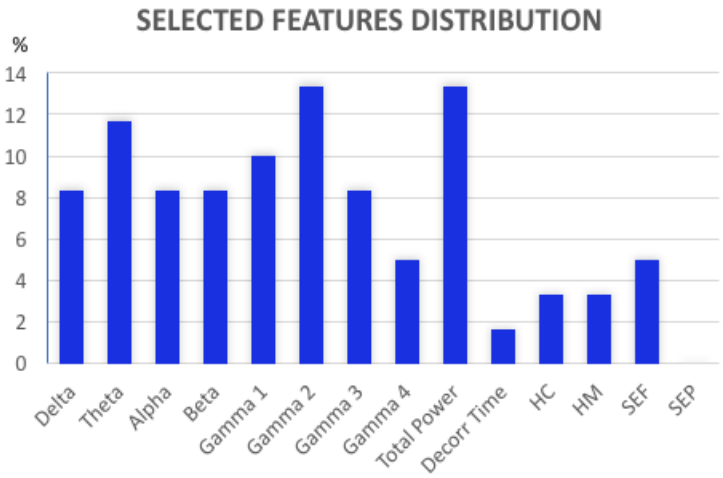

Figure 4.9 Selected features distribution

The seizure prediction algorithm showed good performance on all 3 dogs with average sensitivity of 84.82% and TIW of 0.1. Recently, our group proposed a GA-based feature selection method for seizure prediction [18]. However, the GA fitness function was the classification loss of the K-Nearest Neighbor classifier which requires under-sampling the interictal class to balance the preictal one, resulting in non-optimal optimization. In this work, proposing the PR-AUC fitness function allowed inclusion of the whole interictal training set in the algorithm's cost function. To our knowledge, no previous seizure prediction investigations have explored fitness function insensitive to skewed class distribution. Common methodology has randomly under-sampled the interictal class prior to problem optimization or classification. On the other side, the fitness function was based on a probabilistic SVM which was in line with the classification methodology undertaken in this work. The proposed methodology includes the firing power technique as a regularization function. Another advantage of this technique relies on a threshold for alarm generation. The threshold allows compromising between sensitivity and specificity and subsequently adjusts them according to the context of use (advisory/intervention).

A preictal time of 1 hour gave better average predictive performance in terms of sensitivity, TIW and AUC. However, since the firing power technique regularization method structurally increases specificity with longer preictal periods, care must be taken to avoid generalizing the findings to studies using different post-processing techniques.

In a recent clinical trial, Cook et al. 2013 designed a system that includes a series of advisory lights depending on seizure likelihood (low, moderate, or high) [28]. Considering the

probabilistic SVM output adopted in our design, the implementation of an output similar to that proposed in [28] is feasible and will be considered in future investigations.

Reducing the number of electrodes enables a more exhaustive feature search to be conducted (in the case of the genetic algorithm) to determine the most useful features to identify the preictal state. Given limitations in benchmarking prediction performances, sometimes within the same dataset [29], it might have been useful to provide some internal benchmark. However, the algorithmic structure adopted in this work restricts a reliable internal benchmark. Due to the iterative nature of the genetic algorithm and given it starts from a random initial population; it was unfair to compare the performance with other strategies. Furthermore, to be able to perform such an internal benchmark, high computational resources are needed to reach a point where the genetic algorithm has relatively converged in all cases and where it might be possible to compare internal results. This goes beyond the perspectives of this manuscript but will be addressed in future work.

In this work, seizure activity generators/sources were identified on the basis of available iEEG coverage; thus, SOZ may not have been totally sampled. However, the proposed scheme ensured that identified electrodes were the closest to SOZ as seizure activity generators/sources feature the highest causal interactions within the ictal frequency range. Another limitation was the relatively low sampling frequency (400 Hz). Our group is currently assessing the value of the same analytical framework on high-density iEEG recordings obtained from epileptic patients sampled at 2,000 Hz.

4.6 Conclusion

This work can be considered as a “proof of principle” evaluation of seizure forecasting in canine epilepsy. A seizure prediction algorithm was proposed after adaptively identifying seizure activity sources and sinks. The proposed Kmeans-DTF method allowed a quantitative delineation of SOZ in bilateral iEEG recordings avoiding inaccuracies induced by EEG visual interpretations. The use of continuous and long-term EEG recordings (several months duration) allowed performing adequate assessment of the methods presented in this study, a main challenge encountered in prior seizure prediction investigations. The scarcity of EEG recordings and short duration of interictal periods were previously considered as major constraints to proper assessment of false positive rates. The results highlight the possibility of seizure forecasting in canine epilepsy and subsequently the development of an EEG-triggered closed-loop seizure

intervention system for ambulatory implantation in epileptic patients. Final judgment can be made after assessing the proposed framework in a significant number of epileptic patients.

4.7 Acknowledgments

The authors acknowledge financial support from the Natural Sciences and Engineering Research Council of Canada, the Agence universitaire de la francophonie, and the Higher Center of Research-USEK.

4.8 References

[1] J. Tellez-Zenteno, L. Hernandez Ronquillo, F. Moien-Afshari, S. Samuel Wiebe, Surgical outcomes in lesional and non-lesional epilepsy: a systematic review and meta-analysis, *Epilepsy Research*, vol. 89, 2010.

[2] H. Stefan, F.H. Lopes da Silva, Epileptic Neuronal Networks: Methods of Identification and Clinical Relevance, *Frontiers in Neurology*, vol. 4, 2013.

[3] C.W.J. Granger, Investigating Causal Relations by Econometric Models and Cross-spectral Methods, *Econometrica*, vol. 37, 1969.

[4] C. Wilke, W. van Drongelen, M. Kohrman, B. He, Neocortical seizure foci localization by means of a directed transfer function method, *Epilepsia*, vol. 51, 2010.

[5] E.B. Assi, M. Sawan, D.K. Nguyen, S. Rihana, A 2D clustering approach investigating inter-hemispheric seizure flow by means of a Directed Transfer Function, in: *2016 3rd Middle East Conference on Biomedical Engineering (MECBME)*, 2016, pp. 68-71.

[6] K. Gadhoumi, J.-M. Lina, F. Mormann, J. Gotman, Seizure prediction for therapeutic devices: A review, *Journal of Neuroscience Methods*, vol. 260, 2015.

[7] C. Alexandre Teixeira, B. Direito, M. Bandarabadi, M. Le Van Quyen, M. Valderrama, B. Schelter, A. Schulze-Bonhage, V. Navarro, F. Sales, A. Dourado, Epileptic seizure predictors based on computational intelligence techniques: A comparative study with 278 patients, *Computer Methods and Programs in Biomedicine*, vol. 114, 2014.

[8] E. Bou Assi, D.K. Nguyen, S. Rihana, M. Sawan, Towards accurate prediction of epileptic seizures: A review, Biomedical Signal Processing and Control, vol. 34, 2017.

[9] K.A. Davis, B.K. Sturges, C.H. Vite, V. Ruedebusch, G. Worrell, A.B. Gardner, K. Leyde, W.D. Sheffield, B. Litt, A novel implanted device to wirelessly record and analyze continuous intracranial canine EEG, *Epilepsy Research*, vol. 96, 2011.

[10] K. Chandler, Canine epilepsy: What can we learn from human seizure disorders?, *The Veterinary Journal*, vol. 172, 2006.

[11] J.J. Howbert, E.E. Patterson, S.M. Stead, B. Brinkmann, V. Vasoli, D. Crepeau, C.H. Vite, B. Sturges, V. Ruedebusch, J. Mavoori, K. Leyde, W.D. Sheffield, B. Litt, G.A. Worrell, Forecasting Seizures in Dogs with Naturally Occurring Epilepsy, *PLoS ONE*, vol. 9, 2014.

[12] B.H. Brinkmann, E.E. Patterson, C. Vite, V.M. Vasoli, D. Crepeau, M. Stead, J.J. Howbert, V. Cherkassky, J.B. Wagenaar, B. Litt, G.A. Worrell, Forecasting Seizures Using Intracranial EEG Measures and SVM in Naturally Occurring Canine Epilepsy, *PLoS ONE*, vol. 10, 2015.

[13] M. Kaminski, M. Ding, W.A. Truccolo, S.L. Bressler, Evaluating causal relations in neural systems: granger causality, directed transfer function and statistical assessment of significance, *Biol. Cybern*., vol. 85, 2001.

[14] R. Kus, M. Kaminski, K.J. Blinowska, Determination of EEG activity propagation: pair-wise versus multichannel estimate, *IEEE Transactions on Biomedical Engineering*, vol. 51, 2004.

[15] E.B. Assi, S. Rihana, M. Sawan, Kmeans-ICA based automatic method for ocular artifacts removal in a motor imagery classification, in: *2014 36th Annual International Conference of the IEEE Engineering in Medicine and Biology Society*, IEEE, Chicago, IL, 2014.

[16] E. B. Assi, S. Rihana, Kmeans-ICA based automatic method for EOG denoising in multi-channel EEG recordings, in: *11th IASTED International Conference on Biomedical Engineering*, Zurich, Switzerland, 2014.

[17] F. Mormann, R.G. Andrzejak, C.E. Elger, K. Lehnertz, Seizure prediction: the long and winding road, *Brain*, vol. 130, 2007.

[18] E.B. Assi, M. Sawan, D.K. Nguyen, S. Rihana, A hybrid mRMR-genetic based selection method for the prediction of epileptic seizures, in: *Biomedical Circuits and Systems Conference (BioCAS)*, IEEE, 2015, pp. 1-4.

[19] B. Direito, F. Ventura, C. Teixeira, A. Dourado, Optimized feature subsets for epileptic seizure prediction studies, in: *Annual International Conference of the IEEE Engineering in Medicine and Biology Society (EMBC)*, 2011, pp. 1636-1639.

[20] J. Davis, M. Goadrich, The relationship between Precision-Recall and ROC curves, in: *Proceedings of the 23rd international conference on Machine learning,* Pittsburgh, Pennsylvania, USA, 2006, pp. 233-240.

[21] B. Bhanu, Y. Lin, Genetic algorithm based feature selection for target detection in SAR images, *Image and Vision Computing*, vol. 21, 2003.

[22] J. Platt, Probabilistic Outputs for Support Vector Machines and Comparisons to Regularized Likelihood Methods, in: *Advances in large margin classifiers*, 1999, pp. 61-74.

[23] C. Teixeira, B. Direito, M. Bandarabadi, A. Dourado, Output regularization of SVM seizure predictors: Kalman Filter versus the "Firing Power" method, in: *Annual International Conference of the IEEE Engineering in Medicine and Biology Society*, IEEE, San Diego, CA, 2012.

[24] B. He, Y. Dai, L. Astolfi, F. Babiloni, H. Yuan, L. Yang, eConnectome: A MATLAB Toolbox for Mapping and Imaging of Brain Functional Connectivity, *Journal of neuroscience methods*, vol. 195, 2011.

[25] B.H. Brinkmann, J. Wagenaar, D. Abbot, P. Adkins, S.C. Bosshard, M. Chen, Q.M. Tieng, J. He, F.J. Muñoz-Almaraz, P. Botella-Rocamora, J. Pardo, F. Zamora-Martinez, M. Hills, W. Wu, I. Korshunova, W. Cukierski, C. Vite, E.E. Patterson, B. Litt, G.A. Worrell, Crowdsourcing reproducible seizure forecasting in human and canine epilepsy, *Brain*, vol. 139, 2016.

[26] Y. Park, L. Luo, K.K. Parhi, T. Netoff, Seizure prediction with spectral power of EEG using cost-sensitive support vector machines, Epilepsia, vol. 52, 2011.

[27] M. Bandarabadi, C.A. Teixeira, J. Rasekhi, A. Dourado, Epileptic seizure prediction using relative spectral power features, *Clinical Neurophysiology*, vol. 126, 2015.

[28] M.J. Cook, T.J. O'Brien, S.F. Berkovic, M. Murphy, A. Morokoff, G. Fabinyi, W. D'Souza, R. Yerra, J. Archer, L. Litewka, S. Hosking, P. Lightfoot, V. Ruedebusch, W.D. Sheffield, D. Snyder, K. Leyde, D. Himes, Prediction of seizure likelihood with a long-term, implanted seizure advisory system in patients with drug-resistant epilepsy: a first-in-man study, *The Lancet Neurology*, vol. 12, 2013.

[29] I. Korshunova, P.J. Kindermans, J. Degrave, T. Verhoeven, B.H. Brinkmann, J. Dambre, Towards improved design and evaluation of epileptic seizure predictors, *IEEE Transactions on Biomedical Engineering*, vol. 65, 2018.

CHAPTER 5 ARTICLE 2 EFFECTIVE CONNECTIVITY ANALYSIS OF OPERCULO-INSULAR SEIZURES

Elie Bou Assi[1], Dang K. Nguyen[2], Sandy Rihana[3] and Mohamad Sawan[1]

[1]Polystim Neurotech Lab, Institute of Biomedical Engineering, Polytechnique Montreal, Montreal, QC, Canada
[2]University of Montreal Hospital Center (CHUM), University of Montreal, Montreal, QC, Canada
[3]Biomedical Engineering Department, Holy Spirit University of Kaslik (USEK), Jounieh, Lebanon

This paper presents the second objective of this thesis, namely the feasibility of quantitative identification of sources and sinks of seizure activity using high density iEEG recordings. We restricted ourselves to a relatively homogeneous group of patients with apparent operculo-insular epilepsy, due to several reasons. These include: 1) the insula is a highly connected brain structure, characterized by fast spreading seizure, thus creating a challenge for localization by means of the swADTF; 2) access to insular recordings was possible given that the CHUM is well-recognized for this particular type of epilepsy and 3) the swADTF was previously tested on temporal lobe epilepsy recordings but not on other types of focal epilepsy. This work was presented as part of insular neural networks investigator workshop at the 71st Annual meeting of the American Epilepsy Society (December 2017, Washington, D.C.) and the manuscript was submitted to Epilepsy Research in July 2018.

5.1 Abstract

Recognition of insular epilepsy may sometimes be challenging due to the rapid speed at which insular seizures can spread throughout the cortex via extensive connections to surrounding cortices. The spectrum weighted adaptive directed transfer function, a multivariate causality-based effective connectivity measure, was applied to intracranial electroencephalography recordings to identify generators of seizure activity. A non-parametric test based on surrogate data testing was used to validate statistical significance of causal relations. Outflow and inflow of seizure activity were extracted from the computed transfer matrix. Recorded data from seven patients were analyzed including five who were rendered seizure-free after operculo-insular resection. Results confirmed an operculo-insular seizure origin in patients with a good post-operative seizure outcome, and for whom the resected region was sampled by intracranial electroencephalography contacts. Different or additional seizure foci were identified in patients

with a bad post-operative seizure outcome. Findings highlight the feasibility of accurate operculo-insular seizure foci localization based on quantitative approaches.

Keywords: Insular Epilepsy, Effective connectivity, Intracranial electroencephalography, Autoregressive modeling, Spectrum weighted adaptive directed transfer function.

5.2 Introduction

Epilepsy is a chronic condition characterized by recurrent seizures (or 'ictus') resulting from abnormal and excessive neuronal discharges. When antiepileptic drugs fail to control seizures, surgical resection of the epileptic focus is recommended if it can be delineated by a set of tests which often include qualitative visual interpretation of intracranial electroencephalography (iEEG) recordings of seizures. Several authors have recently applied quantitative effective connectivity analyses on such recordings to characterize the complex epileptic network of the different brain areas involved in the generation, propagation, and modulation of seizures. By exploiting temporal precedence among a set of signals to reveal information transfers from 'driver' to 'secondary' nodes of the network, effective connectivity analyses may help understand seizure semiology and optimize delineation of the area to be resected for seizure cure [1, 2]. Until now, such methods have mainly been used to analyze temporal or frontal lobe seizures [1, 3-5]. While little attention has been given to insular seizures [6], effective connectivity measures could possibly help explain the diversity in their ictal symptoms and facilitate their identification knowing how complex their ictal intracranial EEG patterns can be (often with the involvement of several distinct structures in as much that visual identification of the area of seizure onset is difficult) [7].

Highly connected to surrounding frontal, temporal and parietal lobes [8], the insula is a multimodal area involved in the processing of several sensory stimuli (viscerosensory, somatosensory, auditory, gustatory, and olfactory) and cognitive processes (attention, social cognition, and decision-making) [9]. Such structural and functional connectivity considerations may explain why insular seizures are diverse in terms of EEG patterns but also in clinical presentation such as early viscerosensory auras (common in temporal lobe seizures), somatosensory auras (as in parietal lobe seizures) and hypermotor symptoms (resembling frontal lobe seizures) [10]. Such mimicry has most likely misled some clinicians into thinking that their patients, suffering from insular epilepsy, had temporal, frontal or parietal lobe seizures leading to the resection of the wrong cortical area [11].

Table 5.1 Clinical caracteristics of patients

Patient ID	Gender	DOB	Epilepsy duration (Y)	SOZ	Side	MRI	# of iEEG contacts	Outcome (Engel)	Follow-up (years)
1	F	1974	33	aINS + F op	L	N	110	IA	5
2	M	1967	9	pIINS	L	N	61	IB	4
3	M	1975	10	supINS + F op	R	N	100	IA	7
4	M	1965	31	pINS, P op/T op	L	N	91	IA	5
5	F	1997	9	sup INS, F op	L	N	114	IA	2
6	F	1977	14	pINS, T op/P op	R	N	74	IIIA	5
7	M	1975	4	aINS, F op	R	N	112	IIIA	2

F: female; M: male; DOB: date of birth; Y: years; aINS: anterior insula; F op: frontal operculum; pINS: posterior insula; supINS: superior insula; P op: parietal operculum; T op: temporal operculum; L: left; R: right, MRI: magnetic resonance imaging, N: normal

A long list of measures has been proposed for the study of effective connectivity and neuronal network dynamics. Compared to bivariate measures, multivariate approaches showed more accurate performances in estimating causal relations during seizure initiation and spread [12, 13]. The directed transfer function (DTF), a multivariate directional connectivity measure, has been validated for quantifying causal relations when quasi-stationarity requirements are met [5, 14]. Although quasi-stationary EEG signals can be identified when analyzing a relatively small number of electrodes, it is more difficult when dealing with a higher number of electrodes. To cope with stationarity issues, Wilke et al. (2008) proposed the Adaptive Directed Transfer Function (ADTF), a time varying version of the DTF [15]. However, for both DTF and ADTF, visual analysis remained necessary for identifying frequency ranges of interest. Subsequently, the spectrum weighted ADTF (swADTF) was proposed, taking into account the full frequency range of the signal and weighting each element of the transfer matrix by the sending channel's auto spectrum [1,3]. In this study, we investigate the effective connectivity of apparent operculo-insular seizures of different semiology using the swADTF.

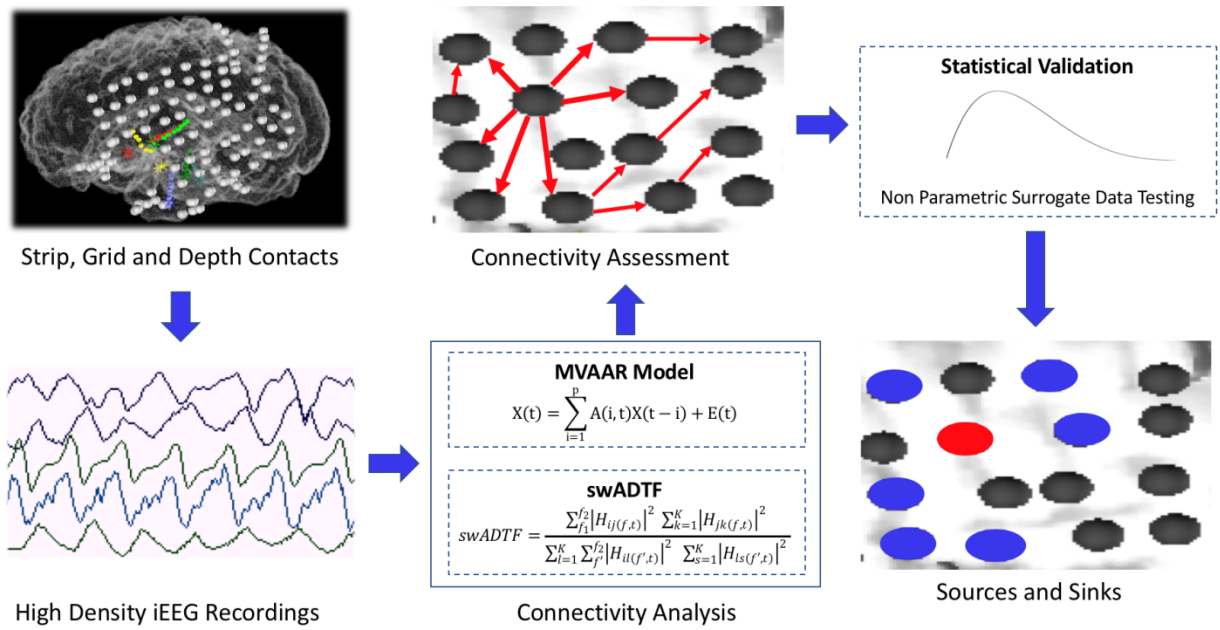

Figure 5.1 Framework of the swADTF-based connectivity implementation (iEEG: intracranial electroencephalography; MVAAR: multivariate adaptive autoregressive model; swADTF: spectrum weighted adaptive directed transfer function)

5.3 Materials and Methods

Figure 5.1 shows the block diagram of the implemented swADTF-based connectivity analysis framework. High-density iEEG recordings following onset of ictal seizure activity were first selected. Connectivity between iEEG electrodes was obtained by applying the swADTF to iEEG time series. Statistical validation was performed by means of surrogate data testing. Outflow and inflow values were quantified, and seizure activity sources and sinks were identified.

5.3.1 Patients

Intracranial EEG recordings of seven patients diagnosed with insulo-opercular epilepsy were retrospectively analyzed (Table 5.1). Patients were selected based on the following inclusion criteria: (1) seizure onset zone located within the insula (with or without extension to the adjacent operculum) as assessed by the clinician of the iEEG study; (2) iEEG electrodes sampled the insula, opercula, as well as temporal, parietal or frontal structures. In 5 patients, focal cortical resection of the seizure onset zone resulted in a good seizure outcome (Engel I) with at least two years of follow-up. The two remaining patients had a poor outcome (Engel IIIA).

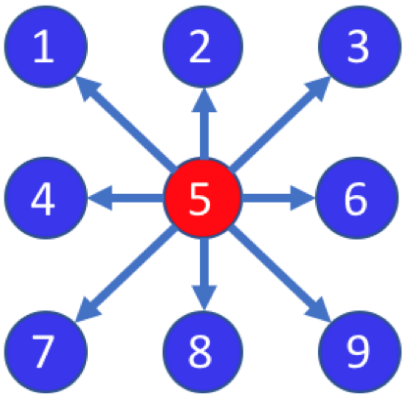

Figure 5.2 Graphical node illustration of the simulated propagation pattern. Node 5 was simulated as a generator of seizure activity that propagates to all remaining nodes (sinks).

Raw iEEG signals were acquired using the Harmonie monitoring system (Stellate Systems Inc.), sampled at 2000 Hz and filtered at 500 Hz. The research protocol was approved by our local ethical research committee.

5.3.2 Spectrum weighted adaptive directed transfer function

For each patient, three iEEG-recorded seizures were randomly chosen and analyzed using swADTF. The ADTF allows investigating time-varying connectivity patterns and does not entail stationarity requirements. It is based on a multivariate adaptive auto regressive model (MVAAR) [15] (1):

$$X(t) = \sum_{i=1}^{p} A(i,t)X(t-i) + E(t) \quad (1)$$

where X(t) is a multivariate signal, A(i,t) is a matrix gathering time varying model coefficients, E(t) is the error matrix and p is the model order.

Non-linear Kalman filtering, based on a combination of observation and state space equations, was used to estimate model's time varying coefficients [15]. The frequency domain transfer matrix $H_{ij}(f,t)$ is obtained by Fourier transforming equation (1). $H_{ij}(f,t)$ displays causal relations from the electrode j to electrode i at time instant t and frequency f.

Although the clinical validity of the ADTF has been demonstrated [15], Mierlo et al. 2013 found that at some frequency f and time t, the term $H_{ij}(f,t)$ may be high even though power of signal j is relatively low [1]. They subsequently proposed the swADTF in which $H_{ij}(f,t)$ is divided by the auto spectrum of the sending channel (2).

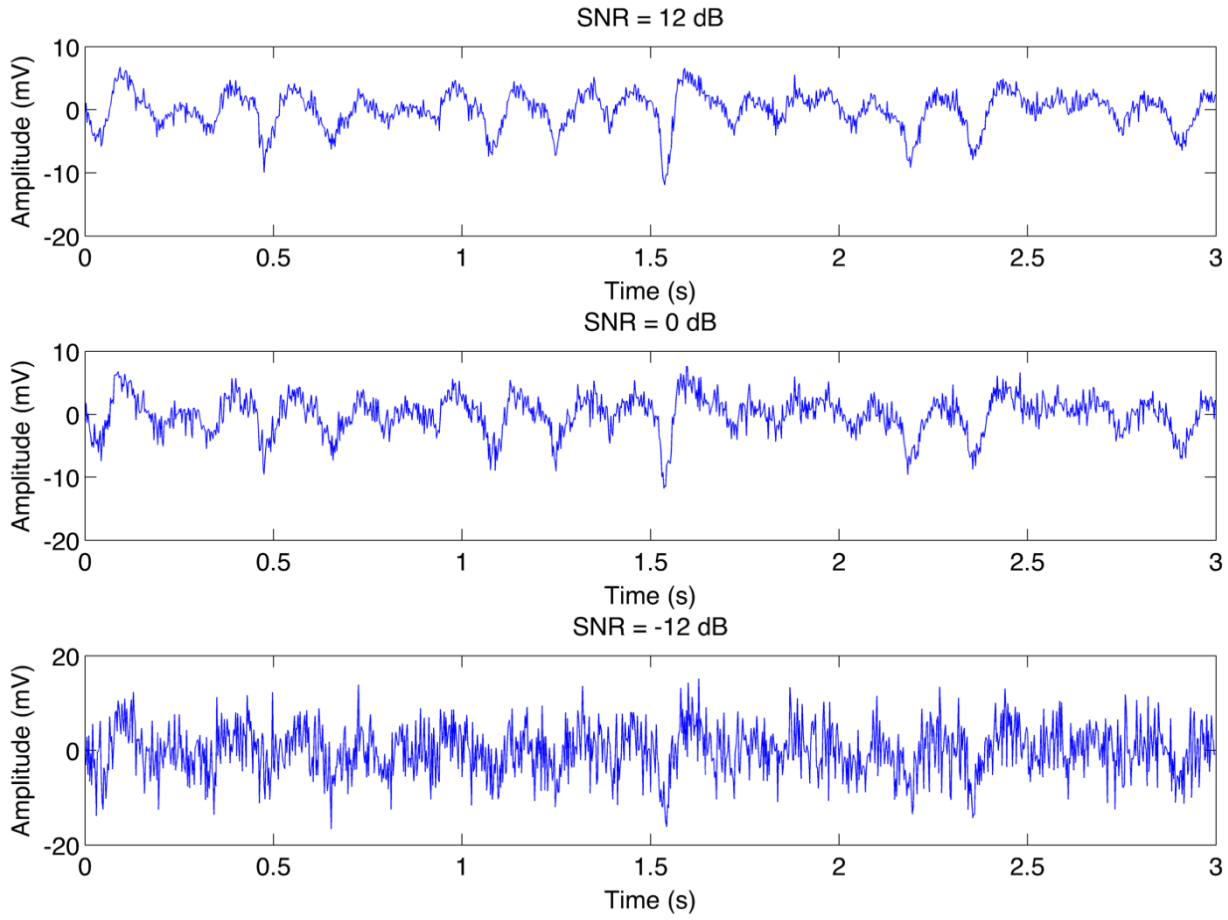

Figure 5.3 Illustrative one-channel raw iEEG recordings with different SNRs. top: SNR = 12 dB; middle: SNR = 0 dB; bottom: SNR= -12 dB. A Gaussian white noise was added with SNRs ranging from -12 dB to 12 dB to assess the proposed framework's robustness to noise; SNR: Signal to noise ratio.

$$swADTF_{ij}(\mathrm{t}) = \frac{\sum_{f=f_1}^{f_2} |H_{ij(f,t)}|^2 \sum_{k=1}^{K} |H_{jk(f,t)}|^2}{\sum_{l=1}^{K} \sum_{f'=f_1}^{f_2} |H_{il(f',t)}|^2 \sum_{s=1}^{K} |H_{ls(f',t)}|^2} \quad (2)$$

where f1 and f2 are frequency bounds of interest, and K is the total number of channels.

Three seizures per patient were randomly chosen and seizure onset was marked by an expert epileptologist (DKN). For each seizure, an ictal segment from 5sec prior to 7sec after the labeled onset was selected for analysis. Extracted epochs were bandpass [0.5 – 40 Hz] filtered using a 6th order zero-phase Butterworth filter. Filtered iEEG signals were then standardized (mean subtraction, and standard deviation division) to avoid any amplitude-based bias. Multivariate autoregressive model orders were adaptively determined by finding the minimum on the Bayesian Information Criterion plot for each individually analyzed seizure [5].

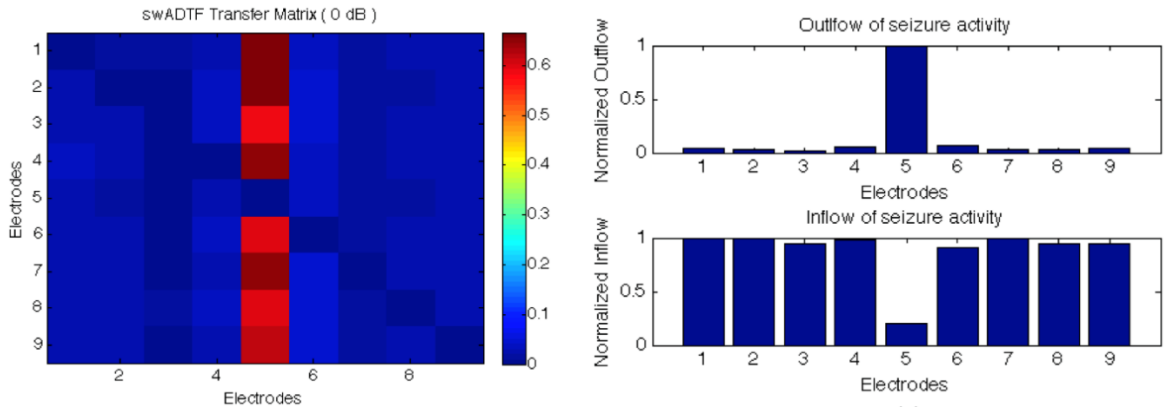

Figure 5.4 Simulation results: swADTF transfer matrix (left), outflow (right, top) and inflow (right, bottom) of seizure activity

Minimum and maximum model order limits were respectively fixed to 1 and 10 with unity increments and an update coefficient of 0.001 was used to compute model coefficients [1].

5.3.3 Surrogate data testing

The swADTF exhibits a highly non-linear relation with the time series from which it is derived resulting in a fairly well-established estimators' distribution under the null hypothesis of no causal interaction. Subsequently, a non-parametric statistical test is required to validate the statistical significance of causal relations among iEEG channels. Surrogate data testing was performed by independently and randomly shuffling Fourier transform phases, thus resulting in a new time series (surrogate). Replicating this operation several times creates an empirical distribution of computed swADTF values under the null hypothesis of no interaction. Statistical significance of causal interactions is then assessed through comparison to the generated empirical/random distribution. The shuffling was repeated 1000 times and a significance level of 0.05 was considered.

5.3.4 Outflow and inflow of seizure activity

Since the swADTF displays causal relations from channel j to channel i, outflow of seizure activity (from channel j to all remaining ones) can be quantified by integrating and normalizing across the transfer matrix's columns (3). Similarly, seizure activity inflow can be determined by repeating the same procedure across the rows of the transfer matrix (4).

$$Outflow(j) = \frac{\sum_{i=1}^{K} swADTF_{ij}}{K} \quad (3)$$

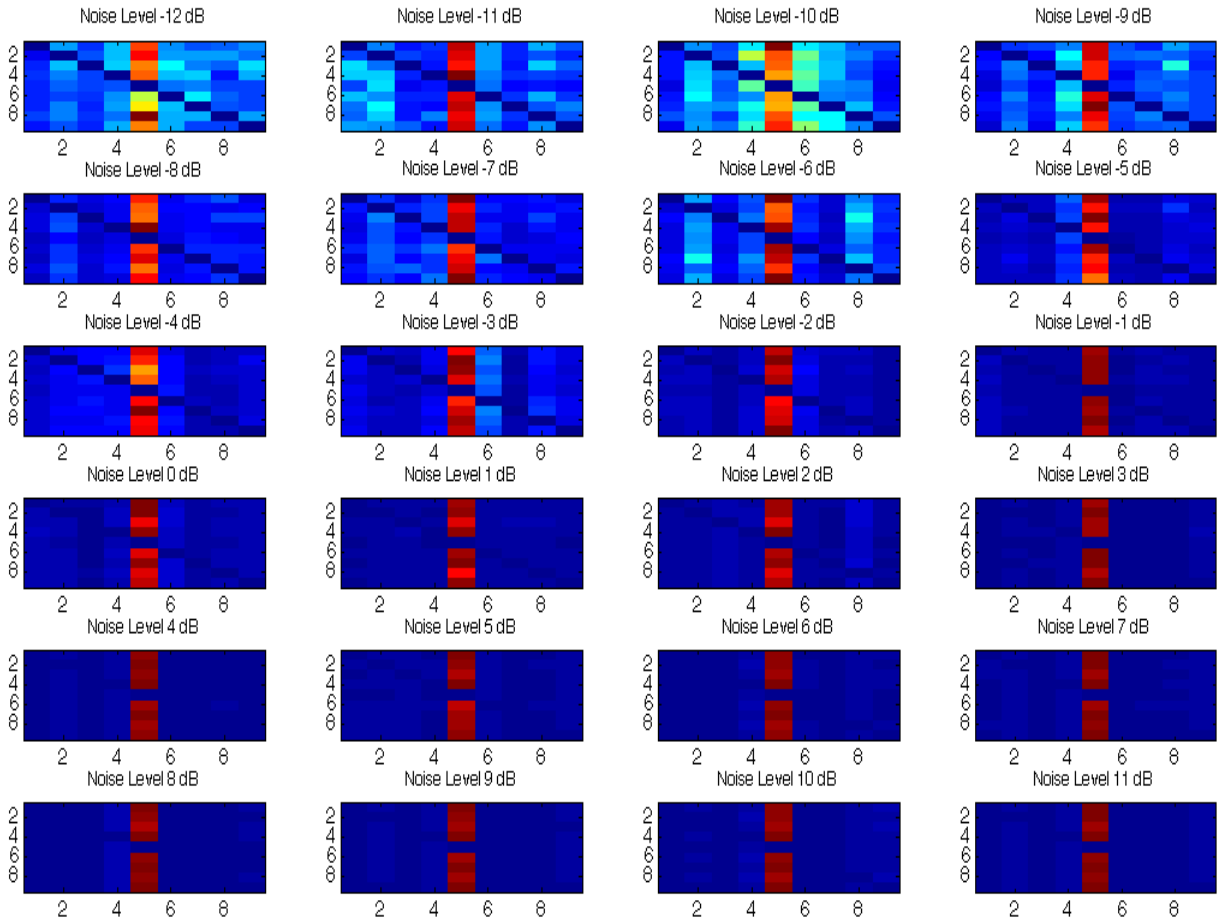

Figure 5.5 Noise simulation results (-12 dB ≤ SNR ≤ 11 dB): The swADTF is stable in identifying node 5 as the generator of seizure activity. Noise simulation results highlight swADTF's resistance to noise for a SNR as low as -12 dB.

$$Inflow\ (i) = \frac{\sum_{j=1}^{K} swADTF_{ij}}{K} \tag{4}$$

for i=1 to K, and j=1 to K where K is the total number of channels.

High outflow or inflow values indicate that a given electrode can be respectively considered as a source or sink of seizure activity. In line with previous investigations, the electrode contact exhibiting the highest outflow across each analyzed seizure was considered the ictal generator [1]. In contrast, to assess the spread of ictal activity, sinks of seizure activity were electrode contacts exhibiting inflow values higher than 80% the maximal inflow value.

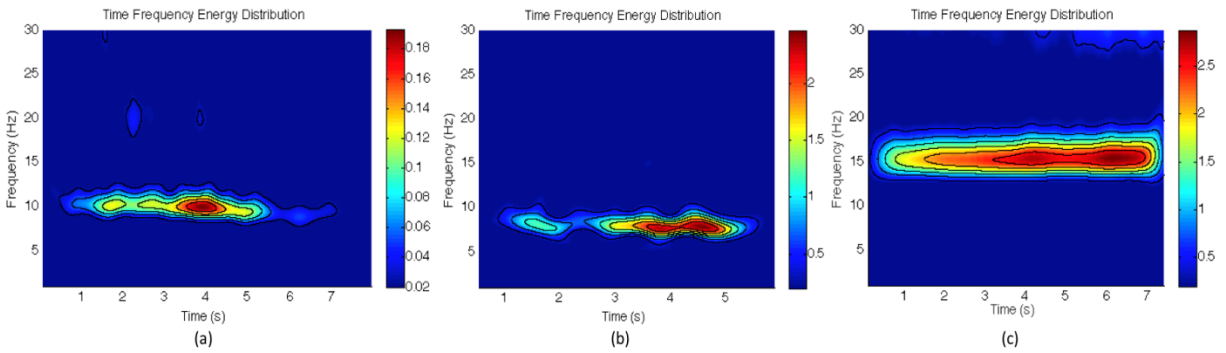

Figure 5.6 Time-Frequency energy distribution for seizures of (a) Patient 1, (b) Patient 2 , and (c) Patient 3

5.3.5 Synthetic iEEG recordings

The implemented swADTF-based seizure generators/sinks identification framework was first tested on a 9-node simulated connectivity pattern (3x3 grid).

A primary generator of seizure activity, consisting of real ictal data (sampled at 400 Hz), was propagated to the 8 remaining nodes. This connectivity propagation model was provided as part of the eConnectome Matlab toolbox for mapping and imaging of brain functional connectivity [14] and was previously used to validate other connectivity methods such as the DTF [5] and the ADTF [15]. The swADTF was evaluated and integrated across frequency range (4-10 Hz) and whole segment duration. Figure 5.2 illustrates the simulated propagation pattern. In order to evaluate the resistance of the proposed analytical framework to noise and interference, an additive Gaussian white noise was imposed to raw iEEG recordings. Recently, Paris et al. 2016 demonstrated that noises interfering with iEEG recordings could be modeled by an additive white Gaussian noise or a causal periodic autoregressive moving average model [17]. Different noise levels were added to the generated 9-node connectivity pattern resulting in signal-to-noise ratios (SNR) between -12 dB and 12 dB (unity increments). Figure 5.3 displays illustrative raw iEEG recordings with SNRs of 12 dB (top), 0 dB (middle), and -12 dB (bottom).

5.4 Results

5.4.1 Simulation results

Figure 5.4 displays the transfer function (0 dB noise), as well as normalized outflow and inflow of seizure activity. Electrode 5 can be quantitatively identified as the source of seizure activity confirming the simulated connectivity pattern.

Table 5.2 Group results in terms of resected regions, sources, and sinks of seizure activity

Patient ID	SOZ	Resection: Ins/op	Seizure Semiology	Outcome (Engel)	Ictal generators	Ictal sinks
1	Ant Ins + F op	Ant and middle/FT	No aura/laughing/complex motor behavior	IA	Ant Ins + Medial OF + ant STG	Lateral OF + Fusiform + Post central gyrus
2	Post Ins	Post/T	R arm painful somatosensory symptoms/Dystonic posturing	IB	Pos Ins	Cingulate +para-central +MFG/SFG
3	Sup Ins + F op	Ant/F	No aura/laughing or swearing, complex motor behavior	IA	Medial OF	Lat OF + SFG + SPL
4	Post Ins, P op/T op	Post/PT	Diurnal: audiogenic reflex L hemiface somatosensory symptoms; Nocturnal: no aura/complex motor behavior	IA	Pos Ins	IFG + Post-central gyrus
5	Sup Ins, F op	Ant/F	Anxiety, palpitations/R dystonic posturing and head deviation	IA	F op	Pre-central + F op
6	Post Ins, T op/P op	Post and Inf/ TP	L hemiface somatosensory, olfactory and auditory auras ± L facial clonic jerks and bilateral convulsive	IIIA	Ant Ins/P op/IFG	Ins + Lat OF
7	Ant Ins, F op	Ant/-	No aura, behavioral arrest, ± bilateral convulsive	IIIA	STG	Fusiform+ T Pole+ Medial OF

SOZ: seizure onset zone; Ant Ins: anterior insula; F op: frontal operculum; Post Ins: posterior insula; Sup Ins: superior insula; P op: parietal opercula; T op: temporal operculum; L: left; R: right; Ins: insular; op: operculum; Ant: anterior; F: frontal: T: temporal; Rad: radical

In addition, contact 5 exhibited highest and lowest outflow and inflow values respectively. Remaining electrodes (sinks of seizure activity) displayed low outflow and high inflow values, as expected.

The entire localizing methodology, including surrogate data testing (1000 times shuffling, α= 0.05) was applied to the simulated data. As shown in Fig. 5.5, the swADTF is stable in identifying node 5 as the generator of seizure activity even in the presence of high noise levels.

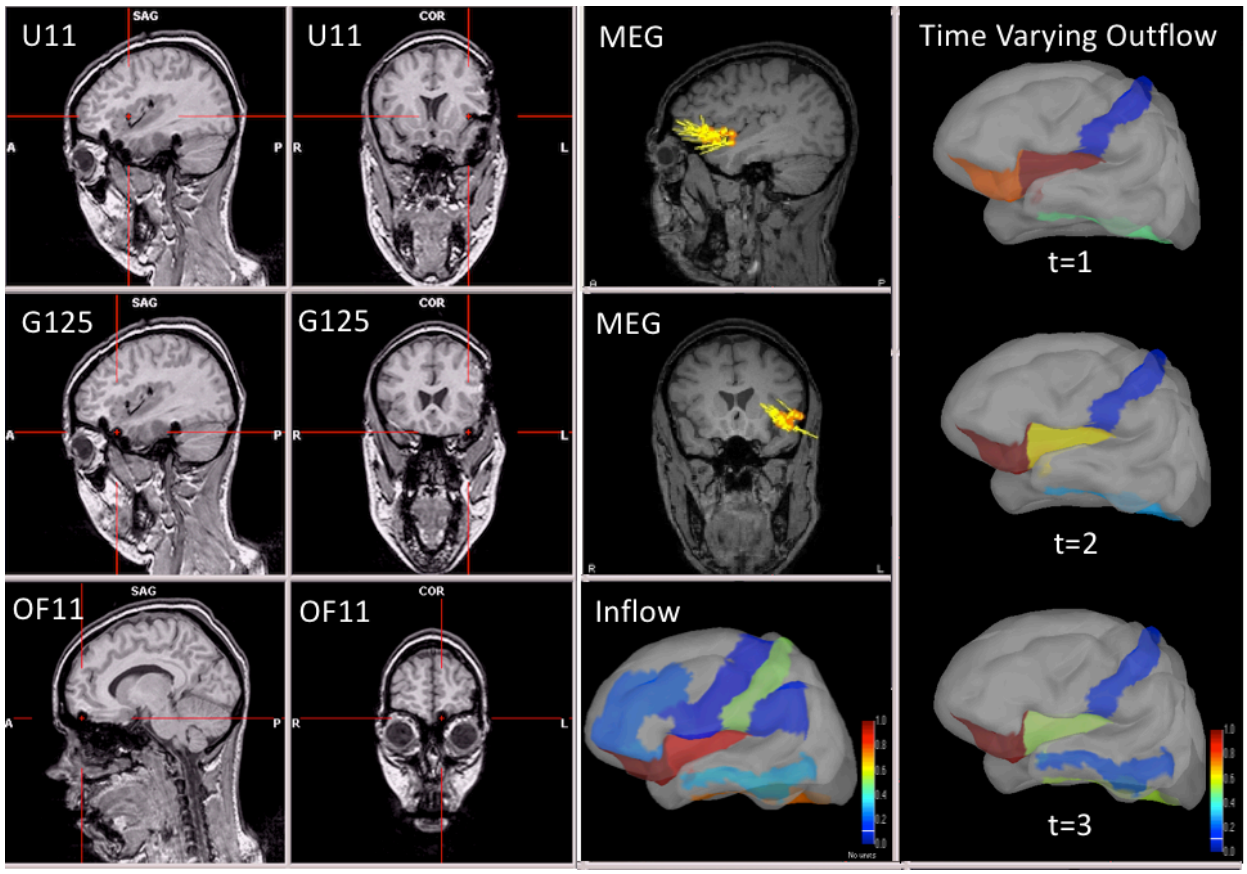

Figure 5.7 Individual swADTF connectivity results for patient 1; U: insular depth electrodes, G: Grid electrodes OF: orbito-frontal strip electrode; MEG: Magnetoencephalography; t: time

5.4.2 Sources of seizure activity – group results

Using the MVAAR model coefficients, swADTF was integrated from f1= 3 Hz to f2= 40 Hz based on equation (2). The high cut-off frequency (3Hz) was chosen in an attempt to exclude low frequency background electrical activity [1]. Complex Morlet wavelet time-frequency analysis was performed to ensure ictal activity, across all analyzed seizures, occurred within the chosen frequency range [18]. Figure 5.6 shows illustrative time-frequency energy distribution of seizure onset patterns for patients 1, 2, and 3. The 5-sec frame prior to seizure onset was discarded from the analysis. It was only included to let the Kalman filter adapt to the iEEG recordings. Outflow and inflow of seizure activity were extracted from the time and frequency integrated swADTF transfer matrices. Table 5.2 depicts results for all patients in terms of regions selected by visual analysis, resected region, as well as swADTF-identified ictal generators and sinks.

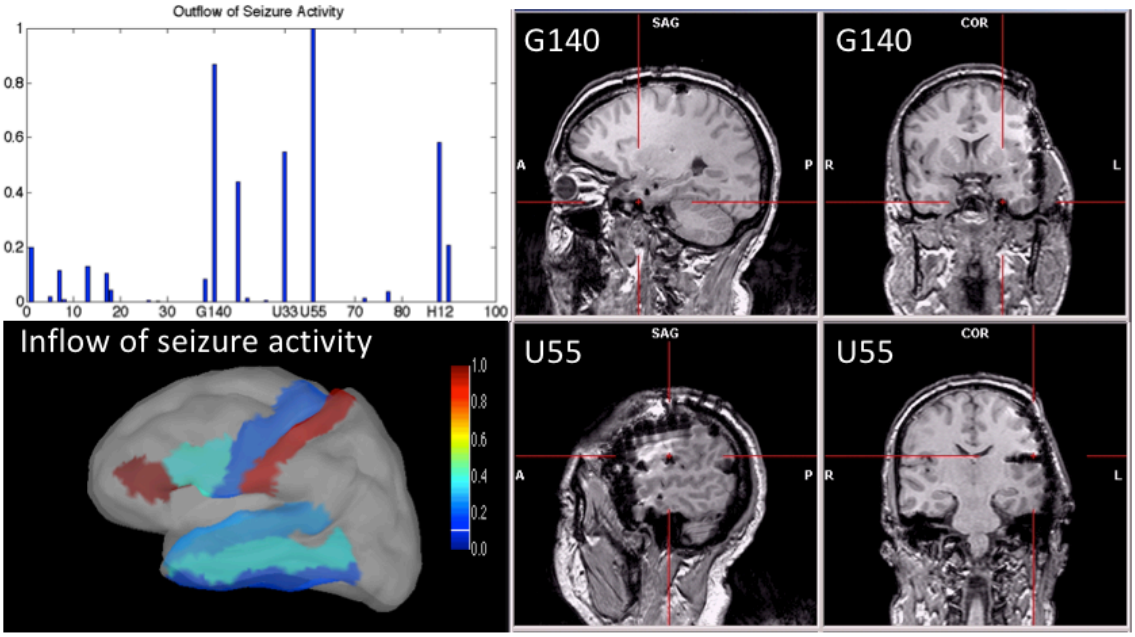

Figure 5.8 Individual swADTF connectivity results for patient 4

For patients with Engel I outcome, and for whom the resected region was sampled by iEEG contacts, ictal generators were within the resected volume and among electrode contacts visually identified by the expert epileptologist. Note however that for patient 1, swADTF identified three ictal generators (different generator for each seizure) from three distinct non-contiguous areas, only one of which was resected to provide seizure freedom. For the remaining two patients (#6 and #7) with poor post-operative seizure outcome, the identified ictal generators were outside of the resected region. For patient 6, while the parietal operculum was resected, two nearby contacts in the anterior insula and inferior frontal gyrus with quasi-similar outflow scores were not. For patient 7, the identified generator in the superior temporal gyrus was right below the resected area (anterior insula).

5.4.3 Individual results

In this section, illustrative cases of patients are discussed. Inflow and outflow of seizure activity were plotted on individual brain surfaces as reconstructed from a T1 magnetic resonance imaging (MRI) volumetric scan using Freesurfer. Individual cortex surfaces were registered to a Desikan-Killiany anatomical atlas using Brainstorm, an open source Matlab toolbox [19].

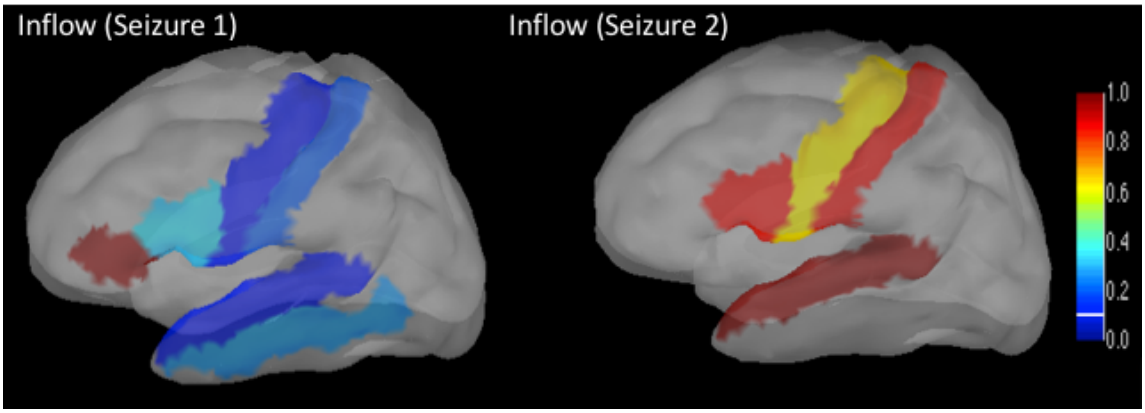

Figure 5.9 Seizure specific swADTF analysis for patient 4. Seizure 1 is a night seizure characterized by complex motor behavior semiology while seizure 2 is a diurnal seizure characterized by somatosensory semiology

To facilitate interpretation, inflow of seizure activity was converted from channels to brain regions. Electrodes on the vertices of a given region as well as the connectivity of pairs of electrodes between two regions were averaged.

5.4.3.1 Illustrative case 1

Patient 1 is a 38-year-old female who suffered from non-lesional focal epilepsy since the age of 5 years. After failing six antiepileptic drugs, she was referred for epilepsy surgery. Clinically, seizures were characterized by sudden non-mirthful laughter and complex motor movements, suggestive of prefrontal lobe involvement. However, non-invasive investigations suggested a seizure focus in the left anterior insula (see magnetoencephalography (MEG) results in Figure 5.7). An intracranial EEG subsequently confirmed a seizure onset zone in the left anterior insula extending to the frontal operculum. She underwent surgical resection of the left anterior and middle insula and part of the adjacent frontal and temporal opercula with good post-operative seizure outcome (Engel IA outcome). As mentioned in Table 5.2, swADTF identified three contacts (one for each individually analyzed seizure). While electrode contact U11 located in the anterior insula was within the seizure onset zone, the other two (contact OF11 in the orbitofrontal cortex and G125 in the superior temporal gyrus) were not. This may suggest that swADTF as integrated across the first seven seconds of the seizure may not always be able to distinguish a primary ictal generator from secondary ictal generators (a node with high inflow but also high outflow). In an attempt to distinguish primary from secondary generators of seizure activity, time-varying outflow of seizure activity was plotted at the early seizure onset. As shown in

Figure 5.7, the insula exhibited the highest outflow of seizure activity at time t =1; afterwards the lateral orbitofrontal gyrus becomes the highest source of seizure activity.

5.4.3.2 Illustrative case 2

Patient 4 is a 46-year-old male with non-lesional drug-resistant epilepsy since age 16 years. He presented diurnal seizures manifesting as paroxysmal pain over the right face often triggered by loud noises, suggestive of a focus involving the posterior insula at the junction of the secondary somatosensory cortex (pain) and the auditory cortex both in the parietal operculum, and possibly also the inferior primary sensory cortex (face sensory). He also presented sleep-related episodes with complex motor behaviours suggesting prefrontal propagation. Invasive EEG recordings confirmed the location of the seizure onset zone in the left posterior insula extending to the adjacent parietal and temporal opercula; a subsequent left operculo-insular resection led to seizure-freedom (Engel IA outcome). The electrode contact identified as the maximal source of outflow based on swADTF was indeed located within the resected volume which led to seizure-freedom (Figure 5.8). Averaging inflow activity across three seizures, the highest inflow of seizure activity included the inferior frontal gyrus and the post central gyrus (where the primary and secondary somatosensory functional cortices are located). Because diurnal and nocturnal seizures were different, we individually analyzed each seizure type. As shown in Figure 5.9, the analyzed nocturnal seizure which was not triggered by loud noises and featured complex motor behaviour (suggestive of prefrontal involvement) exhibited high activation of the left inferior frontal gyrus while the analyzed diurnal audiogenic reflex painful somatosensory seizure exhibited propagation to the post central gyrus (primary and secondary somatosensory cortices), the temporal neocortex and the pars opercularis.

5.4.3.3 Illustrative case 3

Patient 7 is a 36-year-old male with non-lesional predominantly nocturnal epilepsy since age 31 years. Seizures were characterized by sudden awakening, fixed gaze and behavioral arrest followed by limb hypertonia. MEG and ictal single-photon emission computed tomography (SPECT) (Figure 5.10) suggested a left operculo-insular focus. Intracranial EEG revealed interictal broadly distributed spikes involving the anterior insula, the frontal operculum, the orbitofrontal cortex and temporal areas.

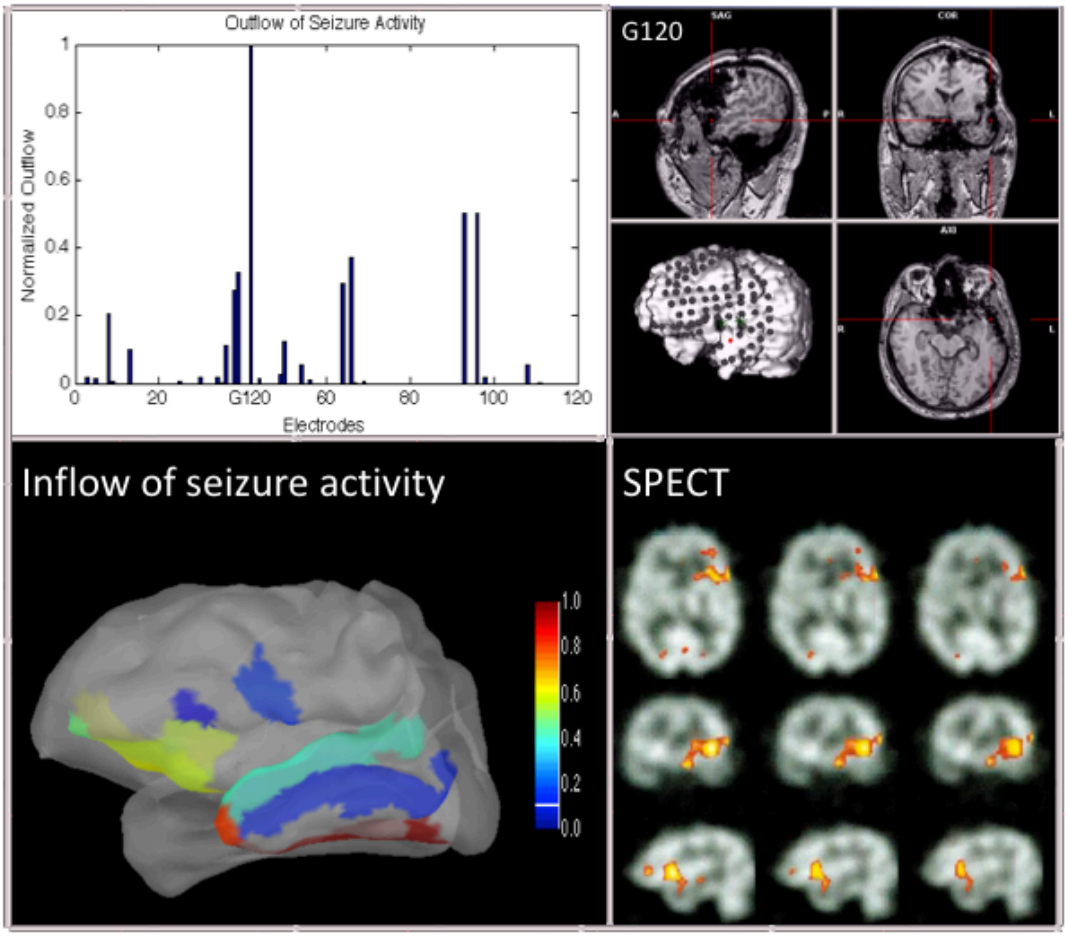

Figure 5.10 Individual swADTF connectivity results for patient 7; SPECT: single-photon emission computed tomography

Seizures started with a broadly distributed spike and wave discharge followed by relatively diffuse low-voltage fast activity involving several contacts. Based on visual analysis, maximum evolution was felt to be in the anterior insula, inferior frontal gyrus, superior temporal gyrus, and orbitofrontal gyrus. The anterior insula and frontal operculum were resected (sparing Broca's language area) with a worthwhile seizure reduction but not seizure freedom (Engel III outcome). Interestingly, swADTF analysis identified the maximum outflow of seizure activity in the superior temporal gyrus which was not part of the resection volume. The region exhibiting highest inflow of seizure activity was the fusiform gyrus, the temporal pole and the medial orbitofrontal gyrus.

5.5 Discussion

In this work, we have investigated the ability of the swADTF in identifying seizure foci in patients with apparent operculo-insular seizures. More specifically, we applied the swADTF to iEEG recordings of seven patients with insular epilepsy who underwent an operculo-insular resection guided by iEEG findings, five of whom with subsequent good outcome and 2 with poorer outcome. To our knowledge, this is the first study to use multivariate autoregressive modeling based effective connectivity for the analysis of operculo-insular seizures.

For four of the five patients with good outcome, swADTF-identified the electrode contact exhibiting highest outflow within the resected volume. For one of these four patients however, more than one electrode contact was identified as a possible generator. For this patient (#1), three different non-contiguous electrode contacts were identified, indicating that swADTF as integrated across the first seven seconds of the seizure may not always be able to distinguish a primary ictal generator from secondary ictal generators and that visual inspection of the time-varying outflow of seizure activity may be necessary. Regarding the single patient with good outcome for whom swADTF identified a generator in the medial orbitofrontal gyrus rather than in the insula, it should be noted that the depth electrode initially destined to reach the anterior insula was found to be located on the post-implantation MRI in the posterior insula close to the second depth electrode positioned in the posterior insula (as intended). This is a reminder that swADTF cannot obviously identify the ictal generator if the epileptic zone is not sampled. However, the identified generator was located within the iEEG-sampled region close to the anterior insula (resected region-not sampled by iEEG contacts for this patient). Structural connectivity results from our group have suggested that the orbitofrontal gyrus and anterior insula are highly connected brain regions [8]. For the final two patients with a poor post-operative seizure outcome, the swADTF-identified contact of maximum outflow was outside the surgical volume, suggesting resection of the wrong area or only part of it (albeit this cannot be verified as both patients declined a second iEEG study). Our observations are in line with previous investigations applying the swADTF to patients with other types of focal epilepsy [1]. In a series of 8 temporal lobe epilepsy patients operated successfully (Engel I outcome), Van Mierlo et al. (2013) showed that the electrode contact with the highest outflow, so called “driver”, was within the region clinically identified as the epileptogenic zone and resected volume [1]. In another series of eleven pediatric patients with frontal or parietal lobe epilepsies, Wilke et al. (2010) applied the DTF to selected quasi-stationary

iEEG epochs and integrated the transfer matrix across the frequency range of interest (as identified by means of Morlet wavelet-based time frequency analysis) [5]. They showed that electrode contacts with normalized outflow values higher than 0.8 (DTF-identified generators) highly correlated with seizure onset zones identified by expert epileptologists.

Although very preliminary, initial observations also suggest that regions identified as generators (defined as the contact of maximal outflow) or sinks (defined as areas of inflow values higher than 80%) of seizure activity, appeared to correlate with seizure semiology. For the three patients who exhibited somatosensory auras (#2, 4, and 6), all had ictal generators in the posterior insula or parietal operculum which are known to produce such symptoms when electrically stimulated. We also note that two out of the three patients with complex motor behaviours (#1 and 2) had sinks of seizure activity in the orbitofrontal cortex (an area which is typically expected to be involved during such manifestations, in addition to the medial prefrontal region); the third (#3), who did not have electrodes sampling the orbitofrontal cortex nor the medial prefrontal region, had an identified-sink in the nearby inferior frontal gyrus.

Our study has some merit and limitations. First, the recordings we used to perform multivariate effective connectivity were obtained from a high number of intracranial electrode contacts (mean of 95) sampling a number of brain areas. Previous investigations used a limited number of electrodes [3], shorter analysis segments [5], or visually identified regions of interest [1, 6]. Still, we acknowledge that some of regions of interest were probably not recorded. Computational requirements of adaptive multivariate modeling with surrogate based statistical validation can constitute a major constraint. In this work, we took advantage of high computational capabilities (160 cores, 1TB RAM, IBM X3850 X5, 8* Intel E7-8870 CPU) to include all implanted electrodes in swADTF analysis. In addition, simulations were optimized and parallelized over available cores using Matlab© parallel computing toolbox. Despite computational requirements, the swADTF is preferred as compared to other quantitative measures based on Granger causality. The major advantage of using the swADTF is that it allows to overcome the non-stationary nature of iEEG recordings, previously considered as an issue when using traditional autoregressive modeling strategies. The relatively small number of patients is another limitation. Although an increasing number of cases are being identified, operculo-insular epilepsy cases remain small in comparison with temporal or frontal lobe epilepsy. In addition, we chose to restrict ourselves to a relatively homogeneous group of patients

with operculo-insular epilepsy to better understand this focal epileptic condition at times considered as a great mimicker due to the variety of associated ictal manifestations. Obviously, larger studies are necessary to reproduce our preliminary findings, both for operculo-insular epilepsy or any type of focal epilepsy. Recent studies have demonstrated that high frequency oscillations (HFOs) may be correlated with the seizure onset zone. Due to limitations imposed by under sampling iEEG time series to cope with computational requirements, we were unable to study interactions within HFOs. Future perspectives include additional processing and swATDF computational optimization to study seizure onset patterns within HFOs.

5.6 Conclusion

In this work we examined the ability of the swADTF in localizing the seizure onset zone in patients with apparent operculo-insular epilepsy. Preliminary results showed that, despite the rapid spread of seizure activity, swADTF is a promising tool to complement visual assessment of seizure origin and propagation. Caveats include adequate sampling by electrode contacts of suspected areas of epileptogenicity, separately analyzing different seizure types if more than one seizure focus is suspected, and using a time-varying outflow representation when swADTF is unable to distinguish a primary ictal generator from secondary ictal generators. Larger prospective studies are obviously necessary before considering translation into clinical practice.

5.7 Acknowledgements

Authors acknowledge financial support from the Natural Sciences and Engineering Research Council of Canada, Epilepsy Canada and the Institute for Data Valorization (IVADO). DKN holds the Canada Research Chair in Epilepsy and Functional anatomy of the Human Brain.

5.8 References

[1] P. van Mierlo, E. Carrette, H. Hallez, R. Raedt, A. Meurs, S. Vandenberghe, et al., "Ictal-onset localization through connectivity analysis of intracranial EEG signals in patients with refractory epilepsy," *Epilepsia,* vol. 54, pp. 1409-1418, 2013.

[2] H. Jia, X. Hu, and G. Deshpande, "Behavioral Relevance of the Dynamics of the Functional Brain Connectome," *Brain Connectivity*, vol. 4, pp. 741-759, 2014.

[3] J. D. Martinez-Vargas, G. Strobbe, K. Vonck, P. van Mierlo, and G. Castellanos-Dominguez, "Improved Localization of Seizure Onset Zones Using Spatiotemporal Constraints and Time-Varying Source Connectivity," *Frontiers in Neuroscience*, vol. 11, p. 156, 2017.

[4] S. Klamer, S. Rona, A. Elshahabi, H. Lerche, C. Braun, J. Honegger, et al., "Multimodal effective connectivity analysis reveals seizure focus and propagation in musicogenic epilepsy," *NeuroImage*, vol. 113, pp. 70-77, 2015.

[5] C. Wilke, W. van Drongelen, M. Kohrman, and B. He, "Neocortical seizure foci localization by means of a directed transfer function method," *Epilepsia*, vol. 51, 2010.

[6] K. Hagiwara, J. Jung, R. Bouet, C. Abdallah, M. Guénot, L. Garcia-Larrea, et al., "How can we explain the frontal presentation of insular lobe epilepsy? The impact of non-linear analysis of insular seizures," *Clinical Neurophysiology*, vol. 128, pp. 780-791, 2017.

[7] A. Levy, Yen Tran Tp, O. Boucher, A. Bouthillier, and D. K. Nguyen, "Operculo-Insular Epilepsy: Scalp and Intracranial Electroencephalographic Findings," *Journal of Clinical Neurophysiology*, vol. 34, 2017.

[8] J. Ghaziri, A. Tucholka, G. Girard, J.-C. Houde, O. Boucher, G. Gilbert, et al., "The Corticocortical Structural Connectivity of the Human Insula," *Cerebral Cortex*, vol. 27, pp. 1216-1228, 2017.

[9] L. Q. Uddin, N. J. S., Hebert-Seropian B., Ghaziri J., and O. Boucher, "Structure and Function of the Human Insula," *Journal of Clinical Neurophysiology*, vol. 34, 2017.

[10] S. Obaid, Y. Zerouali, and D. K. Nguyen, "Insular Epilepsy: Semiology and Noninvasive Investigations," *Journal of Clinical Neurophysiology*, vol. 34, pp. 1537-1603, 2017.

[11] A. Harroud, A. Bouthillier, A. G. Weil, and D. K. Nguyen, "Temporal lobe epilepsy surgery failures: a review," *Epilepsy Research and Treatment*, vol. 2012, 2012.

[12] M. Kaminski, M. Ding, W. A. Truccolo, and S. L. Bressler, "Evaluating causal relations in neural systems: granger causality, directed transfer function and statistical assessment of significance," *Biological Cybernetics*, vol. 85, 2001.

[13] E. B. Assi, M. Sawan, D. K. Nguyen, and S. Rihana, "A 2D clustering approach investigating inter-hemispheric seizure flow by means of a Directed Transfer Function," in *2016 3rd Middle East Conference on Biomedical Engineering (MECBME),* 2016, pp. 68-71.

[14] B. He, Y. Dai, L. Astolfi, F. Babiloni, H. Yuan, and L. Yang, "eConnectome: A MATLAB Toolbox for Mapping and Imaging of Brain Functional Connectivity," *Journal of neuroscience methods*, vol. 195, pp. 261-269, 2011.

[15] C. Wilke, Ding L., and B. He, "Estimation of time-varying connectivity patterns through the use of an adaptive directed transfer function," *IEEE Transactions on Biomedical Engineering*, vol. 55, 2008.

[16] A. Schlögl, G. Dorffner, B. Kemp, A. Värri, T. Penzel, and S. Roberts. (2000) The Electroencephalogram and the Adaptive Autoregressive Model: Theory and Applications, *Shaker Publishing*.

[17] A. Paris, G. K. Atia, A. Vosoughi, S.A. Berman, "A New Statistical Model of Electroencephalogram Noise Spectra for Real-Time Brain Computer Interfaces", *IEEE Transactions on Biomedical Engineering*, vol. 64, 2016.

[18] L. Qin, Ding L., and B. He, "Motor imagery classification by means of source analysis for brain-computer interface applications", *Journal of Neural Engineering* , vol. 1, 2004.

[19] F. Tadel, S. Baillet, J. C. Mosher, D. Pantazis, R.M. Leahy, " Brainstorm: A User-Friendly Application for MEG/EEG Analysis ", Computational Intelligence and Neuroscience, vol. 13, 2011.

CHAPTER 6 ARTICLE 3 LEVERAGING HIGHER ORDER SPECTRA AND ARTIFICIAL NEURAL NETWORKS: TOWARDS NEW PRECURSORS OF SEIZURE ACTIVITY

Elie Bou Assi[1], Laura Gagliano[1], Sandy Rihana[2], Dang K. Nguyen[3], and Mohamad Sawan[1]

[1]Polystim Neurotech Lab, Institute of Biomedical Engineering, Polytechnique Montreal, Montreal, QC, Canada

[2]Biomedical Engineering Department, Holy Spirit University of Kaslik (USEK), Jounieh, Lebanon

[3]University of Montreal Hospital Center (CHUM), University of Montreal, Montreal, QC, Canada

This article addresses the third objective of this thesis, namely the assessment of the feasibility of seizure forecasting based on higher order spectra features. The revised version of the manuscript, based on reviewers' comments was submitted to Scientific Reports in July 2018.

6.1 Abstract

The ability to accurately forecast seizures could significantly improve the quality of life of patients with drug-refractory epilepsy. Prediction capabilities rely on the adequate identification of seizure activity precursors from electroencephalography recordings. Although a long list of features has been proposed, none of these is able to independently characterize the brain states during transition to a seizure. This work assessed the feasibility of using the bispectrum, an advanced signal processing technique based on higher order statistics, as a precursor of seizure activity. Quantitative features were extracted from the bispectrum and passed through two statistical tests to check for significant differences between preictal and interictal recordings. Results showed statistically significant differences ($p<0.05$) between preictal and interictal states using all bispectrum-extracted features. We used normalized bispectral entropy, normalized bispectral squared entropy, and mean of magnitude as inputs to a 5-layer multi-layer perceptron classifier and achieved respective held-out test accuracies of 78.11%, 72.64%, and 73.26%.

Keywords: Epilepsy, seizure prediction, intracranial electroencephalography (iEEG), feature engineering, cross frequency coupling, bispectrum, multi-layer perceptron

6.2 Introduction

Epilepsy is a chronic condition characterized by recurrent 'unpredictable' seizures. While the first line of treatment consists of long-term drug therapy, more than a third of patients are pharmaco-resistant [1]. The availability of several new antiepileptic drugs over the last two decades helped in reducing the risk of adverse events but their impact on the rate of seizure control is only modest [2]. In addition, recourse to epilepsy surgery remains low in part due variable success rates depending on the complexity of the case at hand, accessibility, and persisting negative attitudes towards it and fear of complications [3,4].

Predicting the possible occurrence of seizures is an unmet medical need and such capability can lead to novel therapeutic avenues to treat patients with refractory epilepsy. Unlike seizure detection, seizure prediction can foresee the possibility of future occurrence of seizure in advance, thus allowing medical intervention to potentially prevent the seizures or reduce their magnitude and/or frequency. However, the ability to accurately identify the pre-seizure state remains elusive. Despite several attempts to identify a specific and unique feature that can be used to predict seizures, no single characteristic has been established as a potential and universal precursor of epileptic seizure activity [5-7].

The commonly used feature in seizure prediction, the spectral band power, is derived from the frequency domain characteristics of electroencephalography (EEG) signals [8]. It quantifies amplitude modulations across time, within the defined frequency bands. While the spectral band power displays phase changes, it cannot identify interactions among frequency components of the signal. However, information regarding multi-frequency behaviors can be captured by more complex metrics, related to the concept of cross-frequency coupling (CFC) [9]. Recently, Alvarado-Rojas et al. (2014) introduced a new measure of brain excitability based on phase-amplitude coupling (PAC), consisting of a slow (delta, theta) modulation of high (gamma) frequency intracranial EEG (iEEG) signal's components [10]. They reported promising prospective results suggesting that preictal PAC modulations may be significant for the whole group of patients ($p<0.05$). We later showed the existence of significant difference in mean PAC distribution between the preictal and interictal states on bilateral canine iEEG recordings [11]. Furthermore, Bandarabadi et al. (2015) reported promising results with a new bivariate feature (although not termed as CFC) quantifying the cross-power information between two different

frequency bands (assessed in terms of power spectral density) and two different channels [12]. Overall, these findings suggest that seizure prediction may be possible using cross-frequency coupling. In contrast to the previously discussed measures, higher order spectral measures based on CFC have been proposed to be the carrier mechanism for the relationship between global and local neuronal processes [9].

The bispectrum is an advanced signal processing technique based on higher order statistics which considers both the amplitude and the degree of phase coupling of a signal. In contrast to traditional power spectrum, which quantifies the power of a time series over frequency, higher order spectral (HOS) analysis employs the Fourier transform of higher order correlation functions to explore the existence of quadratic (and cubic) non-linear coupling information. Although the bispectrum has shown promising results within the context of seizure detection and EEG signals classification [13], it has not yet been used for seizure prediction. In this work, we investigated the suitability of the bispectrum in quantifying changes between the interictal and preictal states. Adequate statistical tests were employed to assess if there are significant differences among the quantified changes. A seizure prediction algorithm employing a multi-layer perceptron (MLP) neural network was used, showing good performances in classifying preictal and interictal samples. The seizure prediction algorithm was designed and tested to perform an automatic classification of preictal and interictal samples. Such algorithm could eventually be embedded in an advisory/intervention closed-loop system, resulting in a life-changing solution for patients with refractory epilepsy.

6.3 Methods

6.3.1 Database

HOS analysis features were extracted from interictal and preictal iEEG recordings of 3 mixed hounds implanted with the NeuroVista ambulatory monitoring device. These recordings were downloaded from the NIH-sponsored international electrophysiology portal (https://www.ieeg.org/). The NeuroVista ambulatory monitoring device consists of an implantable lead assembly in line with a telemetry unit and a personal advisory device. Data were acquired at 400 Hz using 16 channels (4×4 contact electrode strips) implanted bilaterally according to a standardized canine implantation protocol [14]. Preictal and interictal segments were extracted from the iEEG recordings of 3 dogs with naturally occurring focal epilepsy. In

line with previous investigations [11, 15, 16] and the American Epilepsy Society seizure prediction challenge consensus, preictal segments consisted of recordings of 1 hour prior to seizure onset with a 5 min intervention time. Interictal segments were randomly chosen from the entire recording with a restriction of 4 hours before or after a seizure.

6.3.2 Higher order spectra

Higher order spectral analysis is an advanced signal processing method that allows exploring the existence of quadratic (and cubic) non-linearities. In contrast to traditional power spectrum, which quantifies the power of a time series over frequency, HOS analysis employs the Fourier transform of higher order correlation functions investigating non-linear coupling information. The bispectrum splits the skewness (third order moment) of a signal over its frequencies, quantifying the coupling between a signal's oscillatory components. The bispectrum, quantifying oscillatory relationships between basic frequencies f1, f2, and their harmonic component "f1+f2", is computed from the Fourier transform of the third-order correlation (1).

$$Bis(f_1, f_2) = \lim_{T \to \infty} \left(\frac{1}{T}\right) E[X(f_1 + f_2)X^*(f_1)X^*(f_2)] \quad (1)$$

where *X(f)* is the Fourier transform of a time series *x(t), (*)* is the complex conjugate, and *E* denotes the arithmetic average estimator.

6.3.3 Higher order spectra features

In order to characterize and compare time series, quantitative features must be extracted from the bispectral density array. Bispectrum analysis yields a 2D mapping of the level of interaction between all frequency pairs in the signal. In order to characterize and compare time series, quantitative features must be extracted. In this work, three features were computed from the non-redundant region (shown in Fig. 6.1): the mean magnitude (Mave) of the bispectrum, the normalized bispectral entropy (P1) and the normalized squared bispectral entropy (P2). The mathematical equations of extracted features are briefly explained:

The first feature, bispectrum's mean of magnitude (Mave) (2), has been used commonly to extract quantitative information from the bispectrum [13, 17].

$$Mave = \frac{1}{L}\sum_{\Omega} |Bis(f_1, f_2)| \quad (2)$$

where L is the total number of sample points in the bispectral density array non-redundant region (Ω) defined in Fig. 6.1.

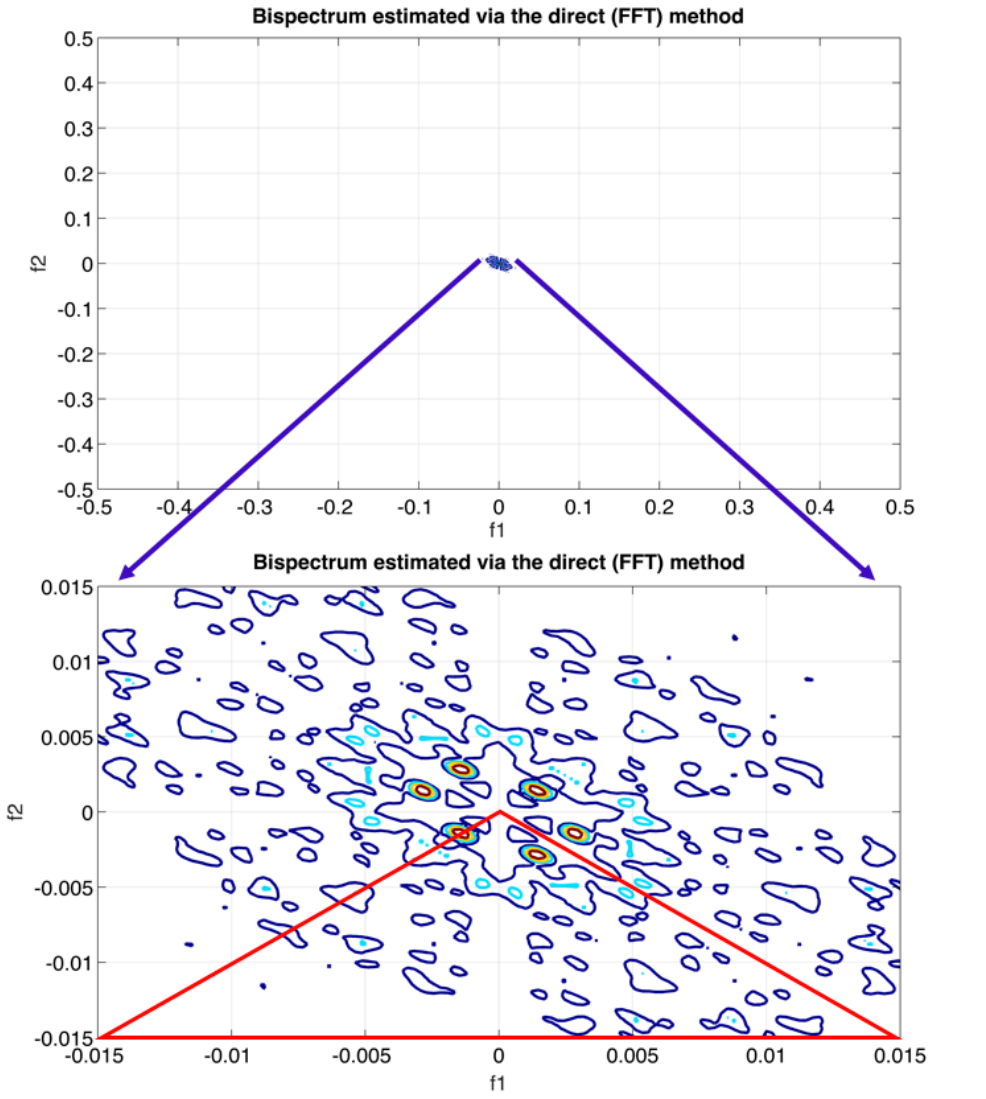

Figure 6.1 2D Bispectrum color map highlighting the non-redundant region used in feature extraction; FFT = Fast Fourier Transforms. Axes coordinates display relative/normalized frequencies where 0.5 represents the maximum frequency (180 Hz). Color indicates degree of coupling (Bispectral value) between f_1 and f_2.

In an attempt to extract regularity from bispectrum plots, normalized bispectral entropy (P1) and normalized bispectral squared entropy (P2) have been proposed recently and were used in this work [13]:

$$P_1 = -\sum_n p_n log p_n \tag{3}$$

$$p_n = \frac{|Bis(f_1,f_2)|}{\sum_\Omega |Bis(f_1,f_2)|} \tag{4}$$

$$P_2 = -\sum_n q_n log q_n \tag{5}$$

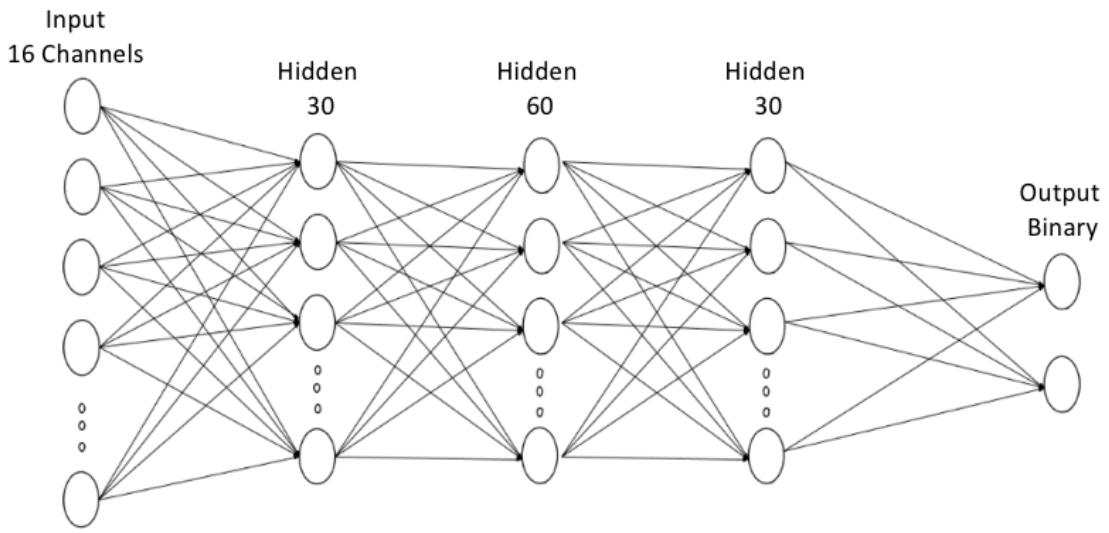

Figure 6.2 Artificial neural network architecture. The input layer consists of 16 nodes. The first, second, and third hidden layers respectively consists of 30, 60, and 30 nodes. The output layer features 2 nodes for a binary classification.

$$q_n = \frac{|Bis(f_1,f_2)|^2}{\sum_{\Omega}|Bis(f_1,f_2)|^2} \quad (6)$$

where *n=0, 1, ... L-1*; L is the total number of sample points in the bispectral density array non-redundant region (Ω). A 30-sec non-overlapping moving window was used to compute the bispectrum and its subsequent features from epileptic canine iEEG recordings. Zero-phase notch (cut-off frequency=60 Hz) and band pass filtering in the frequency range [0.5 - 180] Hz were performed to keep signals' phase intact. The higher order spectral analysis (HOSA) Matlab© toolbox was used to extract the bispectrum. Following equation (1), the bispectrum matrix was estimated for all possible frequency pairs (f_1, f_2) in the range [0.5 - 180] Hz based on the direct fast Fourier transform approach.

6.3.4 Statistical analysis

To assess bispectrum related features' capability in distinguishing between interictal and preictal iEEG recordings, a statistical analysis was performed to measure the level of statistically significant differences between the three features extracted from 30-sec non-overlapping windows. Firstly, the general level of interaction between the type of recordings (interictal vs. preictal) and the values of each feature were evaluated for each dog, using one-way ANOVA. This analysis indicates whether there is a statistically significant difference between preictal and interictal recordings for each of the three features.

Table 6.1 Mean values of HOS features and One-Way ANOVA global statistical analysis results

Dog ID	Nb. Seizures	M_{ave}			P1			P2		
		Pre	Inter	F, p	Pre	Inter	F, p	Pre	Inter	F, p
0002	17 (4'080)	3.31e3 ±3.30e3	3.49e3 ±2.57e3	F = 6.07, P = 0.0138	4.79 ±0.30	4.94 ±0.21	F = 2480, P = 0*	3.45 ±0.53	3.71 ±0.45	F = 2800, P = 0*
0003	17 (4'080)	1.79e3 ±1.04e3	2.02e3 ±1.24e3	F = 167, P = 4.113e-38	4.49 ±0.24	4.75 ±0.28	F = 98.3, P = 3.67822e-23	3.35 ±0.46	3.26 ±0.43	F = 346, P = 5.50e-77
0004	11 (2'640)	7.44e3 ±1.46e3	5.99e3 ±4.33e3	F = 18.5, P = 1.75e-5	4.05 ±0.38	4.72 ±0.34	F = 2340, P = 0*	3.04 ±0.59	3.28 ±0.51	F = 1360, P = 3.262e-292

Mean values and standard deviation of HOS features for each dog were computed using recordings from all available seizures. Independent Analysis of Variance tests comparing preictal and interictal HOS feature distributions were conducted on recordings of each dog. Nb. Seizures: total number of seizures; the numbers in parentheses indicate the total number of 30-sec data samples used in the comparison; F: F statistic of one-way ANOVA; *p*: *p*-value of one-way ANOVA indicating probability that the null hypothesis (H_O) is falsely rejected (H_O: preictal and interictal feature distributions have equal means), **p*-value is less than Matlab's digit precision = 4.9407e-324.

One-Way ANOVA was preferred over Student's *t*-test, since the data were randomly and independently selected from the entire record and multiple features were compared.

Then, to assess the spatial localization of the change in bispectral features during the preictal period, the distribution of each feature for each hour of the preictal recordings (120 samples) was compared to the features for one hour of the interictal recordings, selected from the same electrode, with the restriction of 4 hours prior to the preictal time, by the Mann-Whitney U-Test. A p-value <0.05 from this test indicates statistically significant difference.

Finally, for each feature, a color map of the brain was created to visualize the percentage of the seizures at each electrode for which the difference measured by the Mann-Whitney U-Test is significant at a confidence level of at least 95%. This representation allows a visualization and identification of the brain regions where the changes in bispectral features are most prominent during preictal periods.

6.3.5 Seizure prediction algorithm

6.3.5.1 Network architecture

To assess the feasibility of seizure prediction based on bispectral features, a 5-layer MLP neural network classifier was trained to differentiate preictal and interictal recordings. Different classifier configurations were trained for each feature.

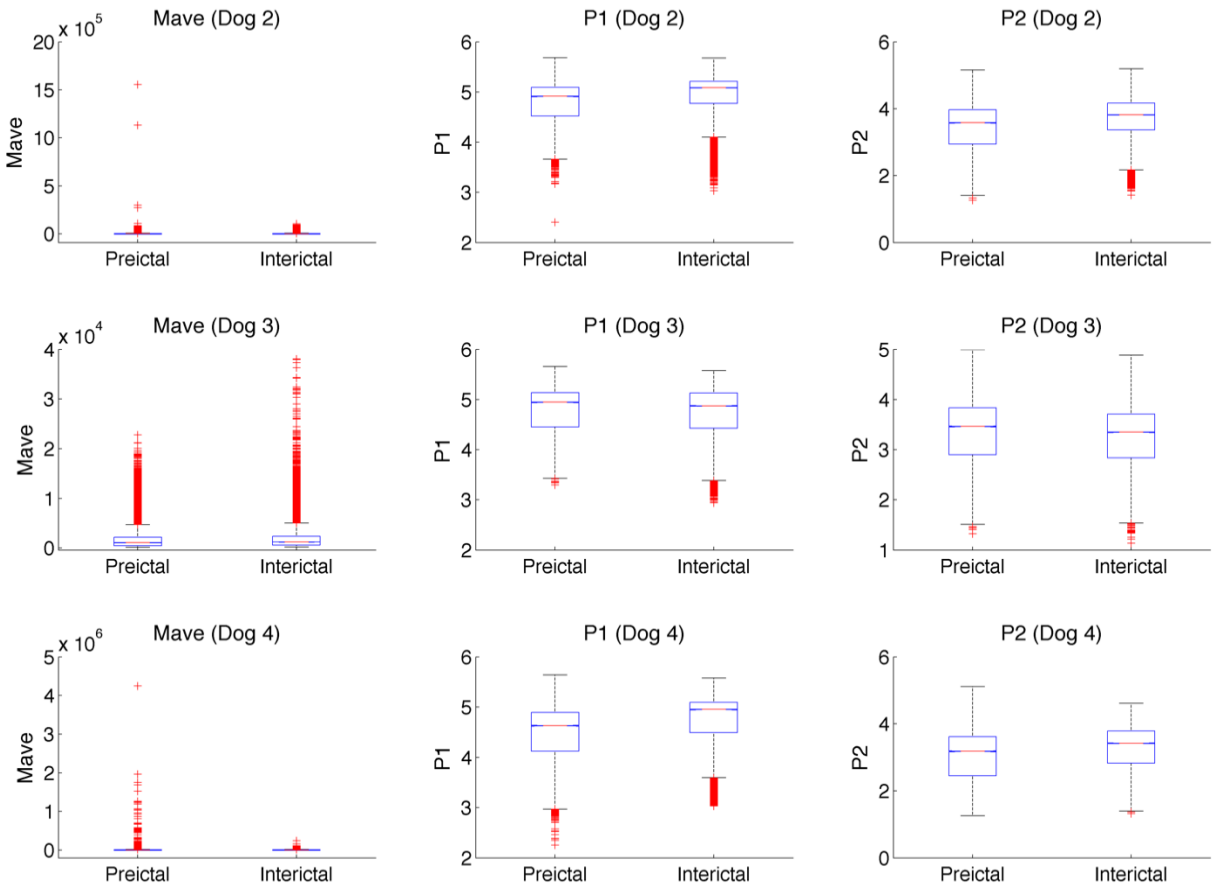

Figure 6.3 Box and Whisker plots for all features from all three dogs. The red central mark indicates the median, the bottom and top edges of the box indicate the 25th and 75th percentiles, respectively, and the whiskers extend to the most extreme data points to a maximum of 1 times the interquartile range. Outliers are points located beyond the whiskers and are marked with a red '+'. The columns from left to right show plots for *Mave*,, *P1* and *P2,* while the rows correspond to the 3 dogs. All available seizures are included in these box plots.

The input layer consisted of 16 nodes (corresponding to 16-input channels). The first, second and third hidden layers, respectively, consisted of 30, 60, and 30 nodes (ReLu activation function). The output layer contains 2 nodes for a binary decision function (Preictal vs Interictal). A stochastic gradient decent optimizer was used during backpropagation. The fitness function was the classification cross entropy. Training iterated through 10,000 epochs with a learning rate of 0.001 and a training and validation batch size of 200 samples. Figure 6.2 shows the architecture of the implemented neural network. All algorithmic development steps were performed on PyTorch, an open source Python-based machine learning library.

6.3.5.2 Data splitting and training strategy

Held-out validation and test were performed. A total of 45 seizures were included in the analysis. A subject-specific algorithm was implemented. Features were extracted using a 30-sec non-overlapping moving window (total of 10,800 classification samples). Training, validation, and testing data were respectively in the following proportions: 40%, 30%, and 30%. To avoid any contamination, time correlation or leakage, the data (train, validation, and test) were split on a seizure per seizure basis. More specifically, the whole preictal period (1 hour segmented using a 30-sec non-overlapping window) of a considered seizure was used for either training, validation, or testing. Splitting samples from the same preictal period (although not identical) into training, validation, and testing may prompt the classifier to learn temporal correlations rather than class information. This, in turn, would result in overoptimistic classification performances. The proposed strategy ensured that preictal samples originating from seizures used in training were neither assessed during validation nor testing.

6.4 Results

6.4.1 Statistical Analysis

6.4.1.1 ANOVA- Global assessment of significance

One-way ANOVA tests were conducted for each dog to compare HOS features extracted from preictal and interictal iEEG recordings. Results from these variance tests are shown in Table 1 and in the box-and-whisker plots in Figure 6.3. For the bispectral magnitude (*Mave*), the distributions from two of the three dogs show a slight decrease in magnitude during the preictal phase, while the ANOVA tests for all three dogs indicate that preictal and interictal *Mave* distributions are statistically different at a confidence of at least 95% (Dog 2: $F_{1,4078} = 6.07$, $p < 0.05$; Dog 3: $F_{1,4078} = 167$, $p < 0.001$; Dog 4: $F_{1,2638} = 18.5$, $p < 0.001$). As for the normalized bispectral entropy (*P1*), distributions from all three dogs show a general decrease in *P1* values during the preictal phase and the ANOVA tests confirm that the difference in *P1* distributions between preictal and interictal recordings is statistically significant in all three dogs (Dog 2: $F_{1,4078} = 2480$, $p < 0.001$; Dog 3: $F_{1,4078} = 98.3$, $p < 0.001$; Dog 4: $F_{1,2638} = 2340$, $p < 0.001$). Finally, the normalized squared bispectral entropy (*P2*) values generally decrease while variances of the distributions increase during transition to seizure. The differences between the *P2* distributions are statistically significant for all three dogs (Dog 2: $F_{1,4078} = 2800$, $p < 0.001$; Dog 3:

$F_{1,4078}$ = 346, p <0.001; Dog 4: $F_{1,2638}$ = 1360, p <0.001). These strong significant differences imply that interictal and preictal recordings are statistically distinguishable based on the three HOS features tested.

6.4.1.2 Mann Whitney - inter seizure assessment of significance

The second statistical test aimed to evaluate the potential patient-specific seizure prediction capability of the three HOS parameters by analyzing the spatial distribution of the iEEG channels, for which the bispectral changes are most prominent. The HOS parameters extracted from 30-sec non-overlapping windows for a total of 45 preictal hours were compared to 45 interictal hours channel per channel. The Mann-Whitney U test was used to compare specific bispectral feature distributions for each seizure and each channel. The results of the specific statistical comparison tests are presented in Figure 6.4. The colormaps represent the percent of predictable seizures, occurring in each dog, for which each specific feature distribution is statistically different (p <0.05) during the preictal hour at that channel. For dog 2, the *P1* and P2 distributions change significantly during the preictal periods for 100% of the seizures (n = 17) at several contacts located in both hemispheres (Fig. 6.4, top).

Furthermore, these specific regions of consistent bispectral change coincide with the regions of most prominent cross-frequency phase-amplitude coupling (PAC) change, which we identified in an earlier study [11]. These regions include channels 2 and 5 in the left hemisphere and channels 10 and 14 in the right hemisphere. For dog 3, mean magnitude (*Mave*) and normalized bispectral entropy (*P1*) show significant distribution changes during preictal periods for 100% of the seizures (n = 17). As shown in Figure 6.4 (middle), these distribution changes are most prominent at channels 1, 5 and 6 in the left hemisphere and channels 10 and 13 in the right hemisphere. This spatial distribution of preictal bispectral feature change, again, coincides with the spatial distribution of preictal PAC change for this dog identified in our previous study [11]. Finally, for dog 4, the mean bispectral magnitude and normalized bispectral entropy showed most consistent seizure prediction potential.

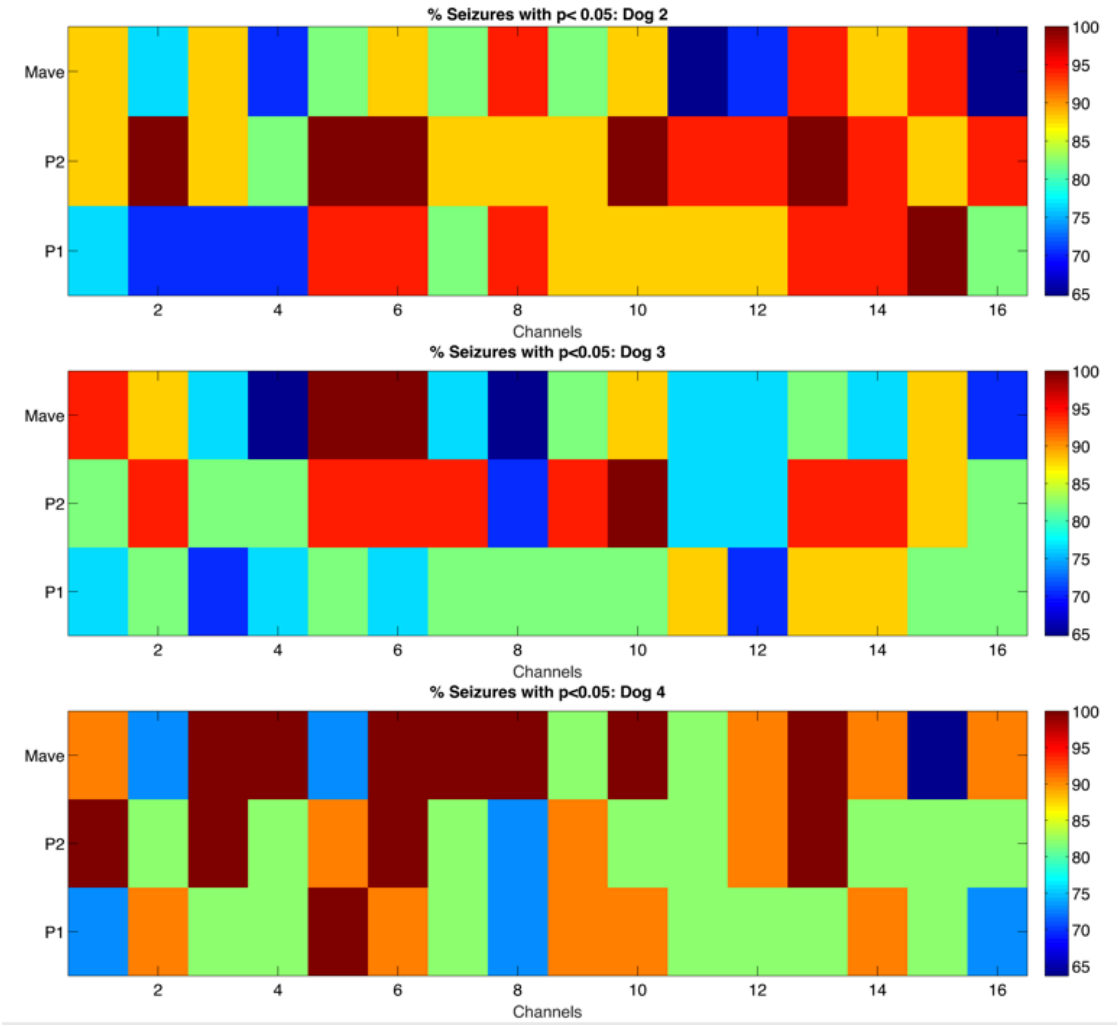

Figure 6.4 Mann-Whitney statistical test results: percentage of predictable seizures using each of the extracted features ($p<0.05$). From top to bottom: Dog 2, Dog 3, Dog 4. Each cell represents a combination of a HOS feature and a contact. Dark red color indicates that 100% of seizures showed a statistically significant change in that feature during the preictal period at that specific contact.

Table 6.2 Multi-Layer Perceptron-based classification results

	P1		P2		Mave	
	Train Acc. (%)	**Test Acc. (%)**	**Train Acc. (%)**	**Test Acc. (%)**	**Train Acc. (%)**	**Test Acc. (%)**
Dog A002	84.23	76.71	79.81	77.61	94.23	61.84
Dog A003	71.71	67.23	75.58	61.52	79.26	67.15
Dog A004	90.89	90.40	83.36	78.78	94.58	90.80
Mean	82.8	**78.11**	79.58	**72.64**	89.36	**73.26**

Once again, as shown in Figure 6.4 (bottom), there was a statistically significant change in *Mave* and *P1* during progression to seizure for 100% of the seizures (n = 11) in bilateral regions, which coincide with those we identified as PAC change regions in Gagliano et al. (2018) [11]. These channels include 3, 4, 6, 7 and 8 in the left hemisphere and channel 13 in the right hemisphere.

6.4.2 Seizure prediction algorithm

As previously mentioned, a 5-layer MLP was trained to classify interictal and preictal samples. As shown in Table 6.2, average test accuracies of 78.11%, 72.64%, and 73.26% were achieved using features *P1*, *P2*, and *Mave,* respectively. Table 6.2 reports performance results, in terms of accuracy, during training and testing, for all features from the 3 dogs. Training and testing performances were close in the case of *P1* and *P2,* whereas it was not in the case with the *Mave* feature, suggesting that the latter may be less useful for seizure prediction. An early stopping strategy was used during training. Training and validation were iterated through 10,000 epochs. Checkpointing was performed on a 10 epochs basis (save classifier model). The best model was chosen as the latest saved classifier model before validation loss starts increasing. The model was then assessed on held-out test data.

6.5 Discussion

In this work, we have examined the ability of HOS features in distinguishing preictal from interictal iEEG recordings in canines implanted with the NeuroVista ambulatory monitoring device. To our knowledge, this is the first investigation of the bispectrum within the context of seizure prediction. Unlike power spectrum (commonly used in forecasting studies), the bispectrum preserves phase information, which is useful for displaying quadratic nonlinear coupling between the different frequency components of the signal. Results highlight the feasibility of seizure forecasting, based on higher order spectra. These results compliment previous investigations of cross-frequency analysis, namely phase-amplitude coupling for seizure forecasting [10,11]. In addition, prominent performances of EEG-bispectrum features were reported within the context of EEG signal classification [13]. Chua et al. 2009 demonstrated a significant difference between EEG recordings from healthy and epileptic patients, using a one-way ANOVA test [13].

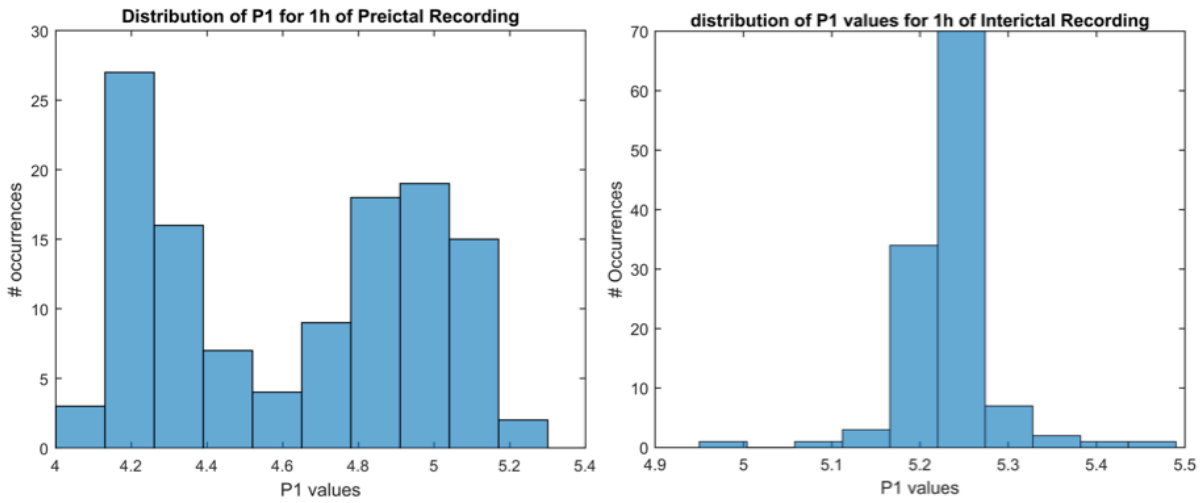

Figure 6.5 Distribution of P1 values during preictal (left) and interictal (right) periods. Each represents values extracted from 1h of continuous recording from Dog 2.

ANOVA statistical analysis results revealed a general tendency for *P1* and *P2* features to decrease during the preictal state (decrease in mean amplitude for all 3 dogs). As these features display irregularity in the properties of iEEG signals, it seems that the iEEG characteristics tend to become more regular during the preictal state. These findings are in agreement with previous dimension analysis of EEG studies, which showed that seizures can be considered as emergent brain states with reduced complexity as compared to non-seizure activity [18, 19]. As emphasized in [20], it appears that a loss of complexity is associated with functional impairment of biological systems. In addition, Mann-Whitney test results confirmed the observed decrease of irregularity, while displaying a more normal distribution of interictal values as compared to preictal ones (Fig. 6.5).

The use of the NeuroVista database allowed investigating the bilateral nature of HOS changes. Although dogs were diagnosed with focal epilepsy [11, 15], bilateral preictal HOS changes were found in all 3 dogs. Interestingly, these findings correlate with our previous PAC-based preictal changes [11]. Unfortunately, we were unable to correlate these findings with respect to the exact location of the seizure onset zone, as this information is not provided within the dataset.

Recent reports have shown that high frequency oscillations can be used as a predecessor of seizure activity [21]. Considering the sampling frequency limitation imposed by the NeuroVista ambulatory monitoring device (Fs=400 Hz), we were unable to explore quadratic non-linear coupling at the HFO level.

In this work, we did not explore the interaction among pre-defined frequency bands (standard iEEG frequency bands). The whole available frequency range was included in the analysis. The fact that standard iEEG frequency bands are used in power spectrum-based analysis does not necessarily justify their use in bispectrum analysis. Although this research avenue is tempting, it goes beyond the focus of this manuscript.

In this manuscript, we have demonstrated the suitability of MLP neural networks for the classification of interictal and preictal samples based on bispectrum-extracted features. Considering the image-based nature of bispectrum plots, it would be interesting to investigate the use of other types of neural networks' architectures, namely, convolutional neural networks (CNNs). The design of seizure predictors, combining raw bispectrum plots and CNNs, is a tempting approach that may improve seizure prediction capabilities.

Each of the aforementioned features was used as an input to a seizure prediction algorithm. To avoid any bias, no previous assumption (based on the statistical analysis) was included during the seizure forecasting algorithm design. For each feature, all electrodes were used as inputs to a 5-layer MLP neural network. We ensured adequate performance evaluation and employed rigorous methodology to avoid reporting overoptimistic results: (1) data were split into training, validation, and testing; (2) Splitting was performed on a seizure per seizure basis to avoid leakage, or time correlation; and (3) Held-out validation and testing were performed. As in previous seizure forecasting investigations, results highlight that changes are not homogenous across the tested dogs and that subject-specific algorithms are required. It is worth mentioning that no post-processing has been performed in this work in an attempt to improve forecasting capabilities. Our objective was to test the capability of a neural network for individually classifying feature samples extracted from 30-sec iEEG samples as preictal or interictal. Future perspectives include extrapolating this methodology to a continuous seizure prediction framework which considers time-based modulation of HOS features. Such algorithms could be implemented into closed-loop intervention systems for advisory or intervention purposes.

6.6 Conclusion

In conclusion, this work can be considered as a proof of principle study on the feasibility of seizure prediction based on HOS features. We have demonstrated statistically significant differences between preictal and interictal iEEG recordings for all the computed features. In addition, HOS analysis showed promising forecasting performances, when used as inputs to a

neural network classifier. Additional studies assessing the performance of HOS features for seizure forecasting, ideally in a quasi-prospective setting, are necessary to advance the development of seizure advisory/intervention devices.

6.7 Acknowledgements

Authors acknowledge financial support from the Natural Sciences and Engineering Research Council of Canada (NSERC), Epilepsy Canada, and the Institute for Data Valorization (IVADO). DKN holds the Canada Research Chair in Epilepsy and Functional Anatomy of the Human Brain.

6.8 References

[1] P. Kwan and J. W. Sander, "The natural history of epilepsy: an epidemiological view," *Journal of Neurology, Neurosurgery & Psychiatry*, vol. 75, 2004.

[2] M. R. Keezer, S. M. Sisodiya, and J. W. Sander, "Comorbidities of epilepsy: current concepts and future perspectives," *The Lancet Neurology*, vol. 15, pp. 1474-4465 (Electronic), 2016.

[3] T. Cloppenborg, T. W. May, I. Blümcke, P. Grewe, L. J. Hopf, T. Kalbhenn, et al., "Trends in epilepsy surgery: stable surgical numbers despite increasing presurgical volumes," *Journal of Neurology, Neurosurgery & Psychiatry*, vol. 87, 2016.

[4] N. Jette and J. Engel, "Refractory epilepsy is a life-threatening disease: Lest we forget," *Neurology*, vol. 86, 2016.

[5] E. Bou Assi, D. K. Nguyen, S. Rihana, and M. Sawan, "Towards accurate prediction of epileptic seizures: A review," *Biomedical Signal Processing and Control*, vol. 34, pp. 144-157, 2017.

[6] K. Gadhoumi, J.-M. Lina, F. Mormann, and J. Gotman, "Seizure prediction for therapeutic devices: A review," *Journal of Neuroscience Methods*, vol. 260, 2015.

[7] F. Mormann, T. Kreuz, C. Rieke, R. G. Andrzejak, A. Kraskov, P. David, et al., "On the predictability of epileptic seizures," *Clinical Neurophysiology*, vol. 116, pp. 569-587, 2005.

[8] F. Mormann, R. G. Andrzejak, C. E. Elger, and K. Lehnertz, "Seizure prediction: the long and winding road," *Brain,* vol. 130, pp. 314-333, 2007.

[9] V. Jirsa and V. Muller, "Cross-frequency coupling in real and virtual brain networks," *Frontiers in Computational Neurocience*, vol. 7, 2013.

[10] C. Alvarado-Rojas, M. Valderrama, A. Fouad-Ahmed, H. Feldwisch-Drentrup, M. Ihle, C. A. Teixeira, et al., "Slow modulations of high-frequency activity (40–140 Hz) discriminate preictal changes in human focal epilepsy," *Scientific Reports*, vol. 4, 2014.

[11] L. Gagliano, E. Bou Assi, D. K. Nguyen, S. Rihana, and M. Sawan, "Bilateral preictal signature of phase-amplitude coupling in canine epilepsy," *Epilepsy Research*, vol. 139, pp. 123-128, 2018.

[12] M. Bandarabadi, C. A. Teixeira, J. Rasekhi, and A. Dourado, "Epileptic seizure prediction using relative spectral power features," *Clinical Neurophysiology*, vol. 126, pp. 237-248, 2015.

[13] K. C. Chua, V. Chandran, U. Rajendra Acharya, and C. M. Lim, "Analysis of epileptic EEG signals using higher order spectra," *Journal of Medical Engineering & Technology*, vol. 33, pp. 42-50, 2009.

[14] B. H. Brinkmann, E. E. Patterson, C. Vite, V. M. Vasoli, D. Crepeau, M. Stead, et al., "Forecasting Seizures Using Intracranial EEG Measures and SVM in Naturally Occurring Canine Epilepsy," *PLoS ONE*, vol. 10, 2015.

[15] J. J. Howbert, E. E. Patterson, S. M. Stead, B. Brinkmann, V. Vasoli, D. Crepeau, et al., "Forecasting Seizures in Dogs with Naturally Occurring Epilepsy," *PLoS ONE*, vol. 9, 2014.

[16] E. B. Assi, D. K. Nguyen, S. Rihana, and M. Sawan, "A Functional-Genetic Scheme for Seizure Forecasting in Canine Epilepsy," *IEEE Transactions on Biomedical Engineering*, vol. 65, pp. 1339-1348, 2018

[17] N. Tian-Tsong, C. Shih-Fu, and S. Qibin, "Blind detection of photomontage using higher order statistics," in *2004 IEEE International Symposium on Circuits and Systems*, 2004, pp. 688-691, vol.5.

[18] K. Lehnertz and C. E. Elger, "Spatio-temporal dynamics of the primary epileptogenic area in temporal lobe epilepsy characterized by neuronal complexity loss," *Electroencephalography and Clinical Neurophysiology*, vol. 95, pp. 108-117, 1995.

[19] K. Lehnertz and C. E. Elger, "Can Epileptic Seizures be Predicted? Evidence from Nonlinear Time Series Analysis of Brain Electrical Activity," *Physical Review Letters,* vol. 80, pp. 5019-5022, 1998.

[20] J. Röschke, J. Fell, and P. Beckmann, "The calculation of the first positive Lyapunov exponent in sleep EEG data," *Electroencephalography and Clinical Neurophysiology*, vol. 86, pp. 348-352, 1993.

[21] L. Menendez de la Prida, R.J. Staba, and J.A. Dian, "Conundrums of high-frequency oscillations (80-800 Hz) in the epileptic brain," *Journal of Clinical Neurophysiology*, vol. 32, pp. 207-219, 2015.

CHAPTER 7 GENERAL DISCUSSION

This thesis confirms the feasibility of seizure forecasting based on long term continuous iEEG recordings. The transition into the ictal state is not random with a build-up leading to seizures. Throughout this thesis, we attempted to address the main perspectives recently proposed by the seizure prediction community. These includes: 1) the need for bilateral long term continuous iEEG recordings [49], 2) the adequate identification of the epileptogenic network and electrodes' location for seizure prediction [48, 50], 3) the clinical utility of probabilistic outputs as compared to binary classification [127], and 4) the need for new precursors of epileptic activity [48, 49, 127]. First, an accurate seizure forecasting algorithm was proposed after adaptively identifying sources and sinks of seizure activity in bilateral continuous canine iEEG recordings (objective 1). Then, to allow reproducing such methodology in high density human iEEG recordings, the swADTF was validated as a quantitative tool for the determination of seizure origin and propagation (objective 2). In parallel, new precursors of seizure activity were proposed and used as inputs to an MLP classifier (objective 3).

7.1 Summary of contributions

Accurate seizure forecasting is currently an important target in the epilepsy research community. For a long time, the paucity of iEEG recordings, the limited amounts of ictal events, and the short duration of interictal periods have been the major obstacles for adequate assessment of the seizure forecasting algorithms. The first objective of this thesis was the development and validation of an accurate seizure forecasting algorithm combining effective connectivity measures for seizure onset zone localization and artificial intelligence techniques for algorithm's development. To our knowledge, no previous seizure prediction investigation had undertaken ***effective-connectivity based raw electrode selection prior to algorithm's implementation***. Reported performance measures were assessed on a total of ***893 days of ambulatory iEEG recordings***. We proposed the use of Kmeans-directed transfer function, an adaptive effective connectivity method intended for the seizure onset zone localization in bilateral iEEG recordings. Electrodes identified as seizure activity sources and sinks were then used to implement a seizure-forecasting algorithm on long-term continuous recordings in dogs with naturally-occurring epilepsy. In addition, proposing the precision recall-area under the curve fitness function allowed inclusion of the whole interictal training set in the algorithm's cost function. This is the first

study to explore the use of a ***fitness function insensitive to skewed (unbalanced) class distribution***. Results showed performance improvement compared to previous studies, achieving average sensitivity of 84.82% and time in warning of 10%.

The second objective of this thesis was to propose and validate a quantitative framework for the determination of seizure activity sources and sinks when dealing with ***high density iEEG recordings (mean of 96 electrodes)***. Operculo-insular epilepsy was a suitable model for assessing such a framework as ictal discharges propagate very rapidly through its dense connections to the surrounding lobes. This may explain the reason for the resemblance of insular seizures to parietal lobe seizures (with the presence of somatosensory symptoms), frontal lobe seizures (with the occurrence of hypermotor manifestations) and temporal lobe seizures (when viscerosensory or dysphasic symptoms are present). Because access to the insula is relatively difficult (it is deeply seated, below highly eloquent opercula and above the extreme/external capsules and surrounded by a dense wall of middle cerebral artery branches), only specialized centers such as the CHUM can explore the insula during iEEG studies. This work is likely the ***first investigation of multivariate adaptive autoregressive modeling-based effective connectivity for the analysis of patients with operculo-insular epilepsy.*** The swADTF has been recently proposed as an effective connectivity measure able to cope with iEEG stationarity requirements while considering the full frequency range of the signal. In this work, the ability of the swADTF in localizing the seizure onset zone in 7 patients with apparent operculo-insular seizures was examined. Results confirmed an operculo-insular seizure origin in patients with good post-surgical outcomes while different or additional seizure foci were identified in patients with bad post-operative outcomes. These findings highlight the possibility of using quantitative approaches to accurately identify generators and sinks of seizure activity, based on high density iEEG recordings, thus paving the way for their use in seizure prediction algorithms in human iEEG recordings.

Although several endeavors have been made to identify a unique precursor of seizure activity, no single feature has shown to be capable to individually track changes during the transition to seizures. Spectral band power, the commonly used feature in seizure prediction, cannot identify interactions among frequency components of a signal. In contrast, information regarding multi-frequency behaviors can be captured by more complex metrics related to the concept of cross frequency coupling. The third objective of this thesis was to investigate the suitability of bispectrum-extracted features in quantifying changes between preictal and interictal

states. To our knowledge, this is the ***first investigation of the use of the bispectrum for seizure forecasting***. The mean of magnitude, normalized bispectral entropy, and normalized squared bispectral entropy were extracted from the bispectrum, estimated for all possible frequency pairs (f_1, f_2) in the range [0.5 - 180] Hz. To analyze the general level of interaction between the type of recording and the value of each feature, as well as the spatial localization of bispectral features' changes, One-Way ANOVA and Mann-Whitney U-test statistical tests were respectively performed. In addition, a 5-layer MLP was trained to automatically classify preictal and interictal samples and showed promising performances. This work can be considered as a preliminary investigation on the feasibility of seizure forecasting based on higher order spectra features.

7.2 Adequate assessment of seizure forecasting

Throughout the whole thesis, we ensured a rigorous methodology and an adequate performance evaluation to avoid reporting overoptimistic performances. Data were always split into train, validation, and test on a seizure-pre-seizure basis, to avoid contamination or time correlation. Scaling parameters were always assessed based solely on the training set.

In the first reported work, we made sure that seizures undergoing connectivity analysis were neither subjected to validation nor to test. In addition, we attempted to imitate a real clinical scenario: the first cluster of each dog was used for training and validation while all the remaining recording was subjected to test in a quasi-prospective manner. While a great majority of previous seizure forecasting investigations reported testing performances on less than 30% of the data, we assessed our algorithm's performance on more than 90% of the available data. Using such large amounts of data for testing allows assessing long-term seizure forecasting capabilities. To our knowledge, this is one of the first studies to include a high percentage of days in the testing set. In the prospective trial led by Cook et al. (2013), the percentage of days used for test was an average of 16.32% [70]. Subsequently, Karoly et al. (2017) used 62.61% of total data for testing [128]. In a follow-up study, Kiral-Kornek et al. (2018) increased the proportion of test data to 88.9 % [129]. In addition, although long-term quasi-prospective testing (with relatively high number of testing days) was performed, we statistically validated the significance of reported performances by comparison to a Poison-process chance forecasting algorithm, as proposed by Snyder [50]. The proposed methodology achieved average sensitivity of 84.82% and average

time in warning of 10% significantly beating a random predictor by an average of 74.82% for all three dogs ($p<0.01$).

In the analysis-based-studies, we ensured using adequate statistical tests. Surrogate data testing was specifically designed and used to validate the significance of causal relations. We imposed a significance level of 0.05 to ensure the statistical significance of reported results.

In the third reported work, we made sure not to include any prior assumptions (based on statistical results) during the design of the seizure forecasting algorithm. The two sub-parts of this study were conducted separately.

7.3 Bilateral recordings for seizure prediction

Although the dogs were diagnosed with focal epilepsy, the implantation of electrodes covered both hemispheres and allowed investigation of the bilateral nature of preictal changes. The DTF identified focal generators in all the dogs, confirming the diagnosis of focal epilepsy and sinks spanned both hemispheres in 2 of the 3 dogs, suggesting an interhemispheric communication during seizure initiation. Analyzing the spatial distribution of the iEEG channels for which bispectrum-extracted features were most prominent, bilateral preictal changes were found in all the 3 dogs. The spatial distribution of preictal changes coincided with that of PAC preictal changes, reported in our previous study [130]. It has been previously suggested that CFC changes, namely in terms of PAC, vary within different brain areas in a subject specific manner [25]. However, the analysis was limited to electrodes implanted within the SOZ as identified by visual inspection. These results suggest that, although not considered in earlier seizure prediction investigations, bilateral iEEG recordings may represent an added value in seizure forecasting. This observation is in line with the recently proposed recommendations, by Gadhoumi et al. 2015 [49].

7.4 Electrode selection based on raw recordings

The effective connectivity-based approach discussed in this thesis allowed a sort of electrode selection based on raw data, which reduced computational requirements of the GA, that is considered as a main constraint for the development of seizure predictors. In contrast, recent studies have discussed a degradation of classifier's performance over time, due to the non-stationary nature of iEEG recordings [127, 128]. Subsequently, Kiral-Lornek et al. (2018)

proposed a dynamic seizure prediction strategy, allowing for the algorithm to be retrained with the 30 most recent days [129]. Using an electrode selection based on raw data rather than electrode-feature combinations makes such retraining strategy possible in real clinical settings. More specifically, the proposed framework allows independently identifying the network of seizure activity (sources and sinks) from high density iEEG recordings, followed by algorithmic development. Only selected electrodes are kept during device deployment. Since electrodes are chosen based on raw data, and thus are feature-independent, new features can be re-selected at any time during re-training without changing electrode positions or requiring the implantation of new electrodes. In this work (Objective 1), we did not attempt to investigate the effect of time on the performance of the proposed algorithm. Nevertheless, reported performances suggest that a system able to autonomously operate over long time periods, without the need for reconfiguration or maintenance, is feasible.

7.5 Performance comparison

Due to the absence of an established gold standard for the assessment of seizure forecasting, we could only compare prediction performances with those achieved by previous endeavours [49]. Interestingly, the long term ambulatory continuous canine iEEG recordings used in this thesis allowed a comparison with the work reported by Howbert et al. (2014) [38]. On the other hand, a seizure prediction competition was recently held on Kaggle.com (a platform for data science and machine learning competitions) during which data scientists and researchers from all around the world designed algorithms for the classification of non-continuous 10-minutes “interictal” and “preictal” iEEG clips of canine and human recordings. Although direct comparison to the results of the contest is not possible due to the reasons stated above, comparable performances were achieved. While the six winning teams of the contest reported an average AUC of 0.74 (min: 0.59, max: 0.79), our strategy achieved an average AUC of 0.87 (1-hour preictal time and 5 min intervention time). Despite the fact that canine epilepsy is a suitable model for human epilepsy, with similar electrophysiology, epidemiology, clinical representation and therapeutic response [131], it would be interesting to investigate how our proposed methodology can be translated to human models of epilepsy. Recently, Cook et al. implanted 15 patients with the same NeuroVista ambulatory monitoring device [70]. Subsequently, the same group proposed two seizure forecasting algorithms based on a logistic regression classifier [128] and a deep learning approach [129]. Unfortunately, comparison with the aforementioned studies is not possible since

the data has not been made publicly available. Should such long-term iEEG human recordings become available in the future, it would be highly valuable to the seizure prediction community. The availability of such recordings could advent the possibility of benchmarking for new studies exploring seizure prediction.

7.6 Ambulatory iEEG recordings

One of the limitations of previous seizure prediction investigations, namely those based on the Freiburg seizure prediction database, is the non-availability of information regarding medication levels and vigilance states [49]. Although iEEG recordings acquired during presurgical evaluation of patients with refractory epilepsy represent a tempting opportunity to investigate seizure forecasting capabilities, such data are usually discontinuous, of relatively short duration, and affected by drug tapering and effects of surgery [38]. Taking into account the established effect of the aforementioned factors on EEG recordings' dynamics [132, 133], they should be considered with more precaution in future seizure forecasting studies, based on such recordings. As addressed in [47], this could be a challenge to overcome in seizure prediction investigations, but in practice, a seizure forecasting algorithm can be considered as "clinically useful", if it can operate on long-term continuous iEEG data that captures different conditions and states. Interestingly, the ambulatory monitoring recordings used in this thesis (Objectives 1 and 3) allowed overcoming the above challenges by testing the algorithm on long-term recordings, eventually covering several states and conditions.

7.7 New precursors of seizure activity

Traditionally, we and others have extracted power-spectrum based features and used them as inputs to classifiers [38, 45, 72, 128, 134]. Although band power has proved to be one of the most successful features used in seizure prediction, it only displays a partial description of signal's characteristics. Considering uniform and Gaussian white noises, two discrete random processes commonly used in signal processing; both can share similar spectral characteristics though their time series are different [135]. In such case, power spectrum is not able to distinguish between them. In contrast, extending the power spectra to orders higher than 2 makes such distinction possible [135]. The third objective of this thesis explored the use of higher order statistics (also known as higher order spectra) within the context of seizure prediction. Promising performances were reported highlighting the feasibility of seizure forecasting based on bispectrum-extracted

features. Normalized spectral and squared bispectral entropies showed the most statistically significant differences. As these features have been associated with irregularity properties of EEG signals, it seems that iEEGs tend to be more regular during the preictal state (decrease in mean P1 and P2 values across 3 dogs). Results are in agreement with previous investigations which showed that seizures are emergent brain states with decreased complexity [136, 137].

7.8 Limitation of iEEG recordings

Although iEEG electrodes can capture potential changes occurring over few millimeters of cortex with a relatively high temporal resolution, they are subjected to spatial resolution and coverage constraints. Throughout this thesis, generators and sinks of seizure activity as well as prominent electrodes recording preictal changes were assessed on the basis of available iEEG coverage. Thus, iEEG contacts may have not sampled the complete SOZ. However, the proposed methodology ensured the identification of most prominent contacts for seizure prediction based on the available iEEG coverage as guided by non-invasive pre-surgical investigations.

In contrast, several studies have investigated the use of functional and effective connectivity measures to locate seizures from scalp EEG using source space connectivity [138, 139]. Employing a connectivity approach based on scalp EEG recordings to guide the implantation of intracranial electrodes is an interesting approach, yet to be explored within the context of seizure prediction and surgical planning.

CHAPTER 8 CONCLUSION AND RECOMMENDATIONS

The findings of this thesis highlight the feasibility of seizure forecasting, in long-term canine epilepsy model, assessed in a pseudo-prospective setting. Combining artificial intelligence and effective connectivity approaches has the potential to improve seizure forecasting capabilities. One of the major caveats of early seizure forecasting investigations was an inadequate assessment of seizure forecasting capabilities. The guidelines for adequate performance evaluation have paved the way for more reproducible performances although less optimistic. This thesis has also established a new strategy for data splitting in ambulatory recordings allowing for a quasi-prospective testing of seizure forecasting capabilities. On the other hand, bispectrum-extracted features showed promising performances as a possible new biomarker for seizure forecasting. Obviously, larger studies, ideally with human recordings, are required before the translation of current approaches into clinical practice. We hope that this thesis will serve as a motivation for further progress towards the development of seizure forecasting devices which could be a life changing solution for patients with refractory epilepsy.

In a recent survey led by the Epilepsy Foundation, the most significantly disabling aspect of epilepsy was the unpredictable nature of seizures, which creates a constant source of anxiety for the patients and puts them at a high risk of injury. There is currently an unmet demand for a system that can provide warnings for high seizure likelihood. Considering the complex nature of epilepsy and its underlying mechanisms, there are several theoretical and technological constraints that need to be overcome for the development of a practical seizure advisory device. Based on findings discussed above, several avenues can be explored to pinpoint towards the short-term availability of such solutions to patients with refractory epilepsy.

With current advances in signal processing and artificial intelligence techniques, investigations are being conducted for proposing powerful algorithms for predicting epileptic seizures, sometimes combining features and classifiers. These powerful algorithms are implemented on electrodes within and outside the seizure onset zone, classified visually by expert neurophysiologists. Our findings highlight the importance of selecting appropriate electrodes in seizure-prediction studies. In the 3 sub-studies of this work, we ensured to include the complete set of available electrodes in our analysis. Interestingly, bilateral preictal changes were found in

dogs with naturally occurring focal epilepsy (Articles 1 and 3). In contrast, while connectivity-based estimations of sources and sinks of seizure activity were in-line with the regions identified by clinical interpretation (patients with good post-surgical outcomes), additional or different generators were sometimes found in the case of patients with poor post-surgical outcomes (Article 2). Considering the retrospective nature of this study, it was not possible to investigate whether the resection of suggested brain regions would have rendered the patients seizure-free, and thus if the identified regions contained the actual generators of seizure activity. Although this thesis highlights the potential of electrode selection based on effective connectivity, further efforts with larger cohorts are required.

Future algorithm-based studies should investigate features and classifications that can be interpreted physiologically, which in turn could provide more insights into the mechanisms of ictogenesis. These algorithms should be simple, so that they can be correlated with clinical events. Combining features and selecting the most discriminative ones to create a subject-specific predictor, is likely to be a convenient approach. Since the information provided by different extracted features may be complementary in some cases, we recommend using feature-selection algorithms to search for the best combination of features instead of ranking them. In contrast, very interesting studies have been published in the field of seizure detection. In terms of feature extraction, Tzallas et al. 2009 [140] reported high classification abilities of time-frequency based feature extraction in epileptic seizure detection. In addition, Rivero et al. (2015) [141] and (2013) [142] demonstrated the suitability of automatic feature extraction, namely genetic programming, in the detection of the seizure onset as well as for EEG signal classification. Subassi et al. (2007) [143] demonstrated the potential of a mixture of expert models in detecting epileptic seizures. Classification has also been well-tackled in the field of seizure detection. For example, Rivero et al. (2009) [144] proposed a new evolutionary classification approach based on forward and recurrent neural networks. They reported promising performances in detecting epileptic seizures [144]. For a detailed review of different transforms applied to EEG recordings, feature extraction strategies and classification methods developed within the context of seizure detection, readers are referred to [145]. It is highly recommended that these methodologies be extrapolated to the problem of seizure forecasting.

Our third finding highlights the feasibility of seizure forecasting based on bispectrum-extracted features. Although not included in this thesis, we have also investigated the use of

phase-amplitude coupling and bicoherence, which reported less promising performances [130]. Interestingly, the bispectrum can be extrapolated to its bivariate form called “cross-bispectrum”, which is asymmetric and thus allows to evaluate coupling directionality. Investigating multi-frequency behaviours among different channels is a promising avenue that could be explored in future studies. An additional perspective is to assess the feasibility of seizure forecasting, based on bispectrum-extracted features on human high density iEEG recordings.

In many studies, relatively low sampling frequency is considered to be a constraint, and predictive capability is found to correlate with sampling frequency [65]. Therefore, new approaches should benefit from currently-available signal acquisition systems allowing higher sampling rates and detection of high frequency oscillations (80-500 Hz).

We and others have demonstrated the feasibility of seizure forecasting on desktop computers, which are obviously not very practical for clinical use [33, 48, 49, 128, 129]. The NeuroVista ambulatory monitoring device included a rechargeable handheld device containing a processor. However, all subsequently developed algorithms were not subject to any power/processor constraints. Since the design of accurate seizure predictors, based on complex algorithms, requires robust and power-intensive processors, the next challenge for translating seizure prediction to clinical practice is to address the issue of hardware implementation.

Deep learning, a newly investigated approach for seizure prediction, has great potential for answering the question of hardware implementation as it features relatively low power consumption. However, using deep learning to forecast seizures requires specifically tailored approaches and network architectures. Although breakthroughs were recently achieved in intractable classification problems such as natural language processing, EEG-motor signals decoding [146], action recognition, and image classification [147] by applying deep learning approaches [148], these techniques cannot integrate time and magnitude-varying temporal information. In contrast, interesting architectures have been recently deployed by weather forecasters in an attempt to incorporate forecasting algorithm combining spatio-temporal information of multiple scales [149]. On the other hand, iEEG recordings can be easily transformed into 2D images (as in the case of bispectrum), where there is a great potential for convolutional neural networks to perform an image-based classification of preictal and interictal samples.

Finally, a promising avenue for future seizure forecasting investigations is the implementation of advisory devices using simple/minimally invasive measures. The recent progress in smart-wear monitoring allows the retrieval of a large amount of physiological measures using ergonomic and comfortable acquisition techniques. A multimodal setting able to capture complementary measures such as heart rate monitoring, respiration, accelerometry, and even time of day (circadian profile) is an interesting perspective with a broader target/scale.

BIBLIOGRAPHY

[1] S. Wiebe, D. Bellhouse, C. Fallahay, and M. Eliasziw, "Burden of epilepsy: the Ontario Health Survey," *The Canadian journal of neurological sciences,* vol. 26, 1999.

[2] S. Fisher Robert, E. Boas Walter van, W. Blume, C. Elger, P. Genton, P. Lee*, et al.*, "Epileptic Seizures and Epilepsy: Definitions Proposed by the International League Against Epilepsy (ILAE) and the International Bureau for Epilepsy (IBE)," *Epilepsia,* vol. 46, 2005.

[3] T. Blume Warren, O. Lüders Hans, E. Mizrahi, C. Tassinari, W. Van Emde Boas, and J. Engel, "Glossary of Descriptive Terminology for Ictal Semiology: Report of the ILAE Task Force on Classification and Terminology," *Epilepsia,* vol. 42, pp. 1212-1218, 2002.

[4] L. Sörnmo and P. Laguna, *Bioelectrical Signal Processing in Cardiac and Neurological Applications*: Elsevier Academic Press, 2005.

[5] J. J. Falco-Walter, I. E. Scheffer, and R. S. Fisher, "The new definition and classification of seizures and epilepsy," *Epilepsy Research,* vol. 139, pp. 73-79, 2018.

[6] J. Engel, T. A. Pedley, and J. Aicardi, *Epilepsy: A Comprehensive Textbook*: Lippincott-Raven, 1998.

[7] H. Stefan and F. H. Lopes da Silva, "Epileptic Neuronal Networks: Methods of Identification and Clinical Relevance," *Frontiers in Neurology,* vol. 4, p. 8, 2013.

[8] F. Leutmezer, S. Lurger, and C. Baumgartner, "Focal features in patients with idiopathic generalized epilepsy," *Epilepsy Research,* vol. 50, pp. 293-300, 2002.

[9] O. Lüders Hans, J. Turnbull, and F. Kaffashi, "Are the dichotomies generalized versus focal epilepsies and idiopathic versus symptomatic epilepsies still valid in modern epileptology?," *Epilepsia,* vol. 50, pp. 1336-1343, 2009.

[10] S. Pati and A. J. Cole, "How focal is generalized epilepsy: A distinction with a difference?," *Epilepsy & Behavior,* vol. 34, pp. 127-128, 2014.

[11] S. Sanei, J. A. Chambers, S. Sanei, and J. A. Chambers, "Fundamentals of EEG Signal Processing," in *EEG Signal Processing*, ed: John Wiley & Sons Ltd, 2007, pp. 35-125.

[12] P. Gloor, "The work of Hans Berger," *Electroencephalography and Clinical Neurophysiology,* vol. 27, p. 649, 1969.

[13] E. Niedermeyer and F. H. L. da Silva, *Electroencephalography: Basic Principles, Clinical Applications, and Related Fields*: Lippincott Williams & Wilkins, 2005.

[14] F. L. Britton JW, Hopp JLet al., authors; St. Louis EK, Frey LC, "Electroencephalography (EEG): An Introductory Text and Atlas of Normal and Abnormal Findings in Adults, Children, and Infants " *American Epilepsy Society,* 2016.

[15] M. Kreuzer, "EEG Based Monitoring of General Anesthesia: Taking the Next Steps," *Frontiers in Computational Neuroscience,* vol. 11, p. 56, 2017.

[16] P. Gloor, "Neuronal Generators and the Problem of Localization in Electroencephalography: Application of Volume Conductor Theory to Electroencephalography," *Journal of Clinical Neurophysiology,* vol. 2, 1985.

[17] R. Cooper, A. L. Winter, H. J. Crow, and W. G. Walter, "Comparison of subcortical, cortical and scalp activity using chronically indwelling electrodes in man," *Electroencephalography and Clinical Neurophysiology,* vol. 18, pp. 217-228, 1965.

[18] A. Varsavsky, I. Mareels, and M. Cook, *Epileptic Seizures and the EEG: Measurement, Models, Detection and Prediction*: CRC Press, 2016.

[19] B. Graimann, B. Allison, and G. Pfurtscheller, "Brain–Computer Interfaces: A Gentle Introduction," in *Brain-Computer Interfaces: Revolutionizing Human-Computer Interaction*, B. Graimann, G. Pfurtscheller, and B. Allison, Eds., ed Berlin, Heidelberg: Springer Berlin Heidelberg, 2010, pp. 1-27.

[20] N. Foldvary, G. Klem, J. Hammel, W. Bingaman, I. Najm, and H. Lüders, "The localizing value of ictal EEG in focal epilepsy," *Neurology,* vol. 57, p. 2022, 2001.

[21] P. Boon, J. De Reuck, C. Drieghe, K. De Bruycker, I. Aers, and J. Pengel, "Long-Term Video-EEG Monitoring Revisited," *European Neurology,* vol. 34 (suppl 1), pp. 33-39, 1994.

[22] O. Henning, A. Baftiu, S. I. Johannessen, and C. J. Landmark, "Withdrawal of antiepileptic drugs during presurgical video-EEG monitoring: an observational study for evaluation of current practice at a referral center for epilepsy," *Acta Neurologica Scandinavica,* vol. 129, pp. 243-251, 2013.

[23] S. M. LaRoche and S. L. Helmers, "The new antiepileptic drugs: Scientific review," *JAMA,* vol. 291, pp. 605-614, 2004.

[24] P. Kwan and M. J. Brodie, "Early identification of refractory epilepsy," *The New England journal of medicine,* vol. 342, 2000.

[25] K. W. Barañano and A. L. Hartman, "The Ketogenic Diet: Uses in Epilepsy and Other Neurologic Illnesses," *Current treatment options in neurology,* vol. 10, pp. 410-419, 2008.

[26] E. Ben-Menachem, "Vagus nerve stimulation, side effects, and long-term safety," *J. Clin Neurophysiol,* vol. 18, 2001.

[27] P. Jayakar, D. Gaillard William, M. Tripathi, H. Libenson Mark, W. Mathern Gary, and J. H. Cross, "Diagnostic test utilization in evaluation for resective epilepsy surgery in children," *Epilepsia,* vol. 55, pp. 507-518, 2014.

[28] J. Tellez-Zenteno, L. Hernandez Ronquillo, F. Moien-Afshari, and S. Samuel Wiebe, "Surgical outcomes in lesional and non-lesional epilepsy: a systematic review and meta-analysis," *Epilepsy Research,* vol. 89, 2010.

[29] A. Harroud, A. Bouthillier, A. G. Weil, and D. K. Nguyen, "Temporal lobe epilepsy surgery failures: a review," *Epilepsy Research and Treatment,* vol. 2012, 2012.

[30] J. F. Tellez-Zenteno, M. Pondal-Sordo, S. Matijevic, and S. Wiebe, "National and regional prevalence of self-reported epilepsy in Canada," *Epilepsia,* vol. 45, 2004.

[31] M. T. Salam, M. Mirzaei, M. Ly, D. K. Nguyen, and M. Sawan, "An implantable closedloop asynchronous drug delivery system for the treatment of refractory epilepsy," *IEEE transactions on neural systems and rehabilitation engineering,* vol. 20, 2012.

[32] M. T. Salam, J. L. Perez-Velazquez, and R. Genov, "Seizure Suppression Efficacy of Closed-loop Versus Open-loop Deep Brain Stimulation in a Rodent Model of Epilepsy," *IEEE Transactions on Neural Systems and Rehabilitation Engineering,* vol. PP, pp. 1-1, 2015.

[33] F. Mormann, R. G. Andrzejak, C. E. Elger, and K. Lehnertz, "Seizure prediction: the long and winding road," *Brain,* vol. 130, pp. 314-333, 2007.

[34] S. Ramgopal, S. Thome-Souza, M. Jackson, N. E. Kadish, I. Sánchez Fernández, J. Klehm*, et al.*, "Seizure detection, seizure prediction, and closed-loop warning systems in epilepsy," *Epilepsy & Behavior,* vol. 37, pp. 291-307, 2014.

[35] E. B. Assi, D. K. Nguyen, S. Rihana, and M. Sawan, "Refractory epilepsy: Localization, detection, and prediction," in *2017 IEEE 12th International Conference on ASIC (ASICON)*, 2017, pp. 512-515.

[36] M. T. Salam, D. K. Nguyen, and M. Sawan, "A low-power implantable device for epileptic seizure detection and neurostimulation," in *2010 Biomedical Circuits and Systems Conference (BioCAS)*, 2010, pp. 154-157.

[37] M. Mirzaei, M. T. Salam, D. K. Nguyen, and M. Sawan, "A Fully-Asynchronous Low-Power Implantable Seizure Detector for Self-Triggering Treatment," *IEEE Transactions on Biomedical Circuits and Systems,* vol. 7, pp. 563-572, 2013.

[38] J. J. Howbert, E. E. Patterson, S. M. Stead, B. Brinkmann, V. Vasoli, D. Crepeau*, et al.*, "Forecasting Seizures in Dogs with Naturally Occurring Epilepsy," *PLoS ONE,* vol. 9, 2014.

[39] M. J. Morrell, "Responsive cortical stimulation for the treatment of medically intractable partial epilepsy," *Neurology,* vol. 77, pp. 1295-1304, 2011.

[40] B. Lee, M. N. Zubair, Y. D. Marquez, D. M. Lee, L. A. Kalayjian, C. N. Heck*, et al.*, "A Single-Center Experience with the NeuroPace RNS System: A Review of Techniques and Potential Problems," *World Neurosurgery,* vol. 84, pp. 719-726, 2015.

[41] K. A. Davis, B. K. Sturges, C. H. Vite, V. Ruedebusch, G. Worrell, A. B. Gardner*, et al.*, "A novel implanted device to wirelessly record and analyze continuous intracranial canine EEG," *Epilepsy Research,* vol. 96, pp. 116-122, 2011.

[42] L. D. Coles, E. E. Patterson, W. D. Sheffield, J. Mavoori, J. Higgins, B. Michael*, et al.*, "Feasibility study of a caregiver seizure alert system in canine epilepsy," *Epilepsy Research,* vol. 106, pp. 456-460, 2013.

[43] N. Moghim and D. W. Corne, "Predicting Epileptic Seizures in Advance," *PLoS ONE,* vol. 9, 2014.

[44] I. Korshunova, P. J. Kindermans, J. Degrave, T. Verhoeven, B. H. Brinkmann, and J. Dambre, "Towards improved design and evaluation of epileptic seizure predictors," *IEEE Transactions on Biomedical Engineering,* vol. 65, 2017.

[45] M. Bandarabadi, C. A. Teixeira, J. Rasekhi, and A. Dourado, "Epileptic seizure prediction using relative spectral power features," *Clinical Neurophysiology,* vol. 126, pp. 237-248, 2015.

[46] M. Bandarabadi, J. Rasekhi, C. A. Teixeira, M. R. Karami, and A. Dourado, "On the proper selection of preictal period for seizure prediction," *Epilepsy & Behavior,* vol. 46, pp. 158-166, 2015.

[47] F. Mormann, T. Kreuz, C. Rieke, R. G. Andrzejak, A. Kraskov, P. David*, et al.*, "On the predictability of epileptic seizures," *Clinical Neurophysiology,* vol. 116, pp. 569-587, 2005.

[48] E. Bou Assi, D. K. Nguyen, S. Rihana, and M. Sawan, "Towards accurate prediction of epileptic seizures: A review," *Biomedical Signal Processing and Control,* vol. 34, pp. 144-157, 2017.

[49] K. Gadhoumi, J.-M. Lina, F. Mormann, and J. Gotman, "Seizure prediction for therapeutic devices: A review," *Journal of Neuroscience Methods,* 2015.

[50] D. E. Snyder, J. Echauz, D. B. Grimes, and B. Litt, "The Statistics of a Practical Seizure Warning System," *Journal of neural engineering,* vol. 5, pp. 392-401, 2008.

[51] K. Gadhoumi, J.-M. Lina, and J. Gotman, "Discriminating preictal and interictal states in patients with temporal lobe epilepsy using wavelet analysis of intracerebral EEG," *Clinical Neurophysiology,* vol. 123, pp. 1906-1916, 2012.

[52] F. Mormann, T. Kreuz, R. G. Andrzejak, P. David, K. Lehnertz, and C. E. Elger, "Epileptic seizures are preceded by a decrease in synchronization," *Epilepsy Research,* vol. 53, pp. 173-185, 2003.

[53] M. D'Alessandro, G. Vachtsevanos, R. Esteller, J. Echauz, S. Cranstoun, G. Worrell*, et al.*, "A multi-feature and multi-channel univariate selection process for seizure prediction," *Clinical Neurophysiology,* vol. 116, pp. 506-516, 2005.

[54] C. Wilke, W. van Drongelen, M. Kohrman, and B. He, "Neocortical seizure foci localization by means of a directed transfer function method," *Epilepsia,* vol. 51, 2010.

[55] E. B. Assi, M. Sawan, D. K. Nguyen, and S. Rihana, "A 2D clustering approach investigating inter-hemispheric seizure flow by means of a Directed Transfer Function," in *2016 3rd Middle East Conference on Biomedical Engineering (MECBME)*, 2016, pp. 68-71.

[56] J. D. Martinez-Vargas, G. Strobbe, K. Vonck, P. van Mierlo, and G. Castellanos-Dominguez, "Improved Localization of Seizure Onset Zones Using Spatiotemporal Constraints and Time-Varying Source Connectivity," *Frontiers in Neuroscience,* vol. 11, p. 156, 2017.

[57] N. Czarnek, K. Morton, L. Collins, S. Tantum, and C. Throckmorton, "The impact of time on seizure prediction performance in the FSPEEG database," *Epilepsy & Behavior,* vol. 48, pp. 79-82, 2015.

[58] B. Direito, F. Ventura, C. Teixeira, and A. Dourado, "Optimized feature subsets for epileptic seizure prediction studies," in *Engineering in Medicine and Biology Society, EMBC, 2011 Annual International Conference of the IEEE*, 2011, pp. 1636-1639.

[59] E. B. Assi, M. Sawan, D. K. Nguyen, and S. Rihana, "A hybrid mRMR-genetic based selection method for the prediction of epileptic seizures," in *Biomedical Circuits and Systems Conference (BioCAS)*, 2015, pp. 1-4.

[60] C. Alvarado-Rojas, M. Valderrama, A. Fouad-Ahmed, H. Feldwisch-Drentrup, M. Ihle, C. A. Teixeira*, et al.*, "Slow modulations of high-frequency activity (40–140 Hz) discriminate preictal changes in human focal epilepsy," *Scientific Reports,* vol. 4, 2014.

[61] Z. Rogowski, I. Gath, and E. Bental, "On the prediction of epileptic seizures," *Biological Cybernetics,* vol. 42, pp. 9-15, 1981.

[62] Y. Salant, I. Gath, and O. Henriksen, "Prediction of epileptic seizures from two-channel EEG," *Medical and Biological Engineering and Computing,* vol. 36, pp. 549-556, 1998.

[63] L. D. Iasemidis, J. C. Sackellares, H. P. Zaveri, and W. J. Williams, "Phase space topography and the Lyapunov exponent of electrocorticograms in partial seizures," *Brain Topography,* vol. 2, pp. 187-201, 1990.

[64] S. S. Spencer, D. K. Nguyen, and R. B. Duckrow, "Invasive EEG in Presurgical Evaluation of Epilepsy," in *The Treatment of Epilepsy*, ed: Wiley-Blackwell, 2009, pp. 767-798.

[65] C. Alexandre Teixeira, B. Direito, M. Bandarabadi, M. Le Van Quyen, M. Valderrama, B. Schelter*, et al.*, "Epileptic seizure predictors based on computational intelligence techniques: A comparative study with 278 patients," *Computer Methods and Programs in Biomedicine,* vol. 114, pp. 324-336, 2014.

[66] J. Rasekhi, M. R. K. Mollaei, M. Bandarabadi, C. A. Teixeira, and A. Dourado, "Preprocessing effects of 22 linear univariate features on the performance of seizure prediction methods," *Journal of Neuroscience Methods,* vol. 217, pp. 9-16, 2013.

[67] A. Schulze-Bonhage, H. Feldwisch-Drentrup, and M. Ihle, "The role of high-quality EEG databases in the improvement and assessment of seizure prediction methods," *Epilepsy & Behavior,* vol. 22, Supplement 1, pp. S88-S93, 2011.

[68] A. Stuart, "Rank Correlation Methods. By M. G. Kendall, 2nd edition," *British Journal of Statistical Psychology,* vol. 9, pp. 68-68, 1956.

[69] J. Klatt, H. Feldwisch-Drentrup, M. Ihle, V. Navarro, M. Neufang, C. Teixeira*, et al.*, "The EPILEPSIAE database: An extensive electroencephalography database of epilepsy patients," *Epilepsia,* vol. 53, pp. 1669-1676, 2012.

[70] M. J. Cook, T. J. O'Brien, S. F. Berkovic, M. Murphy, A. Morokoff, G. Fabinyi*, et al.*, "Prediction of seizure likelihood with a long-term, implanted seizure advisory system in patients with drug-resistant epilepsy: a first-in-man study," *The Lancet Neurology,* vol. 12, pp. 563-571, 2013.

[71] B. H. Brinkmann, E. E. Patterson, C. Vite, V. M. Vasoli, D. Crepeau, M. Stead*, et al.*, "Forecasting Seizures Using Intracranial EEG Measures and SVM in Naturally Occurring Canine Epilepsy," *PLoS ONE,* vol. 10, 2015.

[72] Y. Park, L. Luo, K. K. Parhi, and T. Netoff, "Seizure prediction with spectral power of EEG using cost-sensitive support vector machines," *Epilepsia,* vol. 52, pp. 1761-1770, 2011.

[73] C. A. Teixeira, B. Direito, H. Feldwisch-Drentrup, M. Valderrama, R. P. Costa, C. Alvarado-Rojas*, et al.*, "EPILAB: A software package for studies on the prediction of epileptic seizures," *Journal of Neuroscience Methods,* vol. 200, pp. 257-271, 2011.

[74] E. B. Assi, S. Rihana, and M. Sawan, "Kmeans-ICA based automatic method for ocular artifacts removal in a motor imagery classification," in *2014 36th Annual International Conference of the IEEE Engineering in Medicine and Biology Society*, Chicago, IL, 2014, pp. 6655-6658.

[75] E. B. Assi and S. Rihana, "Kmeans-ICA based automatic method for EOG denoising in multi-channel EEG recordings," in *11th IASTED International Coneference on Biomedical Engineering*, Zurich, Switzerland, 2014.

[76] J. J. Niederhauser, R. Esteller, J. Echauz, G. Vachtsevanos, and B. Litt, "Detection of seizure precursors from depth-EEG using a sign periodogram transform," *IEEE Transactions on Biomedical Engineering,* vol. 50, pp. 449-458, 2003.

[77] M. Le Van Quyen, J. Martinerie, M. Baulac, and F. Varela, "Anticipating epileptic seizures in real time by a non-linear analysis of similarity between EEG recordings," *Neuroreport,* vol. 10, pp. 2149-2155, 1999.

[78] A. Eftekhar, W. Juffali, J. El-Imad, T. G. Constandinou, and C. Toumazou, "Ngram-Derived Pattern Recognition for the Detection and Prediction of Epileptic Seizures," *PLoS ONE,* vol. 9, 2014.

[79] B. Schelter, M. Winterhalder, T. Maiwald, A. Brandt, A. Schad, A. Schulze-Bonhage*, et al.*, "Testing statistical significance of multivariate time series analysis techniques for epileptic seizure prediction," *Chaos,* vol. 16, pp. 1054-1500 (Print), 2006.

[80] B. Schelter, M. Winterhalder, T. Maiwald, A. Brandt, A. Schad, J. Timmer*, et al.*, "Do false predictions of seizures depend on the state of vigilance? A report from two seizure-prediction methods and proposed remedies," *Epilepsia,* vol. 47, pp. 2058-2070, 2006.

[81] M. A. Harrison, I. Osorio, M. G. Frei, S. Asuri, and Y. C. Lai, "Correlation dimension and integral do not predict epileptic seizures," *Chaos,* vol. 15, 2005.

[82] P. E. McSharry, L. A. Smith, and L. Tarassenko, "Prediction of epileptic seizures: are nonlinear methods relevant?," *Nat Med,* vol. 9, pp. 241-242, 2003.

[83] A. Aarabi, R. Fazel-Rezai, and Y. Aghakhani, "EEG seizure prediction: Measures and challenges," in *Annual International Conference of the IEEE Engineering in Medicine and Biology Society*, Minneapolis, MN, USA, 2009.

[84] T. Netoff, Y. Park, and K. Parhi, "Seizure prediction using cost-sensitive support vector machine," presented at the Annual International Conference of the IEEE Engineering in Medicine and Biology Society, Minneapolis, MN, USA, 2009.

[85] D. R. Stanski, R. J. Hudson, T. D. Homer, L. J. Saidman, and E. Meathe, "Pharmacodynamic modeling of thiopental anesthesia," *Journal of Pharmacokinetics and Biopharmaceutics,* vol. 12, pp. 223-240, 1984.

[86] K. Gadhoumi, J.-M. Lina, and J. Gotman, "Seizure prediction in patients with mesial temporal lobe epilepsy using EEG measures of state similarity," *Clinical Neurophysiology,* vol. 124, pp. 1745-1754, 2013.

[87] K. Lehnertz, R. G. Andrzejak, J. Arnhold, T. Kreuz, F. Mormann, C. Rieke*, et al.*, "Nonlinear EEG analysis in epilepsy: its possible use for interictal focus localization, seizure anticipation, and prevention," *J. Clin Neurophysiol,* vol. 18, pp. 209-222, 2001.

[88] C. Alvarado-Rojas, M. Valderrama, A. Fouad-Ahmed, H. Feldwisch-Drentrup, M. Ihle, C. A. Teixeira*, et al.*, "Slow modulations of high-frequency activity (40-140-Hz) discriminate preictal changes in human focal epilepsy," *Scientific Reports,* vol. 4, pp. 2045-2322, 2014 2014.

[89] J. Sackellares, D. Shiau, J. Principe, Y. MC., L. Dance, W. Suharitdamrong*, et al.*, "Predictability analysis for an automated seizure prediction algorithm," *Clinical Neurophysiology,* vol. 23, 2006.

[90] M. Winterhalder, T. Maiwald, H. U. Voss, R. Aschenbrenner-Scheibe, J. Timmer, and A. Schulze-Bonhage, "The seizure prediction characteristic: a general framework to assess and compare seizure prediction methods," *Epilepsy & Behavior,* vol. 4, pp. 318-325, 2003.

[91] R. Aschenbrenner-Scheibe, T. Maiwald, M. Winterhalder, H. U. Voss, J. Timmer, and A. Schulze-Bonhage, "How well can epileptic seizures be predicted? An evaluation of a nonlinear method," *Brain,* vol. 126, 2003.

[92] P. Grassberger and I. Procaccia, "Estimation of the Kolmogorov entropy from a chaotic signal," *Physical Review A,* vol. 28, pp. 2591-2593, 10/01/ 1983.

[93] R. Savit and M. Green, "Time series and dependent variables," *Physica D: Nonlinear Phenomena,* vol. 50, pp. 95-116, 1991.

[94] M. G. Rosenblum, A. S. Pikovsky, and J. Kurths, "From Phase to Lag Synchronization in Coupled Chaotic Oscillators," *Physical Review Letters,* vol. 78, pp. 4193-4196, 1997.

[95] F. Mormann, R. Andrzejak, T. Kreuz, P. David, C. E. Elger, and K. Lehnertz, "Automated detection of a preseizure state based on a decrease in synchronization in intracranial electroencephalogram recordings from epilepsy patients," *Physical review. E, Statistical, nonlinear, and soft matter physics,* vol. 67, 2003.

[96] P. Mirowski, D. Madhavan, Y. Lecun, and R. Kuzniecky, "Classification of patterns of EEG synchronization for seizure prediction," *Clinical Neurophysiology,* vol. 120, 2009.

[97] M. Winterhalder, B. Schelter, T. Maiwald, A. Brandt, A. Schad, A. Schulze-Bonhage*, et al.*, "Spatio-temporal patient-individual assessment of synchronization changes for epileptic seizure prediction," *Clin, Neurophysiol,* vol. 117, pp. 2399-2413, 2006.

[98] L. D. Iasemidis, D. S. Shiau, P. M. Pardalos, W. Chaovalitwongse, K. Narayanan, A. Prasad*, et al.*, "Long-term prospective on-line real-time seizure prediction," *Clinical Neurophysiology,* vol. 116, p. 544, 2005.

[99] M. Le Van Quyen, J. Soss, V. Navarro, R. Robertson, M. Chavez, M. Baulac*, et al.*, "Preictal state identification by synchronization changes in long-term intracranial EEG recordings," *Clinical Neurophysiology,* vol. 116, pp. 559-568, 2005.

[100] H. Lee, M. Kohrman, K. Hecox, and W. van Drongelen, "Seizure Prediction," in *Neural Engineering*, B. He, Ed., ed: Springer US, 2013, pp. 685-723.

[101] P. Tass, M. G. Rosenblum, J. Weule, J. Kurths, A. Pikovsky, J. Volkmann*, et al.*, "Detection of n:m Phase Locking from Noisy Data: Application to Magnetoencephalography," *Physical Review Letters,* vol. 81, pp. 3291-3294, 1998.

[102] M. Bandarabadi, C. Teixeira, B. Direito, and A. Dourado, "Epileptic seizure prediction based on a bivariate spectral power methodology," presented at the Annual International Conference of the IEEE Engineering in Medicine and Biology Society, San Diego, CA, 2012.

[103] H. Peng, L. Fulmi, and C. Ding, "Feature selection based on mutual information criteria of max-dependency, max-relevance, and min-redundancy," *IEEE Transactions on Pattern Analysis and Machine Intelligence* vol. 27, pp. 1226-1238, 2005.

[104] A. F. Rabbi, L. Azinfar, and R. Fazel-Rezai, "Seizure prediction using adaptive neuro-fuzzy inference system," presented at the 35th Annual International Conference of the IEEE EMBS, Osaka, Japan, 2013.

[105] P. Ataee, A. Yazdani, S. K. Setarehdan, and H. A. Noubari, "Genetic Algorithm for Selection of Best Feature and Window Length for a Discriminate Pre-seizure and Normal State Classification," in *5th International Symposium on Image and Signal Processing and Analysis*, Istabul, Turkey, 2007, pp. 107-112.

[106] R. Costa, P. Oliveira, G. Rodrigues, B. Leitão, and A. Dourado, "Epileptic Seizure Classification Using Neural Networks with 14 Features," presented at the Knowledge-Based Intelligent Information and Engineering Systems, 2008.

[107] N. V. Chawla, N. Japkowicz, and A. Kotcz, "Editorial: special issue on learning from imbalanced data sets," *SIGKDD Explorations Newsletter,* vol. 6, pp. 1-6, 2004.

[108] H. Dickten, C. E. Elger, and K. Lehnertz, "Measuring directed interactions using cellular neural networks with complex connection topologies," presented at the Proceedings of the 5th International Workshop on Seizure Prediction, Dresden, Germany, 2013.

[109] V. Senger and R. Tetzlaff, "Seizure prediction by cellular nonlinear networks?," in *Recent Advances in Predicting and Preventing Epileptic Seizures*, ed: World Scientific, 2013, pp. 228-241.

[110] L. Chisci, A. Mavino, G. Perferi, M. Sciandrone, C. Anile, G. Colicchio*, et al.*, "Real-time epileptic seizure prediction using AR models and support vector machines," *IEEE Transactions on Biomedical Engineering,* vol. 57, pp. 1124-1132, 2010.

[111] C. Teixeira, B. Direito, M. Bandarabadi, and A. Dourado, "Output regularization of SVM seizure predictors: Kalman Filter versus the "Firing Power" method," presented at the Annual International Conference of the IEEE Engineering in Medicine and Biology Society, San Diego, CA, 2012.

[112] E. B. Assi, S. Rihana, and M. Sawan, "33% Classification Accuracy Improvement in a Motor Imagery Brain Computer Interface," *Journal of Biomedical Science and Engineering,* vol. Vol.10No.06, p. 16, 2017.

[113] V. Jirsa and V. Muller, "Cross-frequency coupling in real and virtual brain networks," *Frontiers in Comutational Neurocience,* vol. 7, 2013.

[114] M. Valderrama, B. Crepon, V. Botella-Soler, J. Martinerie, D. Hasboun, C. Alvarado-Rojas M. Baulac*,* C. Adam, V. Navarro, and M. Le Van Quyen, "Human gamma oscillations during slow wave sleep," *PLoS ONE,* vol. 7, 2012.

[115] K. C. Chua, V. Chandran, U. Rajendra Acharya, and C. M. Lim, "Analysis of epileptic EEG signals using higher order spectra," *Journal of Medical Engineering & Technology,* vol. 33, pp. 42-50, 2009.

[116] N. Tian-Tsong, C. Shih-Fu, and S. Qibin, "Blind detection of photomontage using higher order statistics," in *2004 IEEE International Symposium on Circuits and Systems* 2004, pp. V-688-V-691 Vol.5.

[117] C. W. J. Granger, "Investigating Causal Relations by Econometric Models and Cross-spectral Methods," *Econometrica,* vol. 37, pp. 424-438, 1969.

[118] A. Brovelli, M. Ding, A. Ledberg, Y. Chen, R. Nakamura, and S. L. Bressler, "Beta oscillations in a large-scale sensorimotor cortical network: Directional influences revealed

by Granger causality," *Proceedings of the National Academy of Sciences of the United States of America,* vol. 101, pp. 9849-9854, 2004.

[119] R. Goebel, A. Roebroeck D. S. Kim and E. Formisano, "Investigating directed cortical interactions in time-resolved fMRI data using vector autoregressive modeling and Granger causality mapping," *Magnetic Resonance Imaging*, vol. 21, 2004.

[120] R. Kus, M. Kaminski, and K. J. Blinowska, "Determination of EEG activity propagation: pair-wise versus multichannel estimate," *IEEE Transactions on Biomedical Engineering,* vol. 51, 2004.

[121] M. Kaminski, M. Ding, W. A. Truccolo, and S. L. Bressler, "Evaluating causal relations in neural systems: granger causality, directed transfer function and statistical assessment of significance," *Biological Cybernetics,* vol. 85, 2001.

[122] P. J. Franaszczuk and G. K. Bergey, "Application of the directed transfer function method to mesial and lateral onset temporal lobe seizures," *Brain Topograhy* vol. 11, 1998.

[123] P. J. Franaszczuk, G. K. Bergey, and M. J. Kaminski, "Analysis of mesial temporal seizure onset and propagation using the directed transfer function method," *Electroencephalography and Clinical Neurophysiology,* vol. 91, 1994.

[124] C. Wilke, Ding L., and B. He, "Estimation of time-varying connectivity patterns through the use of an adaptive directed transfer function," *IEEE Transactions on Biomedical Engineering,* vol. 55, 2008.

[125] P. van Mierlo, E. Carrette, H. Hallez, R. Raedt, A. Meurs, S. Vandenberghe*, et al.*, "Ictal-onset localization through connectivity analysis of intracranial EEG signals in patients with refractory epilepsy," *Epilepsia,* vol. 54, pp. 1409-1418, 2013.

[126] M. Palus and D. Hoyer, "Detecting nonlinearity and phase synchronization with surrogate data," *Engineering in Medicine and Biology Magazine, IEEE,* vol. 17, pp. 40-45, 1998.

[127] D. R. Freestone, P. J. Karoly, and M. J. Cook, "A forward-looking review of seizure prediction," *Current Opinion in Neurology,* vol. 30, 2017.

[128] P. J. Karoly, H. Ung, D. B. Grayden, L. Kuhlmann, K. Leyde, M. J. Cook*, et al.*, "The circadian profile of epilepsy improves seizure forecasting," *Brain,* vol. 140, pp. 2169-2182, 2017.

[129] I. Kiral-Kornek, S. Roy, E. Nurse, B. Mashford, P. Karoly, T. Carroll*, et al.*, "Epileptic Seizure Prediction Using Big Data and Deep Learning: Toward a Mobile System," *EBioMedicine,* vol. 27, pp. 103-111, 2018.

[130] L. Gagliano, E. Bou Assi, D. K. Nguyen, S. Rihana, and M. Sawan, "Bilateral preictal signature of phase-amplitude coupling in canine epilepsy," *Epilepsy Research,* vol. 139, pp. 123-128, 2018.

[131] K. Chandler, "Canine epilepsy: What can we learn from human seizure disorders?," *The Veterinary Journal,* vol. 172, pp. 207-217, 2006.

[132] K. Lehnertz and C. E. Elger, "Neuronal complexity loss in temporal lobe epilepsy: effects of carbamazepine on the dynamics of the epileptogenic focus," *Electroencephalography and Clinical Neurophysiology,* vol. 103, pp. 376-380, 1197.

[133] W. T. Blume, "Drug effects on EEG," *Clin, Neurophysiol,* vol. 23, 2006.

[134] E. B. Assi, D. K. Nguyen, S. Rihana, and M. Sawan, "A Functional-Genetic Scheme for Seizure Forecasting in Canine Epilepsy," *IEEE Transactions on Biomedical Engineering,* vol. 65, pp. 1339-1348, 2018.

[135] W. B. Collis, P. R. White, and J. K. Hammond, "Higher-order spectra: the bispectrum and trispectrum," *Mechanical Systems and Signal Processing,* vol. 12, pp. 375-394, 1998.

[136] K. Lehnertz and C. E. Elger, "Spatio-temporal dynamics of the primary epileptogenic area in temporal lobe epilepsy characterized by neuronal complexity loss," *Electroencephalography and Clinical Neurophysiology,* vol. 95, pp. 108-117, 1995.

[137] K. Lehnertz and C. E. Elger, "Can Epileptic Seizures be Predicted? Evidence from Nonlinear Time Series Analysis of Brain Electrical Activity," *Physical Review Letters,* vol. 80, pp. 5019-5022, 1998.

[138] W. Staljanssens, G. Strobbe, R. Van Holen, V. Keereman, S. Gadeyne, E. Carrette*, et al.*, "EEG source connectivity to localize the seizure onset zone in patients with drug resistant epilepsy," *NeuroImage: Clinical,* vol. 16, pp. 689-698, 2017.

[139] L. Ding, G. A. Worrell, T. D. Lagerlund, and B. He, "Ictal Source Analysis: Localization and Imaging of Causal Interactions in Humans," *NeuroImage,* vol. 34, pp. 575-586, 2007.

[140] A. T. Tzallas, M. G. Tsipouras, and D. I. Fotiadis, "Epileptic seizure detection in EEGs using time-frequency analysis," *IEEE Transactions on information technology in biomedicine,* vol. 13, pp. 703-710, 2009.

[141] D. Rivero, E. Fernandez-Blanco, J. Dorado, and A. Pazos, "Classification of Two-channel Signals by Means of Genetic Programming," presented at the Proceedings of the Companion Publication of the 2015 Annual Conference on Genetic and Evolutionary Computation, Madrid, Spain, 2015.

[142] E. Fernández-Blanco, D. Rivero, M. Gestal, and J. Dorado, "Classification of signals by means of Genetic Programming," *Soft Computing,* vol. 17, pp. 1929-1937, 2013.

[143] A. Subasi, "EEG signal classification using wavelet feature extraction and a mixture of expert model," *Expert Systems with Applications,* vol. 32, pp. 1084-1093, 2007.

[144] D. Rivero, J. Dorado, J. Rabu, and A. Pazos, "Evolving simple feed-forward and recurrent ANNs for signal classification: a comparison," presented at the Proceedings of the 2009 international joint conference on Neural Networks, Atlanta, Georgia, USA, 2009.

[145] U. R. Acharya, S. Vinitha Sree, G. Swapna, R. J. Martis, and J. S. Suri, "Automated EEG analysis of epilepsy: A review," *Knowledge-Based Systems,* vol. 45, pp. 147-165, 2013.

[146] E. Nurse, B. S. Mashford, A. J. Yepes, I. Kiral-Kornek, S. Harrer, and D. R. Freestone, "Decoding EEG and LFP signals using deep learning: heading TrueNorth," presented at the Proceedings of the ACM International Conference on Computing Frontiers, Como, Italy, 2016.

[147] A. Krizhevsky, I. Sutskever, and G. E. Hinton, "ImageNet classification with deep convolutional neural networks," presented at the Proceedings of the 25th International Conference on Neural Information Processing Systems - Volume 1, Lake Tahoe, Nevada, 2012.

[148] Y. LeCun, Y. Bengio, and G. Hinton, "Deep learning," *Nature,* vol. 521, p. 436, 2015.

[149] L. F. Richardson., "Weather prediction by numerical process. ," *Quarterly Journal of the Royal Meteorological Society,* vol. 48, pp. 282-284, 1922.

[150] L. R. Rabiner, B. Gold, and C. K. Yuen, "Theory and Application of Digital Signal Processing," *Systems, Man and Cybernetics, IEEE Transactions on,* vol. 8, pp. 146-146, 1978.

[151] P. L. Nunez and R. Srinivasan, *Electric fields of the brain: the neurophysics of EEG*: Oxford university press, 2006.

[152] P. Rajdev, M. Ward, J. Rickus, R. Worth, and P. Irazoqui, "Real-time seizure prediction from local field potentials using an adaptive Wiener algorithm," *Comput Biol, Med,* vol. 40, 2010.

[153] F. Takens, "Detecting strange attractors in turbulence," in *Dynamical Systems and Turbulence, Warwick 1980*. vol. 898, D. Rand and L.-S. Young, Eds., ed: Springer Berlin Heidelberg, 1981, pp. 366-381.

[154] P. Grassberger and I. Procaccia, "Characterization of strange attractors," *Physical Review Letters,* vol. 50, pp. 346-349, 1983.

[155] A. Wolf, J. B. Swift, H. L. Swinney, and J. A. Vastano, "Determining Lyapunov exponents from a time series," *Physica D: Nonlinear Phenomena,* vol. 16, pp. 285-317, 1985.

[156] Y. C. Lai, M. F. Harrison M. Frei, and I. Osorio, "Inability of Lyapunov exponents to predict epileptic seizures," *Physical Review Letters,* vol. 91, 2003.

[157] R. T. Canolty and R. T. Knight, "The functional role of cross-frequency coupling," *Trends in Cognitive Neurosciences,* vol. 14, 2010.

[158] L. D. Iasemidis, P. Pardalos, J. C. Sackellares, and D. S. Shiau, "Quadratic Binary Programming and Dynamical System Approach to Determine the Predictability of Epileptic Seizures," *Journal of Combinatorial Optimization,* vol. 5, pp. 9-26, 2001.

[159] K. Kira and L. A. Rendell, "The feature selection problem: traditional methods and a new algorithm," presented at the Proceedings of the tenth national conference on Artificial intelligence, San Jose, California, 1992.

[160] I. Kononenko, "Estimating attributes: analysis and extensions of RELIEF," presented at the Proceedings of the European conference on machine learning on Machine Learning, Catania, Italy, 1994.

APPENDICES

MATHEMATICAL DETAILS OF METHODS DISCUSSED IN THE LITERATURE REVIEW

This appendix presents a mathematical overview of different methods employed in earlier seizure predictions investigations as discussed in the literature review.

A. Preprocessing

1. Finite impulse response (FIR) filter:

FIR filters are usually implemented in a non-recursive form [150]:

$$Y[n] = b_0X[n] + b_1X[n-1] + b_2X[n-2] + \cdots + b_NX[n-N] \quad (1)$$

where Y[n] is the filtered EEG signal, X[n] is the unfiltered EEG signal, and bi are the filter's coefficients also known as the filter's weights.

2. Space differential filtering

Some studies have explored the effect of bipolar (space differential) preprocessing on the performance of seizure prediction algorithms [72]. Since bipolar preprocessing consists of subtracting two single-ended channels, it enhances common mode rejection ratio and it improves the spatial resolution as compared to single single-ended electrodes [151]. In a study including 18 patients from the Freiburg EEG database, Y. Park et al, 2011 showed that bipolar processing significantly improved the performance of the seizure prediction algorithm in terms of sensitivity and specificity [72].

3. Signal Normalization

All seizure prediction studies deal with multichannel signals that are sometimes recorded with different type of electrodes. Therefore, these should be normalized to allow a reliable comparison and feature extraction. The first step is to divide by the maximum value of the EEG signal to normalize its amplitude as shown in eqt.2.

$$X_n = \frac{x}{|\max(x)|} \quad (2)$$

Then the value of the signal is normalized by making its mean equal to zero and its standard deviation equal to 1.

$$X_{GN=}\frac{x-mean(x)}{std(x)} \quad (3)$$

B. Feature extraction

I. Univariate linear measures:

1. Energy and accumulated Energy

The energy and accumulated energy had been commonly employed in seizure prediction studies [43, 106]. The signal energy is the mean energy of a signal over a time period (4).

$$E(t,w)\frac{1}{w}\sum_{i=t}^{t+w} s(i)^2 \quad (4)$$

Long-Term Energy (LTE) and Short Term Energy (STE) have been proposed [106] and used in seizure prediction studies [43]. These corresponded to the energy of the signal averaged over 9s for the STE feature and 180 seconds for the LTE feature. Since the average power of a signal is given by its variance (Parseval's theorem), the accumulated energy at a given time point is computed by summing the variance of all previous time windows [33] (5):

$$AE(t) = \sum_{k=1}^{t} \sigma_k^2 \quad (5)$$

With σ_k^2 the variance of the k^{th} time window.

N. Moghim and D. Come, 2014 [43] computed the accumulated energy by summing the successive values of energy from a series of time moving windows. Although signal energy have been successful employed in some seizure prediction studies, Mormann et al, 2005 [47] found it unable to discriminate between the preictal and the interictal states above chance levels.

2. Autoregressive model

In several seizure prediction studies, the EEG signal was modeled as an autoregressive moving average (ARMA) model and several parameters that describe the evolution of this model were used as features (model order, prediction error, characteristic of the transfer function, coefficients, or power spectrum) . Such a model contains a combination of three linear model processes: an autoregressive model (AR), a random model (white noise), and a moving average model (MA). As shown in (6), an AR model indicates that the value of a signal at a given time point is a linear combination of its past values and a random process ε_i.

$$x_i = \sum_{l=1}^{p} a_l x_{i-l} + \varepsilon_i \quad (6)$$

However, some correlations may occur in the random process and therefore ε_i can be modeled as a moving average process (7).

$$\varepsilon_i = \sum_{k=1}^{q} b_k \varepsilon_{i-k} \quad (7)$$

The combination of equations 6 and 7 results in the ARMA model (8):

$$x_i = \sum_{l=1}^{p} a_l x_{i-l} + \sum_{k=1}^{q} b_k \varepsilon_{i-k} \quad (8)$$

The model coefficients a_l and b_k are found by fitting the data. Several algorithms have been proposed such as the least-squares algorithm. The prediction error (mean square error) derived from such a model has been proposed for seizure prediction [152]. It was stated that as the seizure approaches, the EEG signals are more likely to be predicted by an AR model and thus the prediction error decreases [73]. B. Direito et al, 2011 found the AR model predictive error as the best predictor for the patient exhibiting the highest performance values [58].

3. Wavelets Energy

The wavelets transform is a multi-resolution analysis in which time and frequency resolutions compromise is overtaken by decomposing the signal into a basis of functions [11]. These functions are a set of wavelets $\Phi_{a,b}$. Each wavelet is a scaled and translated version of the mother wavelet (9).

$$\emptyset_{a,b}(t) = \frac{1}{\sqrt{(a)}} \emptyset \left(\frac{t-b}{a}\right) \quad (9)$$

where b is the translation factor, a is the scaling factor and Φ is the mother wavelet.
The continuous wavelet transform is computed as shown in (10).

$$W_x(s,u) = \int_{-\infty}^{+\infty} X(t) \emptyset_{u,s}(t) dt \quad (10)$$

In this way, it is possible to analyze the signal at multiple scales and resolutions at the same time allowing an examination of low frequency components with high frequency resolution and high frequency components with high temporal resolution. In the field of seizure prediction, the wavelet transform was used as quantification of the energy in different frequency bands over a time window [73].

II. Univariate nonlinear measures:

Based on the fact that the brain passes through several dynamical states, a set of non-linear features derived from the theory of dynamical systems has been proposed in an attempt to quantify the properties of state space trajectories in a Cartesian space. The state space trajectory is first reconstructed from the scalar time series x_i (for i=1, … N). Two types of reconstructions have been proposed: a type-delay embedding and spatial embedding [33]. As its name implies, the time-delay embedding (11) is performed by means of time delay coordinates [153].

$$\overrightarrow{X_i} = \left(x_i, x_{i+\tau}, \ldots . x_{i+(m-1)\tau}\right) \quad (11)$$

with i=1,…, M; and M=N-(m-1) τ

where m is the embedding dimension and τ is the time delay. With this configuration, the evolution of the system can be now seen as the projection of Xi into the state space (multidimensional space).

On the other side, in a spatial embedding, mostly used in the study of electroencephalography, each channel is considered as an axis of the Cartesian space. Therefore, the embedding dimension is fixed and is equal to the number of channels. It should be noted that a combination of time-delay and spatial embedding is possible.

Several univariate non-linear measures based on the reconstruction of the state based trajectory have been proposed such as the correlation dimension [154], the largest Lyapunov exponent [155], and the dynamical similarity index. In a comparative study of 30 linear and non-linear features, Mormann et al, 2005 found that the used univariate non- linear measures (correlation dimension, Lyapunov exponent) weren't able to significantly perform better than chance [47].

1. Correlation density

The correlation density estimates the number of active states of a dynamic system [154]. It was explained by Mormann et al, 2007 [33] as the correlation sum of a fixed hypersphere radius. Mormann et al, 2005 [47] found an increase in the correlation dimension prior to seizure onset while Elger and Lehnertz, 2008 [137] reported a decrease 5-25 min prior to the seizure onset. Therefore, contracting evidences have been reported what limited the use of this measure in future studies.

2. Largest Lyapunov exponent (L_{max})

The Largest Lyapunov exponent has been largely employed in early seizure prediction studies as a quantification of the convergence or divergence of nearby state space trajectories. Exponential values of divergence are considered as the most basic indicator of chaos and non-linearity in a univariate EEG time series. The rate at which the distance between two initially close trajectories changes during time is described by an exponent: e^{λ_i} (λ_i being the lyapunov exponent at the i^{th} dimension). In a multidimensional state space, the Lyapunov exponent is the sum of all the exponents (at all dimensions) and indicates the evolution of the so-called hypercube [100]. A positive value of λ_i is indicative of a divergence (chaotic behavior) while negative value indicates

a convergence in the i^{th} dimension. Several studies have adopted the largest exponent as a characterizing measure of EEG signals. As shown in eqt. 12, L_{max} quantifies the expansion of the hypercube along the principal axis (p_i) over a given time interval t [100]:

$$\lambda_i = \lim_{t\to\infty} \frac{1}{t} log_2 \left[\frac{p_i(t)}{p_i(0)}\right] \quad (12)$$

The first algorithm applied to estimate the largest Lyapunov exponent from a measured time series was proposed by Wolf et al, 1985 [155]. The algorithm starts by finding the point nearest to the starting point in the embedded state space then following the trajectories between this point and the starting point during a fixed interval. The next step consists of measuring the initial distance d0 and d1 (the distance after the first-time interval). If d1 is less than a fixed threshold, the procedure is repeated. On the other side, if d1 becomes larger than the threshold, a rescaling of the distance is performed by searching for a new point closer to the reference trajectory [100, 155]. Iasemidis et al, 1990 [63] revised this rescaling algorithm for application to EEG and iEEG. As shown in eqt. 13, the largest Lyapunov is computed by repeating the procedure k times to cover the state space from t_0 to t_k.

$$\lambda_{max} = \frac{1}{t_k - t_0} \sum_{i=1}^{k} \log_2 \left[\frac{d_i}{d_{i-1}}\right] \quad (13)$$

Although first investigation revealed a decrease in Lmax several minutes before seizures [63], contradictory results have been also reported suggesting an increase 30 min prior to seizure onset [47]. Furthermore, Lai et al, 2003 [156] challenged its suitability for seizure prediction.

3. Dynamical Similarity Index

Le Van Quyen et al, 1999 [77] proposed the dynamical similarity index as a measure of dynamical similarity between a reference window (beginning of the recordings, 300s) and a moving test window. Interestingly, the authors preprocessed the signals by segmenting them into 30 sec non- overlapping consecutive windows. These were transformed to the domain of inter-event intervals by taking the sequence of time intervals between the positive-going crossings of a fixed threshold. Then each of the time series was converted into a state space embedding. The dynamical similarity between the two windows was calculated in terms of the cross-correlation index. Thus, changes in the dynamical state leading to an increased non-stationarity of the EEG result in lower values of correlation. The authors evaluated the presence of a preictal state by statistically assessing the deviation of the moving test window from the reference state

(Chebushev's inequality). Persistent deviations from the reference state have been found about 18 min prior to the seizure onset. However, by the turn of the millennium, the reliability of these optimistic results was questioned by Winterhalder et al, 2003 [91].

Other non-linear univariate measures have been proposed such as the correlation entropy [92], the marginal predictability [93], the state space dissimilarity measures, local flow and algorithmic complexity. Since several studies showed non-superiority of univariate non-linear measures as compared to linear ones [47, 82], we will be limited to the most prominent ones in this paper.

4. Phase Frequency Coupling

Additionally, motivated by the fact that human intracranial EEG studies have identified a spatially distributed modulation of cortical high frequency oscillations in the gamma band (40-120 Hz) by theta oscillations (4-8 Hz) [157] and slow waves (0.5-3 Hz) [114], recent studies have adopted the slow modulation of high-frequency gamma activity as a measure of brain excitability [88]. The interaction between the phase of low frequency bands and the amplitude of gamma sub bands was quantified by measuring the mean coupling phases. Interestingly, the authors performed prospective testing and found above chance preictal changes in 13.2% of the patients (7/53). M. Tort et al, 2010 proposed an algorithm for measuring the phase amplitude coupling: It starts by bandpass filtering the signals into the frequencies of interest, then extracting the amplitude and phase using the Hilbert Transform. The analytical representation (X_a) of a signal x (t) is obtained by means of the Hilbert Transform (14).

$$X_a(t) = A_x(t)e^{-j\varphi_x(t)} \tag{14}$$

where A_x is the envelope and φ_x is the instantaneous phase of the filtered signal.

The next step consists of quantifying the modulation between phase-amplitude pairs $(\varphi_x(t), A_x(t))$.

III. Bivariate Linear Measures

1. Maximum linear cross-correlation

As a measure of lag synchronization, the maximum of the normalized cross-correlation (15) is used to quantify the similarity of two time series x_i and y_i [94] and have been employed between EEG signals in seizure prediction studies [47].

$$C_{max} = \max_{\tau}\left\{\left|\frac{C(x,y)(\tau)}{\sqrt{C(x,x)(0).C(y,y)(0)}}\right|\right\} \quad (15)$$

where C(x,y)(τ) is the linear cross correlation function (16).

$$C(x,y)(\tau) = \begin{cases} \frac{1}{N-\tau}\sum_{i=1}^{N-\tau} x_{i+\tau}y_i & \tau \geq 0 \\ C(y,x)(-\tau) & \tau < 0 \end{cases} \quad (16)$$

The value of Cmax is between 0 and 1 with high values indicating time course similarities between the two time series (possibly shifted by a time lag τ) while not correlated signals will show values close to zero (16).

In comparative study with several non-linear bivariate signals, Mormann et al, 2005 [47] found the maximum cross-correlation as one of the most discriminative bivariate measures.

IV. Bivariate non-linear Measures

Bivariate non-linear measures were extensively employed in seizure prediction investigations and showed good predictive performances [33]. Measures based on mutual information and similarity between channels has been used to characterize the level of synchrony between EEG channels at different locations [100]. The advantages of using such measures rely in their capability of capturing the brain's dynamics from a network point of view.

1. Dynamical entrainment

Some non-linear univariate measures described above have been extrapolated into a multichannel version. Iasemidis et al, 2001 [158] proposed the dynamical entrainment, a multichannel version of the Lyapunov exponent that quantifies the statistical difference between the largest Lyapunov exponents Lmax of two signals recorded at two different recording sites (17).

$$T_{xy} = \sqrt{l}\,\frac{|\langle L_{max,x} - L_{max,y}\rangle|}{\sigma_{xy}} \quad (17)$$

where l is the number of consecutive windows, <…> denotes the mean over l and σ_{xy} is the standard deviation [33, 158]. This measure has shown a good predictive power with a relatively low false prediction rate [83].

2. Phase Synchronization Measures

As their name imply, phase synchronization measures tend to quantify the degree at which two or more signals tend to oscillate with repeating sequences of relative phase angles. Different

measures have been applied in EEG time series analysis and seizure prediction and will be discussed:

i- Phase Locking Value

The phase locking value (PLV) has been also used as a measurement of phase synchrony and coupling between two or several signals. Two EEG signals X(t) and Y(t) are said phase locked if the difference of their corresponding phases $\emptyset_x$ and $\emptyset_y$ fluctuates around a constant value (18).

$$\emptyset_x - \emptyset_y = cte \tag{18}$$

The instantaneous phases of each signal are estimated using the Hilbert Transform (previously explained). Le Van Quyen et al, 2005 [99] evaluated the suitability of the phase locking value for all pairs of EEG channels placed of the temporal lobe. A sliding window analysis on 15 frequency bands (between 0 and 30 Hz with 2 Hz steps) has been performed over the entire dataset (305 hours). The authors stated that in 70% of the cases (36 out of 52 seizures), a specific state of synchronization can be observed during a relatively long preictal time of several hours before the seizure onset. No general trend (increase or decrease) of synchronization has been observed but changes were most often localized in the primary epileptogenic zone and occurred within the 4-15Hz frequency band.

ii- Mean Phase coherence

Mormann et al, 2003, [52] used the mean phase coherence and reported a drop in synchronization during the preictal state (19).

$$MPC = \left| \frac{1}{N} \sum_{i=1}^{N} e^{i[\emptyset_x(t_j) - \emptyset_y(t_j)]} \right| \tag{19}$$

In a follow up study, Mormann et al, 2003 [95] used the mean phase coherence as a measure of phase synchronization and the maximum linear cross-correlation (bivariate linear measure) as a measure for lag synchronization for the automatic detection of the preictal state. Interestingly the authors found a similar performance for both synchronization methods in terms of predictive power as well as anticipation times. The authors suggested that the preictal synchronization dynamics can be sufficiently characterized using a linear measure.

Similarly, Winterhalder et al, 2006 [97] investigated short-term changes of increasing and decreasing synchronization during the preictal state (50 min) using the mean phase coherence and the lag synchronization index. In contrast with [52], the results revealed non-uniform changes in

synchronization and the authors stated that evaluating increasing as well as decreasing synchronization may yield to significant prediction performance. These results are concordant with those obtained in the comparative study of the 30 different measures for seizure prediction [47] suggesting that these measures perform better than a random predictor with both an increase and a decrease in synchronization during the preictal state.

iii- Indexes based on conditional probability and Shannon entropy

Indexes based on conditional probability and Shannon entropy have been proposed by Tass et al, 1998 [101] as measures of phase synchronization and have been adopted in earlier seizure prediction studies [47]. A detailed mathematical explanation of these measures has been emphasized in [33]. Morman et al, 2005 [47] compared 8 different bivariate non-linear features. The mean phase coherence, the Shanon entropy index, and the conditional probability index, were calculated based on both the Wavelets Transform and the Hilbert Transform. Two additional measures of non-linear independence were used (called H and R) [47]. High values (close to 1) are obtained when and high-nonlinear dependence exists between two time series and vice versa. The authors found that the mean phase coherence, the Shanonn entropy index, and the conditional probability index computed based on the Hilbert Transform as the best non-linear bivariate measures.

C. Feature selection

1. Minimum normalized difference of percentiles (mNDP)

The basic idea of this method is to minimize the overlap between the percentiles of the samples between the two classes for a given feature. M. Bandarabadi et al, 2012 [102] introduced a new measure to quantify the overlap value (20):

$$NDP = \frac{p_{n1}(\,class\ 1) - p_{n2}(\,class\ 2)}{p_{50}(class\ 2) - p_{50}(class\ 1)} \qquad (20)$$

where p_n is the n^{th} percentile of features' values of the preictal or interictal classes.

The selection method performs a ranking of the features based on their normalized difference of percentiles values. The discriminative features are those which exhibit the minimum normalized difference of percentiles. However, the limitation of this method is the need for finding the adequate values of the percentiles what limited its application in seizure prediction studies. Based

on trial and error, M. Bandarabadi et al, 2012 [102] selected the 70th and 30th percentiles for class 1 and class 2 respectively.

2. Maximum Difference of Amplitude Distribution Histograms (mDAD)

This method was mainly introduced for feature selection in seizure prediction applications [102]. As it name implies, it is based on the amplitude distribution of preictal and non-preictal samples. An amplitude distribution histogram (ADH) represents the histogram of the samples of a feature associated with one class. In seizure prediction studies a binary classification problem is usually addressed, therefore two ADH were considered. To have a good discriminative power, a feature should maximize the difference between the two ADHs. Therefore, the method will search for the features that have the Maximum Difference of ADHs (mDAD). As shown in (21), the difference of ADHs is defined in terms of common area (CA) of the two normalized ADHs:

$$DAD = 1 - CA \tag{21}$$

The common area is computed as the difference of the classes' normalized histograms. The ADH (22) is normalized by dividing the original histograms by the number of samples in each class.

$$ADH_{normj} = \frac{ADH_j}{ns*w} \tag{22}$$

$$CA = w * \sum_{i=1}^{n} \min\left(ADH_{norm1}, ADH_{norm2}\right) \tag{23}$$

Where w is the bin width (of the feature axis), ADH_{normj} is the normalized ADH of class j. The features are ranked in terms of common area. Most discriminative features are those which exhibit the lowest values. This method was first used in [102] in which from 435 features of relative spectral power, an average of 8.75 most discriminative features were selected. The authors compared the performance of the proposed approach (sensitivity: 76.09%; FPR: 0.15; number of selected features: 8.75) to the well-used mRMR (sensitivity: 60.87%; FPR: 0.11; number of selected features: 9.91) method and reported a better mean performance. In a follow-up study, M. Bandarabadi et al, 2015 [45] extended their investigations into long-term continuous EEG recordings of twenty-four patients from the European Epilepsy database. The authors performed a comparative study and found that the mDAD (sensitivity: 75.8%; FPR: 0.10; number of selected features: 9.9) outperformed the mRMR (sensitivity: 64.4%; FPR: 0.09; number of selected features: 11.9) selection method in terms of sensitivity and number of features with comparable performance in terms of FPR.

3. ReliefF feature selection

Relief was first proposed by Kira and Rendel, 1992 [159] as a feature selection algorithm dedicated to binary classification. It was then extrapolated into a multi-class version [160]. In summary, it is an iterative procedure that starts by assigning a zero weight to each feature. The next step consists of sampling a random instance, finding a sample of the closest data instances from the same class, and a sample of the closest data instances form the other classes. Then feature weights are adjusted increasing those of highly discriminative features. A detailed description of the algorithm is available in [160]. N. Moghim and D. Come used the reliefF for feature selection within the framework of the proposed Advanced Seizure Prediction via Preictal Relabeling Algorithm (discussed in the literature review). The algorithm was used to reduce feature dimensions from 204 features to the 14-highest ranked features. The authors fixed the size of the selected subset of features to 14 considering that this may make results benchmarking possible with a previous study that used 14 features based on wavelet transforms, signal energy attributes, and non-linear system dynamics [106]. The authors stated that their results outperformed the benchmarking feature set and the baseline predictors.

D. Regularization

1. Kalman Filtering

L.Chisci et al, 2010 [110] were the first to use the Kalman filtering approach as a regularization method to smooth the output of an SVM classifier. It is a statistical method used to produce estimates that tend to be close to the true measurements. The basic mathematical principle of this method is briefly explained:

The Kalman filter is applied directly on the continuous decision variable (z_k) of the classifier (mainly SVM) which is the real value of the classifier's output signal (before the SVM decision threshold). The idea behind this method is to model the continuous signal (z_k) as a state space model and filter it using the Kalman filter. The continuous variable z_k can be considered as the sum of a noiseless decision variable (d_k) and a noisy measurement process (24).

$$z_k = d_k + v_k \tag{24}$$

where v_k is a zero-mean measurement noise with a standard deviation σv.

Considering that the brain undergoes a smooth transition between different states, the authors proposed to naturally enforce the regularity of the decision variable by means of a White Noise

Acceleration (WNA) model [Y. Bar-Shalom et al, 2001; L.Chisci et al, 2010]. Then the continuous variable zk can be represented by the following state space model (25):

$$\begin{cases} s_{k+1} = \begin{bmatrix} 1 & T_p \\ 0 & 1 \end{bmatrix} s_k + w_k \\ z_k = \begin{bmatrix} 1 & 0 \end{bmatrix} s_k + v_k \end{cases} \quad (25)$$

$$s_k = \left[d_k, \dot{d_k} \right]' \quad (26)$$

where $\dot{d_k}$ is the rate of change of d_k , w_k is the process noise, and T_p is the prediction interval. More details about the Kalman filter implementation and tuning can be found in [110].

E. Additional performance evaluation measures

Some studies have adopted other measures to evaluate the performance of their predictors. N. Moghim and D. Come, 2014 [43] adopted the S1-score which is the harmonic mean of specificity and sensitivity (27). The authors considered that using such a measure may simplify the discussion of the results.

$$S1 = 2\ x\ \left(\frac{Sensitivity\ x\ Specificty}{Sensitivity + Specificity} \right) \quad (27)$$

The time under false warning and warning rate were also proposed as performance evaluation measures in terms of specificity.